

UNCLASSIFIED

AD . 4 2 5 8 7 6

DEFENSE DOCUMENTATION CENTER

FOR

SCIENTIFIC AND TECHNICAL INFORMATION

CAMERON STATION, ALEXANDRIA, VIRGINIA



UNCLASSIFIED

DISCLAIMER NOTICE

**THIS DOCUMENT IS BEST QUALITY
PRACTICABLE. THE COPY FURNISHED
TO DTIC CONTAINED A SIGNIFICANT
NUMBER OF PAGES WHICH DO NOT
REPRODUCE LEGIBLY.**

NOTICE: When government or other drawings, specifications or other data are used for any purpose other than in connection with a definitely related government procurement operation, the U. S. Government thereby incurs no responsibility, nor any obligation whatsoever; and the fact that the Government may have formulated, furnished, or in any way supplied the said drawings, specifications, or other data is not to be regarded by implication or otherwise as in any manner licensing the holder or any other person or corporation, or conveying any rights or permission to manufacture, use or sell any patented invention that may in any way be related thereto.

425876

CATALOGED BY DDC
AS AD No. _____

NEW CATHODE-ANODE COUPLES USING NONAQUEOUS ELECTROLYTE

Technical Documentary Report No. RTD-TDR-63-4083

October 1963

Air Force Aero-Propulsion Laboratory
Research and Technology Division
Air Force Systems Command
Wright-Patterson Air Force Base, Ohio

Project No. 8173

Task No. 817304

DEC 28 1963

(Prepared under Contract No. AF 33(616)7957
by LOCKHEED MISSILES & SPACE COMPANY
Palo Alto, California;

H. F. Bauman, J. E. Chilton, W. J. Conner, and G. M. Cook, authors)

Code No. 2-02-63-3

NOTICES

When Government drawings, specifications, or other data are used for any purpose other than in connection with a definitely related Government procurement operation, the United States Government thereby incurs no responsibility nor any obligation whatsoever; and the fact that the Government may have formulated, furnished, or in any way supplied the said drawings, specifications, or other data, is not to be regarded by implication or otherwise as in any manner licensing the holder or any other person or corporation, or conveying any rights or permission to manufacture, use, or sell any patented invention that may in any way be related thereto.

Qualified requesters may obtain copies of this report from the Defense Documentation Center (DDC), (formerly ASTIA), Cameron Station, Bldg. 5, 5010 Duke Street, Alexandria 4, Virginia.

This report has been released to the Office of Technical Services, U.S. Department of Commerce, Washington 25, D.C., for sale to the general public.

Copies of this report should not be returned to the Aeronautical Systems Division unless return is required by security considerations, contractual obligations, or notice on a specific document.

FOREWORD

This is the second Annual Report prepared by personnel of the Electrochemistry Group, Materials Sciences Laboratory, Lockheed Missiles & Space Company, Palo Alto, California, under Air Force Contract AF 33(616)7957, Task Number 817304, Project Number 8173, entitled "New Cathode-Anode Couples Using Nonaqueous Electrolytes." This work was administered under the direction of the Flight Vehicle Power Branch, Air Force Aero-Propulsion Laboratory, Research and Technology Division, Wright-Patterson Air Force Base, Ohio. Acknowledgment is made of the assistance of Mr. Wayne S. Bishop, task engineer for the Aero-Propulsion Laboratory.

The work reported covers the period October 1962 through September 1963. This report summarizes continued work on nonaqueous electrolyte secondary batteries initially reported in Aeronautical Systems Division Annual Technical Report ASD-TDR-62-837, dated September 1962.

LMSC personnel who have contributed valuable ideas and labor on this project include the following:

Dr. G. B. Adams	Senior Member, Research Laboratory
Mrs. Irene Alves	Research Technician
Mr. H. F. Bauman	Staff Scientist
Dr. J. E. Chilton	Research Scientist
Dr. G. M. Cook	Associate Research Scientist
Mr. W. J. Conner	Senior Research Engineer
Miss S. K. Erickson	Associate Scientist
Mr. H. H. Harris	Associate Scientist
Mr. R. W. Holsinger	Associate Scientist

ABSTRACT

Improvement in the cycle life and energy density of secondary batteries is necessary for extensive aerospace power usage. The properties of a lithium - silver chloride cell using nonaqueous electrolyte have been studied, and sealed cells of 5-amp-hr nominal capacity fabricated and tested. Nonaqueous electrolytes have been formed with AlCl_3 and LiCl additions to propylene carbonate (PC) and nitromethane (NM). The maximum specific conductivity of the propylene carbonate electrolyte is $7 \times 10^{-3} \text{ ohm}^{-1} \text{ cm}^{-1}$ in a 1.2 M LiCl-AlCl_3 solution and for the nitromethane electrolyte is $4.2 \times 10^{-2} \text{ ohm}^{-1} \text{ cm}^{-1}$ at 1.5 M LiCl-AlCl_3 solution. The freezing point of NM-based electrolyte is -70°C at 3 M $\text{AlCl}_3\text{-LiCl}$ level. The freezing point of PC-based electrolyte is below -80°C at 0.8-M $\text{AlCl}_3\text{-LiCl}$ solution. The conductivity of PC- AlCl_3 solution is slightly lowered, while that of the NM- AlCl_3 solution is greatly increased, upon addition of LiCl . A temperature-dependence study of the electrolytes indicates 4-M NM- AlCl_3 solution has an activation energy for ion transport of 1.9 kcal per mole and 3-M NM- $\text{AlCl}_3\text{-LiCl}$ solution 3.3 kcal per mole. A PC- AlCl_3 solution has an activation energy of 4.4 kcal per mole at 0.75-M concentration. Electrolyte electrolysis occurs at potentials greater than 3 v versus a silver-silver chloride electrode for both electrolytes (NM and PC) with AlCl_3 but no LiCl present. A silver-electrode study led to fabrication of silver-silver chloride-graphite pasted electrodes, the mix formed by precipitation of silver chloride in a graphite-silver oxide suspension in water. Thin electrodes and use of mix low in AgCl led to increased utilization of the AgCl during discharge. Graphite was found to increase the AgCl utilization in thick pasted electrodes. Silver chloride solubility in $\text{AlCl}_3\text{-LiCl}$ electrolytes is less than $6 \times 10^{-4} \text{ M}$. An increase in AgCl solubility was found in electrolyte with perchlorate salt added. AgCl is formed from silver by anodic oxidation at 100 percent current efficiency at current densities up to 35 ma/cm^2 . Lithium electrodes were initially formed by dipping nickel screen in molten lithium and are now produced by rolling lithium sheet onto nickel screen in an argon atmosphere.

Lithium deposition occurs up to 100 percent efficiency in concentrated AlCl_3 -LiCl-NM solutions and AlCl_3 -LiCl-PC solutions. A lithium deposit is most metallic in appearance when formed from LiClO_4 -PC solution but did not form well from LiClO_4 -NM solution.

An improved lithium deposit was obtained from the NM system and from mixed solutions of PC and NM. Water addition to both NM and PC systems reduced lithium deposition efficiency. Slight improvement in lithium deposit appearance was noted on addition of certain organic addition agents to PC and NM solution. Lithium is deposited from solution with least alloying effect on nickel or stainless steel matrices. A study of separator material resistivity in PC electrolyte and of reactivity in solvent indicates a glass mat has low resistance, moderate strength, and good solvent resistance. Silver and lithium electrodes have been assembled into cells and inserted into split polypropylene cases or in aluminum cases. Initially, plastic tops were used to close the aluminum cells. In the final development of the cell container, aluminum tops containing terminals were arc welded in an argon atmosphere to the aluminum case, producing a sealed, all-metal case.

Mechanical fastening techniques have been used to assemble multiple electrodes to terminals. Testing equipment for single cells and 5-cell batteries has been designed, assembled, and is being used. The battery charges and discharges cells connected in series at constant current, recording individual cell voltages, battery voltage, and current. Cell cycling tests indicate the best material for lithium electrode support is nickel or stainless steel. The use of soldered electrode-to-terminal connections and aluminum electrode support results in rapid loss of electrodes. Over-charged, over-discharged or reversed-charged cells assembled in a battery configuration cause cell failure. A propylene carbonate electrolyte cell has been cycled for a 90-min period at 12-percent depth of discharge for 110 cycles at current density of 1.3 ma/cm^2 . When cycling cells in a battery configuration, the need for better uniformity of cell components was indicated. A nominal 5-amp-hr lithium-silver chloride cell was fabricated which had the following characteristics: Energy density of 8 w-hr/lb total weight at a 4.5-amp discharge level with an average cell voltage of 2.2 v, and 25 w-hr/lb

total weight at a 0.12-amp discharge level with an average cell voltage of 2.7 v. From cell voltage-current measurements taken at -30°C , a drop in cell voltage of 0.9 v at 10 ma/cm^2 was measured from the cell voltage at room temperature and at the same current density. The low-temperature discharge is limited mainly by solution resistance. Steady-state cell polarization is a major limiting factor in the lithium-silver chloride cell in initial discharge state, and upon charge-discharge cycling an increase in cell resistance occurs.

Transient polarization measurements show that increased lithium resistance occurs with reduced cell capacity on long-term cycling. By calculating the entropy for the reaction of lithium and silver chloride from a determination of the change in cell voltage with temperature, the reaction is shown to occur with components in solid state in PC solutions. Solvent interaction with AgCl and LiCl in NM solutions may occur. In measuring cell heat production with an adiabatic calorimeter on discharge, we found the heat effect to be predominantly due to electrode polarization, with smaller contribution from solution resistance and reaction entropy heat.

The present study of the lithium-silver chloride cell system has led to the development of cells which operate at a current density of 1 to 2 ma/cm^2 at 2.4 to 2.6 v and yield an energy density of 20 w-hr/lb at this rate. The charge-discharge cycles which have been obtained indicate that the cells are reversible and operate as a secondary battery. Improvements in the design and assembly techniques and further material research will enable construction of experimental cells with both increased operational life and higher energy densities.

PUBLICATION REVIEW

The publication of this report does not constitute approval by the Air Force of the findings or conclusions contained herein. It is published for the exchange and stimulation of ideas.

CONTENTS

Section	Page
1 INTRODUCTION	1
2 DISCUSSION OF EXPERIMENTAL WORK	3
2.1 Electrolyte Studies	3
2.1.1 Lithium Chloride Conductivity	3
2.1.2 Aluminum Chloride and Mixed-Salt Conductivity	3
2.1.3 Temperature Dependence of Conductivity	5
2.1.4 Freezing Points of Electrolyte	10
2.1.5 Electrolyte Decomposition Potential	10
2.2 Silver Electrode Studies	15
2.2.1 Anodic Oxidation of Silver	15
2.2.2 Methods of Electrode Preparation	
2.2.3 Additives to Electrode Mix	19
2.2.4 Silver Powder Size	20
2.2.5 Graphite Effects	20
2.2.6 Silver Chloride Concentration	24
2.2.7 Electrode Thickness	26
2.2.8 Present Silver Electrode	26
2.3 Lithium Electrode Studies	28
2.3.1 Electrode Preparation	28
2.3.2 Lithium Electrodeposition	28
2.3.3 Deposition from Various Solvents	29
2.3.4 Deposition from Mixed Solvents	30
2.3.5 Nitromethane Solution Deposition	32
2.3.6 Deposition of Other Metals	32
2.3.7 Addition Agent Effects	33

Section	Page
2.3.8 Pressure Effects	35
2.3.9 Coulombic Efficiency of Electroplated Lithium	36
2.3.10 Lithium Polarization	37
2.4 Separator Material Study	37
2.5 Cell Assembly Techniques	40
2.5.1 Cell Assembly Dry Boxes	40
2.5.2 Materials	43
2.5.3 Initial 5-Amp-Hr Cells	44
2.5.4 Final 5-Amp-Hr Cells	44
2.5.5 Lid-to-Can Sealing	45
2.6 Test Apparatus	47
2.6.1 Constant-Current Cell Cycling Apparatus	47
2.6.2 Battery Testing Equipment	53
2.7 Cell Testing	61
2.7.1 Cells with 4-In. ² Electrodes	61
2.7.2 5-Amp-Hr Cell Tests	67
2.8 Battery Test Results	69
2.9 Cell Thermal Effects	71
2.9.1 Low-Temperature Studies	71
2.9.2 High-Temperature Study	89
2.9.3 Temperature Dependence of Cell Voltage	89
2.9.4 Cell Heat Production	93
2.10 Cell Polarization Study	97
2.10.1 Steady-State Measurements	97
2.10.2 Transient Measurements	97

ILLUSTRATIONS

Figure		Page
1	Specific Conductivity of Nitromethane Solutions with AlCl_3 and LiCl	4
2	Variation of Conductivity of Nitromethane- AlCl_3 Solutions with Addition of LiCl	6
3	Equivalent Conductivity of Dilute Nitromethane- AlCl_3 Solutions	7
4	Temperature Dependence of Specific Conductivity for 4-M AlCl_3 -Nitromethane Electrolyte	8
5	Temperature Dependence of Specific Conductivity for 3-M LiCl-AlCl_3 Nitromethane Electrolyte	9
6	Temperature Dependence of Specific Conductivity for 0.75-M AlCl_3 -Propylene Carbonate Solution	11
7	Freezing Points of LiCl-AlCl_3 Complex in Nitromethane	12
8	Electrode Polarization in Propylene Carbonate Solution	13
9	Electrode Polarization in Nitromethane Solution	14
10	Silver Discharge Polarization for Various Silver Surfaces	18
11	Utilization of AgCl in Various Electrodes	21
12	Silver Discharge Polarization for Various Discharge Cycles	22
13	Silver Polarization for Later Discharge Cycles	23
14	Discharge Characteristics for a Lithium-Silver Chloride Cell	25
15	Silver Chloride Concentration Effect on Utilization	27
16	Lithium Electrode Discharge Polarization	38
17	5-Amp-Hr Lid and Can Assembly	46
18	Lid Assembly Sequence	48
19	Arc-Welded Cell Assembly	49
20	Cell Power and Control Circuit	51
21	Charge-Discharge Circuit	52
22	Constant-Current Charge-Discharge Apparatus	54

Figure		Page
23	Charge-Discharge Curves Obtained with Li-AgCl Nitromethane System	55
24	Battery Cycle Diagram	56
25	5-Amp Power and Control Unit	57
26	Cell Voltage Switch	58
27	Variable Charge-Discharge Unit	59
28	Battery Cycling Unit	60
29	Battery Cycling Data Record	70
30	Cell Discharge Characteristics at 25° C and -30° C	86
31	Cell Characteristics at -57° C	87
32	Cell Characteristics at -56° C	88
33	Cell Characteristics at 74° C	90
34	Temperature Dependence of Open-Circuit Cell Voltage in Propylene Carbonate Solution	92
35	Temperature Dependence of Open-Circuit Cell Voltage in Nitromethane Solution	94
36	Cell Heat Production Measurements	96
37	Cell Discharge Characteristics Study at Various Cycles	98

TABLES

Table		Page
1	Anodic Oxidation of Silver in Selected Systems	16
2	Lithium-Electrolyte Deposition Study	29
3	Solvent Properties	30
4	Lithium Deposition from Mixed Solvents	31
5	Lithium Deposition from Nitromethane Solution	32
6	Metal Deposition	33
7	Effect of Organic Additives on Lithium Deposition	34
8	Lithium Deposition from Systems with LiClO_4	35
9	Separator Materials	41
10	Key to Cell Components	62
11	Cell Test Data	64
12	Cell Cycling Results	66
13	Results of 5-Amp-Hr Cell Testing	68
14	Battery Test Results	72

Section 1
INTRODUCTION

The use of secondary batteries in conjunction with solar-cell charging equipment is a recognized method of supplying and storing electrical power in earth-orbiting satellites. New, improved secondary batteries using new cathode-anode couples, with increased energy per unit weight values and long cycle life, are necessary to improve the load-carrying capability and the useful electrical life of present satellites. Previous work on new cathode-anode couples has indicated that cells composed of alkali metal-metal halide electrodes in conjunction with a nonaqueous electrolyte can have high theoretical energy per unit weight values and high cell voltages, e. g., for a lithium-silver chloride cell, 240 w-hr/lb of reactants and 3-v open circuit. The work leading to the development of the lithium-silver chloride cell and a consideration of other systems is reported in Technical Documentary Report Nos. ASD-TDR-62-1, January 1962, and ASD-TDR-62-837, September 1962, of Aeronautical Systems Division - now called Research and Technology Division - Wright-Patterson Air Force Base, Ohio.

The objective of this program is to continue a study on the properties of a lithium-silver chloride nonaqueous secondary battery in order to improve the life of the battery and increase the energy output by suitable improvements in battery materials selection, and fabrication techniques. Concurrent with the battery study, a research program has been conducted to investigate electrolyte systems containing new solvent or soluble materials and electrode forming techniques which will improve the basic electrochemical processes occurring during charge and discharge cycling steps. The program is divided into four parts:

- The Electrode. Cell component investigation consisting of cathode-anode separator and electrolyte studies to improve the rate of reactions occurring on electrode surfaces and obtain minimum resistance from separators and electrolyte

Manuscript released by the authors November 1963 for publication as an RTD Technical Documentary Report.

- Cell testing. Electrical tests of cells with 2-in. by 2-in. electrodes at varying percent capacity, measuring current and voltage as functions of time
- Battery testing. Electrical tests of battery of 4 to 6 cells, noting the effect of overcharge and reverse charging
- Design and test of a 5-amp-hr nominal size cell and battery

The study outlined is directed toward accomplishing the necessary research leading to the development of a secondary battery with specific properties which include the following as goals:

1. Good shelf life
2. Voltage regulation of 10 percent during discharge
3. Lifetimes of 10,000 charge-discharge cycles at 75 percent rated capacity
4. An energy density of 100 w-hr/lb
5. Operation from -30° F to 150° F (-35° C to 65° C)
6. Operation in space or aerospace environment

Section 2

DISCUSSION OF EXPERIMENTAL WORK

2.1 ELECTROLYTE STUDIES

2.1.1 Lithium Chloride Conductivity

The concentration of saturated solutions of lithium chloride are very small in both propylene carbonate and nitromethane. The solubility products are:

$$K_{\text{nitromethane}} = 10^{-8}$$

$$K_{\text{propylene carbonate}} = 8.27 \times 10^{-8} \text{ (measured by W. S. Harris*)}$$

Because of these small concentrations, conductance experiments yield information at only saturated solutions.

2.1.2 Aluminum Chloride and Mixed Salt Conductivity

The electrical conductivity of various aluminum chloride-nitromethane (NM) solutions were measured using a platinum-electrode cell with a cell constant of 1.0 cm^{-1} . The cell was immersed in an oil bath at a temperature of 25°C . The resistance was measured with an AC bridge operating at 1,000 cps. As shown in Fig. 1, the maximum electrical conductivity for the AlCl_3 -NM system occurs at 2.2-M concentration of $1.5 \times 10^{-2} \text{ ohm}^{-1} \text{ cm}^{-1}$. The maximum obtained with a AlCl_3 -propylene carbonate (PC) system was $7 \times 10^{-3} \text{ ohm}^{-1} \text{ cm}^{-1}$. The electrical conductivity of a (nitromethane) solution

*W. S. Harris, Electrochemical Studies in Cyclic Esters, AEC Report UCRL-8381 (1955)

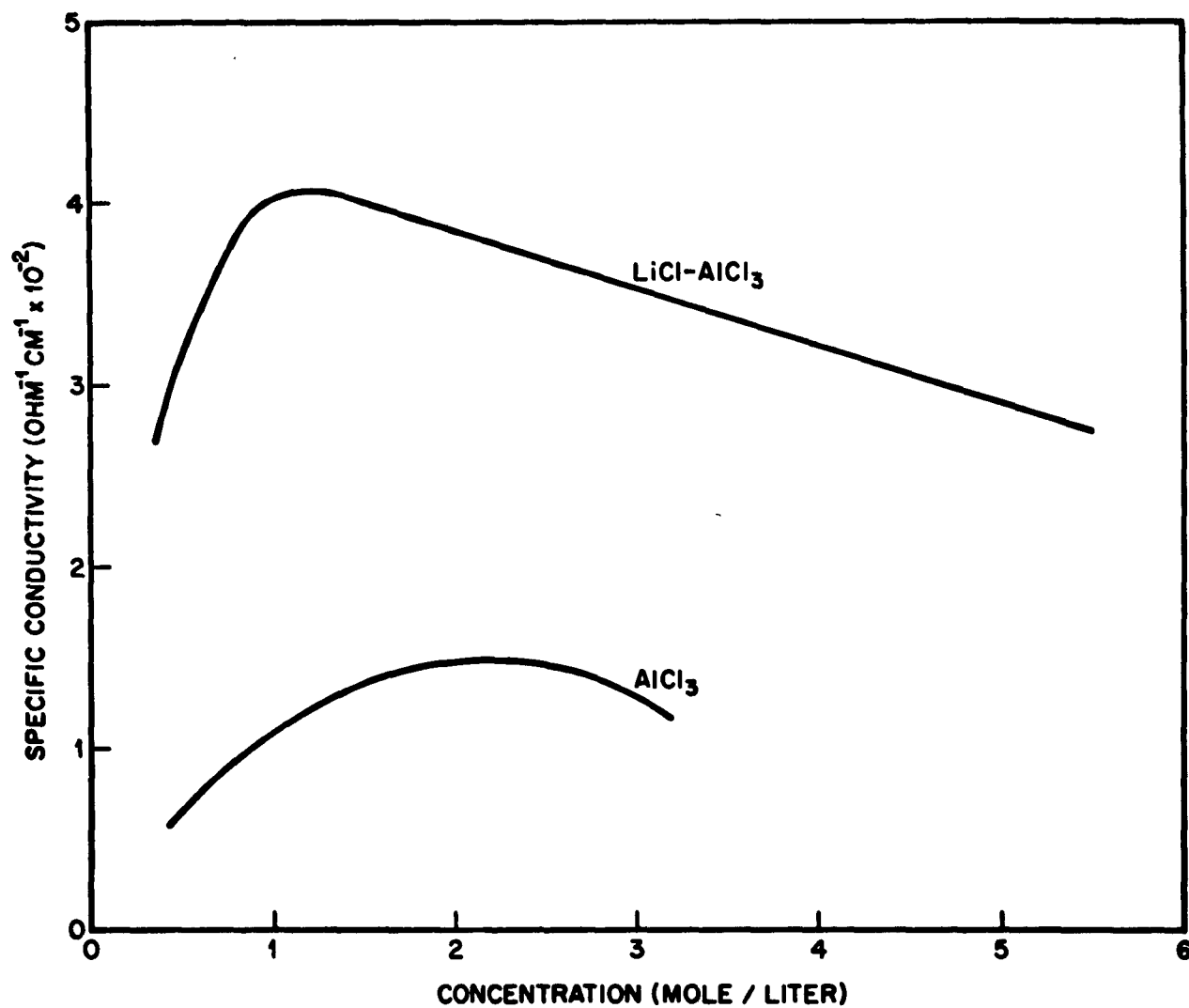


Fig. 1 Specific Conductivity of Nitromethane Solutions with AlCl_3 and LiCl

of AlCl_3 saturated with LiCl was also measured. The maximum value ($4.2 \times 10^{-2} \text{ ohm}^{-1} \text{ cm}^{-1}$) for the AlCl_3 - LiCl -NM system occurs at 1.5-M solute concentration. Thus, there is considerable improvement in the conductivity when LiCl is added to a AlCl_3 -NM solution.

Figure 2 shows the variation in the electrolyte conductivity of a 1.25-M aluminum chloride solution in nitromethane as a function of the amount of lithium chloride added. It is found that it varies in a nearly linear fashion, increasing as the lithium chloride concentration increases to a limit at a mole ratio of one to one of lithium to aluminum compounds.

A 0.75-M aluminum chloride solution was used to make up dilute solutions. Figure 3 shows the variation of the equivalent conductivity with the square root of the concentration. This resulting curve is similar to that obtained with propylene carbonate as the solvent. The master solution was then saturated with lithium chloride. In a similar fashion dilutions were made. Much higher equivalent conductivities were determined at concentrations above 0.388 M. At lower concentrations, a precipitate formed which was rich in lithium chloride. A plot of the equivalent conductivity change with concentration has not been made since the ratio of the concentration of aluminum chloride to lithium chloride is constantly changing. This work indicates that cells using nitromethane as the solvent may have complex equilibria occurring between aluminum chloride-lithium chloride and nitromethane, and solid compounds may form.

2.1.3 Temperature Dependence of the Conductivity

In order to predict the usefulness of the electrolyte at low temperature, it is necessary to determine the variation of the electrolyte conductivity as a function of temperature. The results of these measurements are presented in Figs. 4 and 5. The points in Fig. 5 marked with X's are values calculated from the conductivities of a 3.5-M electrolyte. At the lowest temperature, -55°C , there was a small amount of a brownish-green precipitate, indicating incomplete dissolution of the electrolyte at that low temperature. The activation energy for ion migration can be calculated by using the

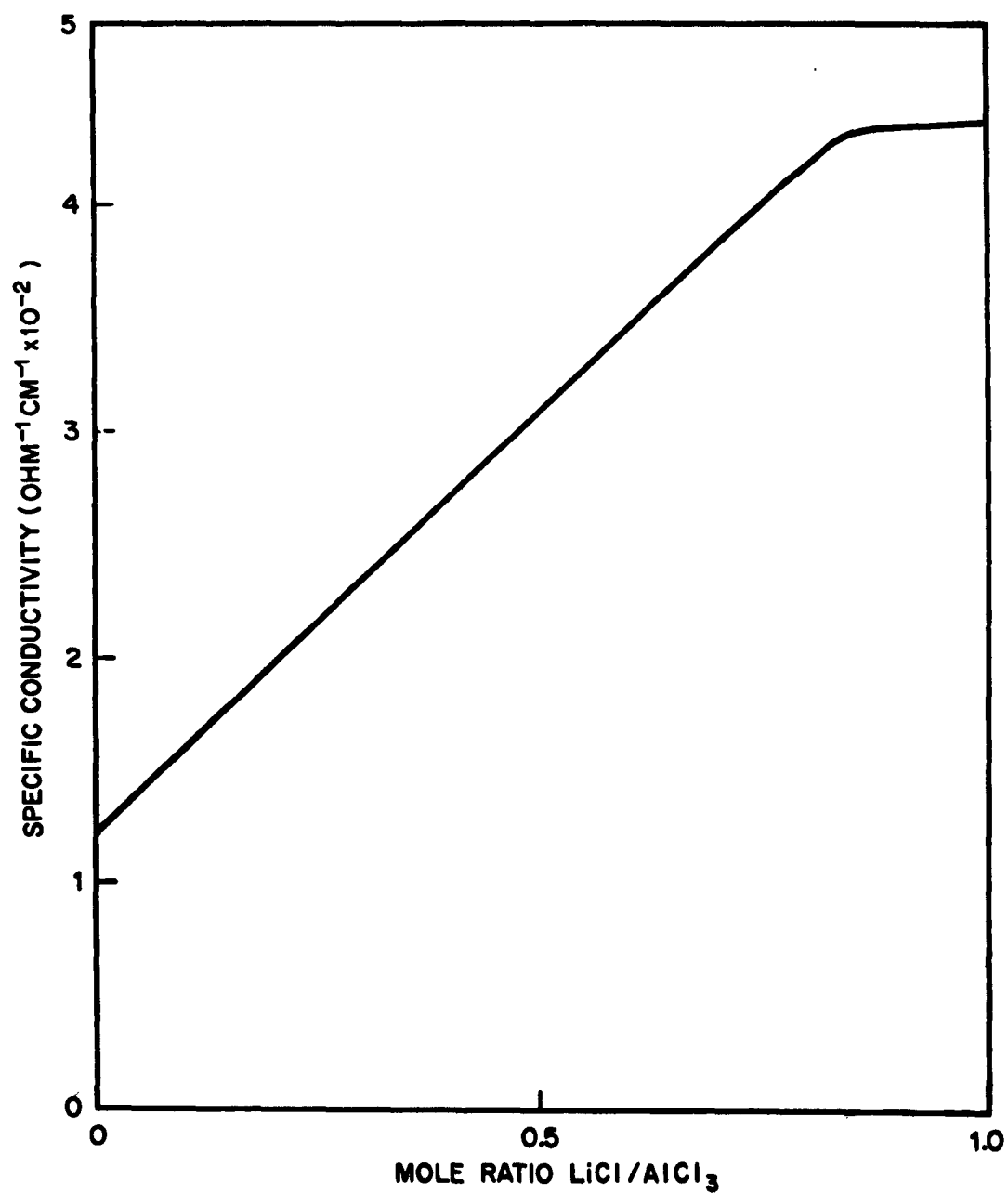


Fig. 2 Variation of Conductivity of Nitromethane-AlCl₃ Solutions with Addition of LiCl

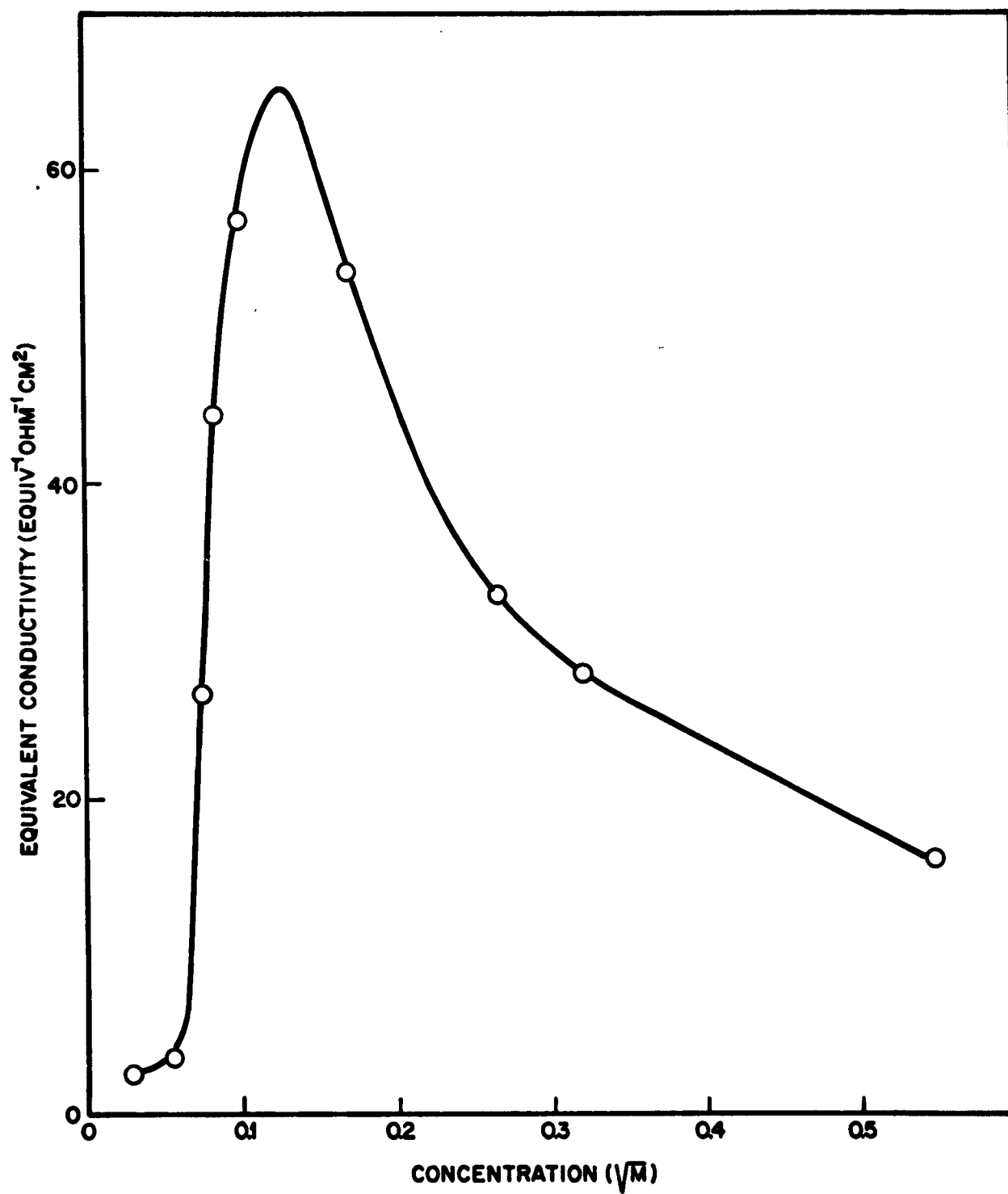


Fig. 3 Equivalent Conductivity of Dilute Nitromethane-AlCl₃ Solutions

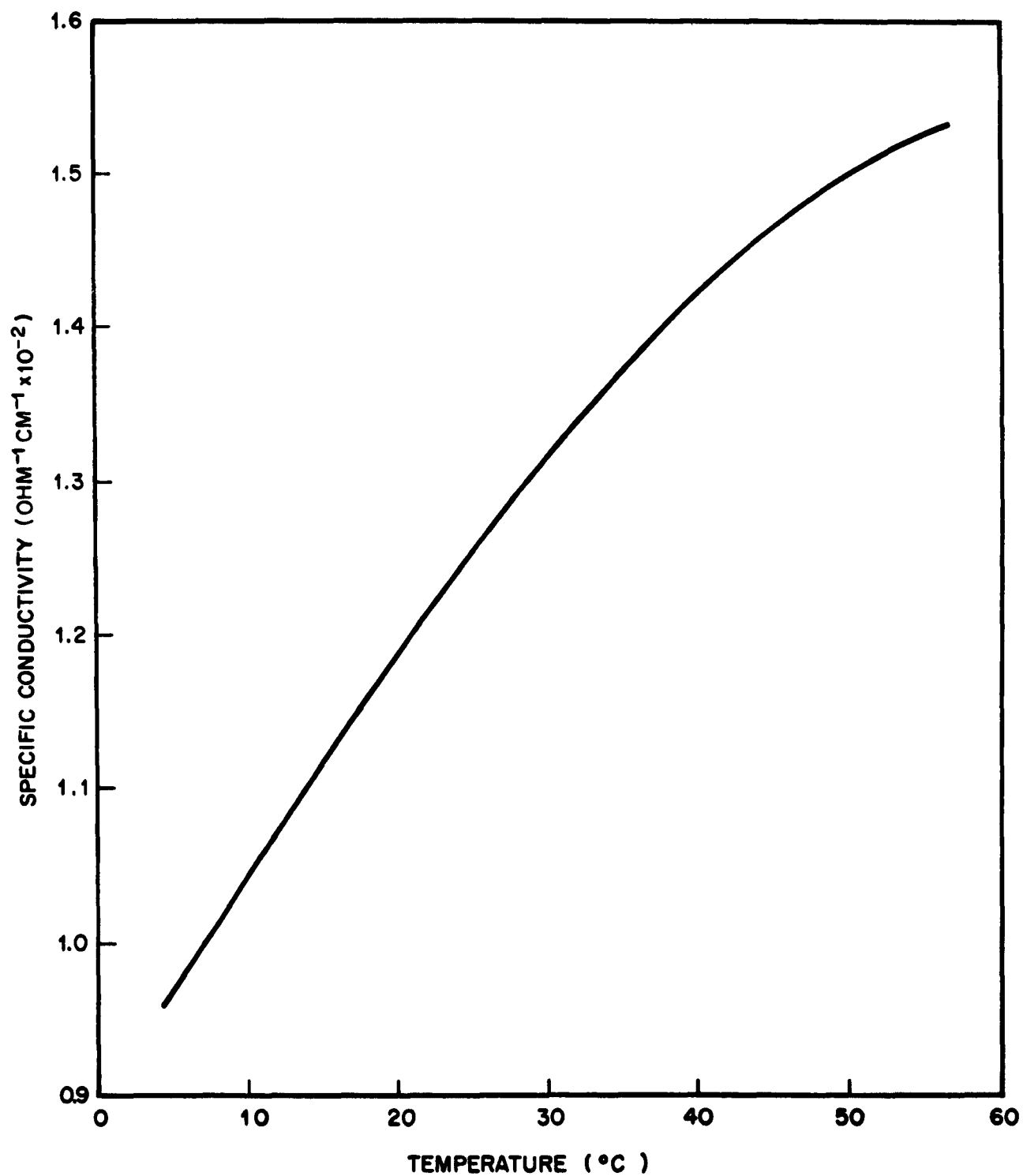


Fig. 4 Temperature Dependence of Specific Conductivity for 4-M AlCl_3 -Nitromethane Electrolyte

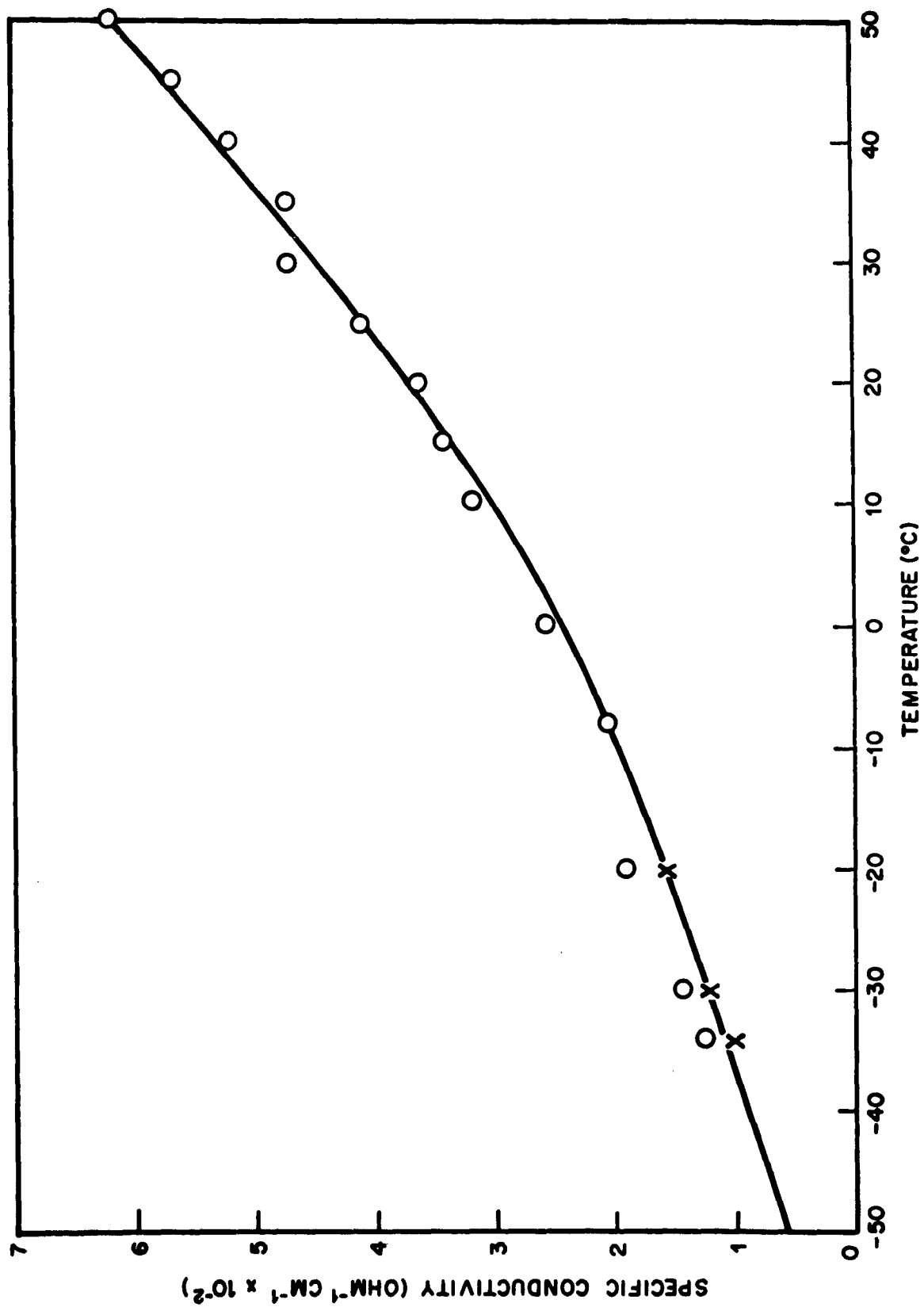


Fig. 5 Temperature Dependence of Specific Conductivity for 3-M LiCl-AlCl₃ Nitromethane Electrolyte

expression: conductance $A e^{-E/RT}$. The values obtained at $T = 298^\circ K$ are 1.94 kcal for a 4-M $AlCl_3$ solution and 3.28 kcal for a 3-M $AlCl_3$ solution which is saturated with LiCl.

Similar studies were performed with propylene carbonate. The value for the activation energy previously obtained for a 0.75-M $AlCl_3$ solution saturated with LiCl was 4.23 kcal. Figure 6 shows the temperature dependence of the conductivity, a similar solution without LiCl. A value of 4.41 kcal was obtained for the activation energy.

2.1.4 Freezing Points of Electrolyte

In order to assess the usefulness of an electrolyte for use at low temperatures, it is of value to know its freezing point. The experiments performed here indicated that the freezing points of the mixtures were not sharp. Propylene carbonate itself can easily be supercooled $25^\circ C$ below its freezing point. The freezing point is given as $-42^\circ C$. A value around $-60^\circ C$ was found for a crystal-liquid mixture. With nitromethane, a literature value of $-29^\circ C$ is reported. We found it to be $-32^\circ C$. The freezing point depression from the addition of LiCl- $AlCl_3$ to nitromethane is shown in Fig. 7. The values are given in terms of mole fraction at concentrations up to 3 M. No values were obtained for the propylene carbonate solutions since they did not freeze at dry-ice temperature ($-80^\circ C$).

2.1.5 Electrolyte Decomposition Potentials

Figure 8 shows the voltage-current density characteristics for oxidation and reduction by means of silver and platinum electrodes, in electrolytes consisting of propylene carbonate solvent with LiCl and/or $AlCl_3$ solutes. The dotted lines indicate the results with LiCl present. The oxidation of the electrolytes on platinum electrodes indicates a difference of chloride activity in the two solutions.

Figure 9 shows similar characteristics for similar electrolytes which use nitromethane as the solvent. The curves representing the reduction of the electrolyte indicate that

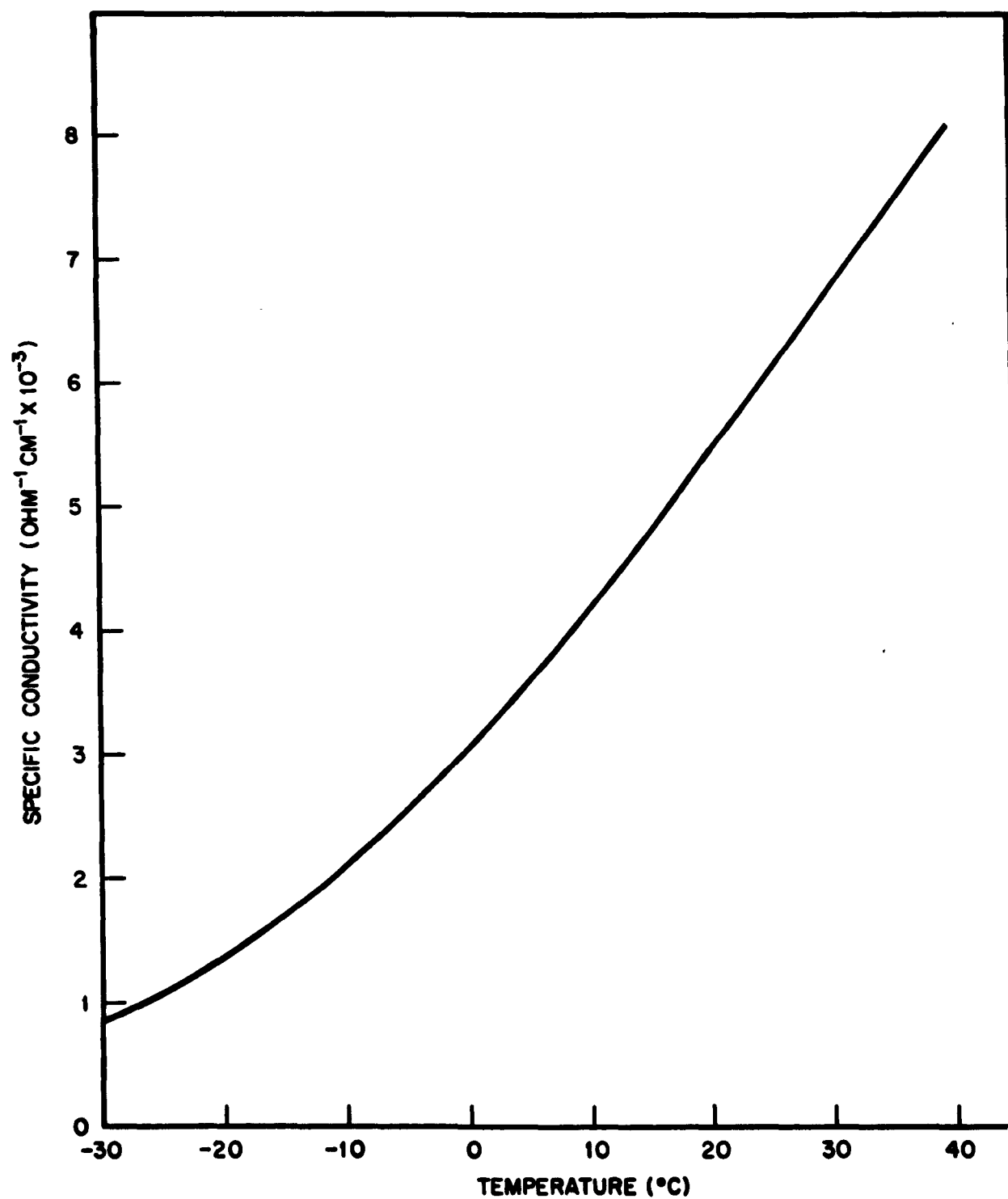


Fig. 6 Temperature Dependence of Specific Conductivity for 0.75-M AlCl_3 -Propylene Carbonate Solution

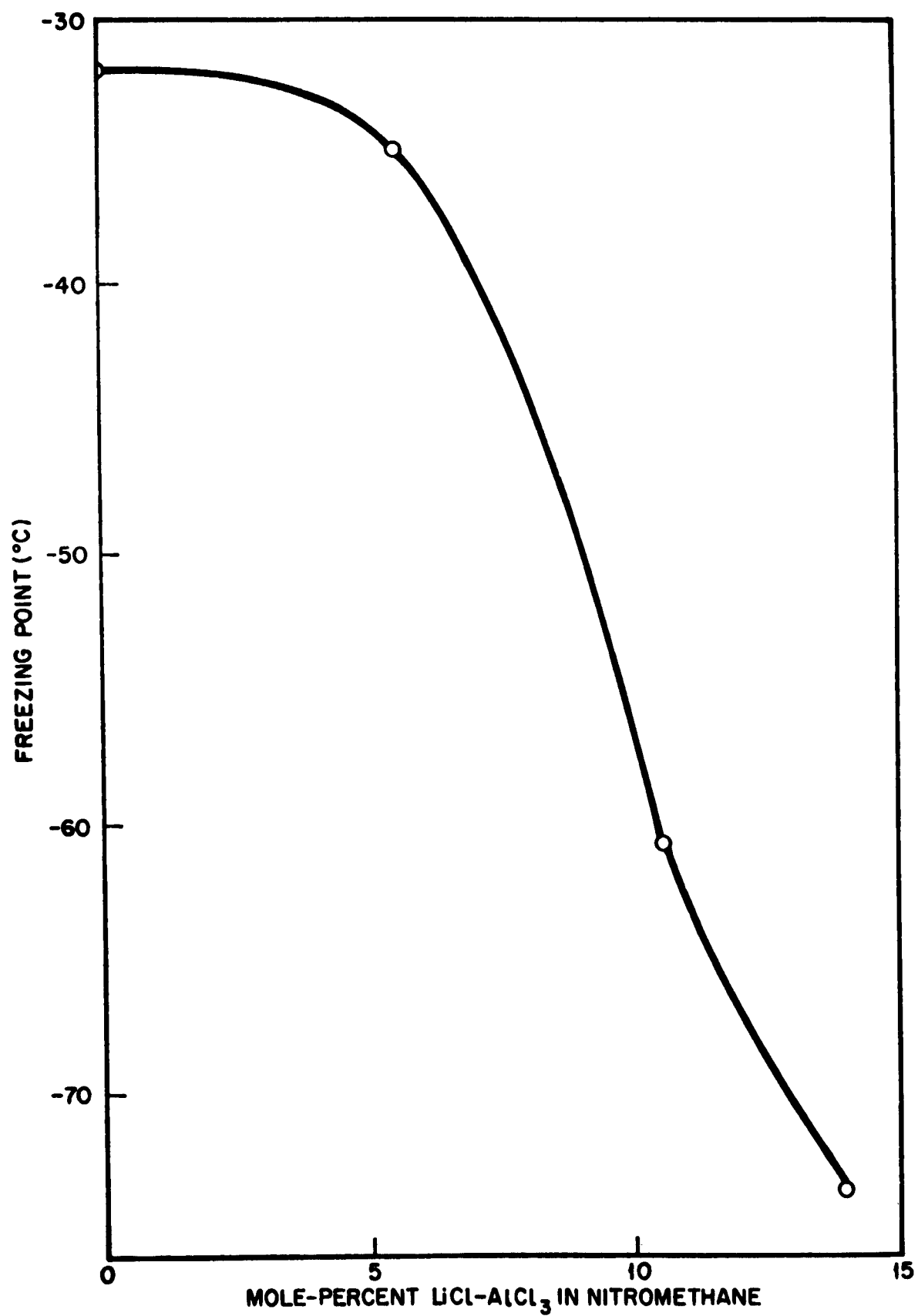
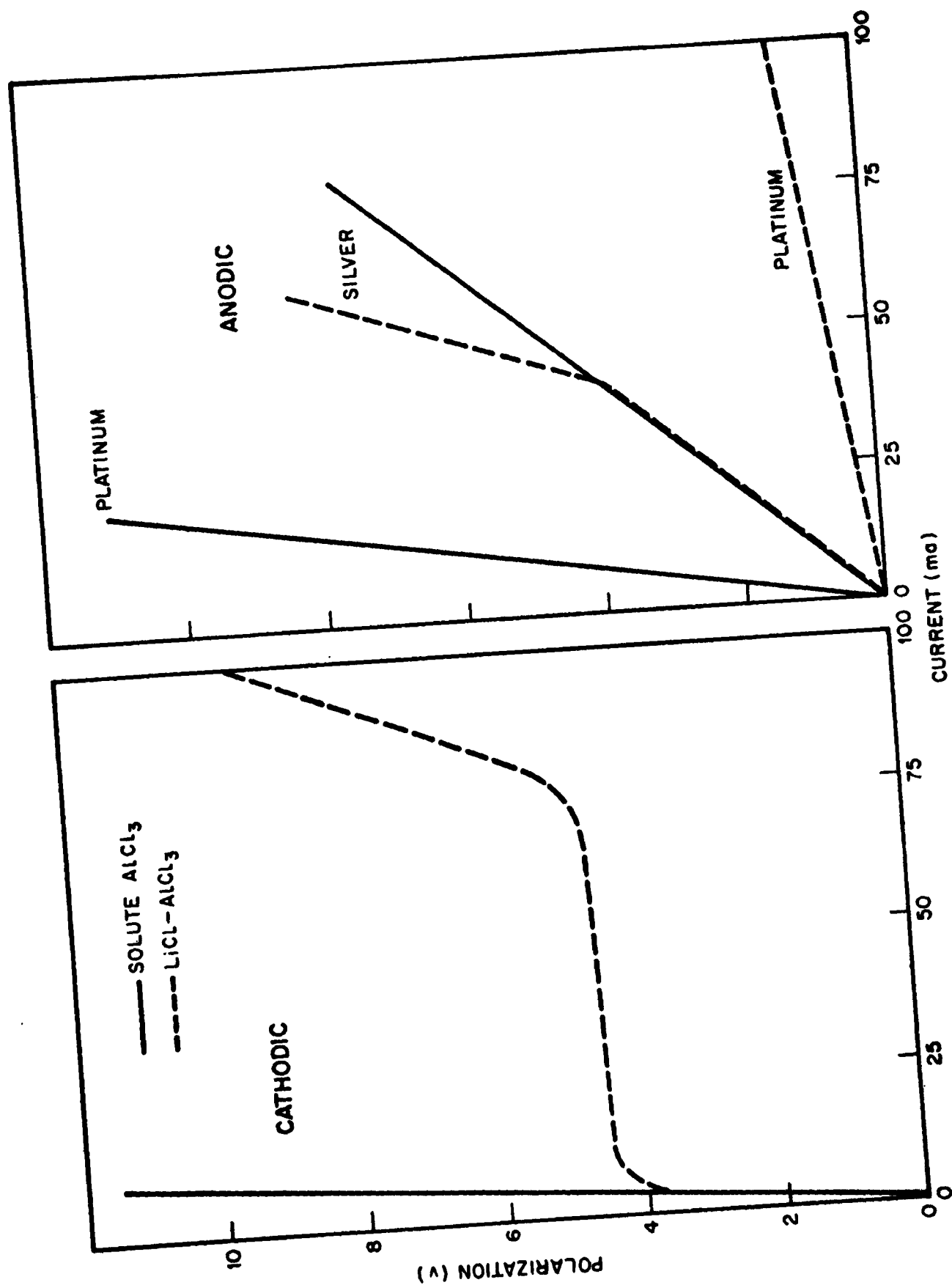


Fig. 7 Freezing Points of LiCl-AlCl₃ Complex in Nitromethane



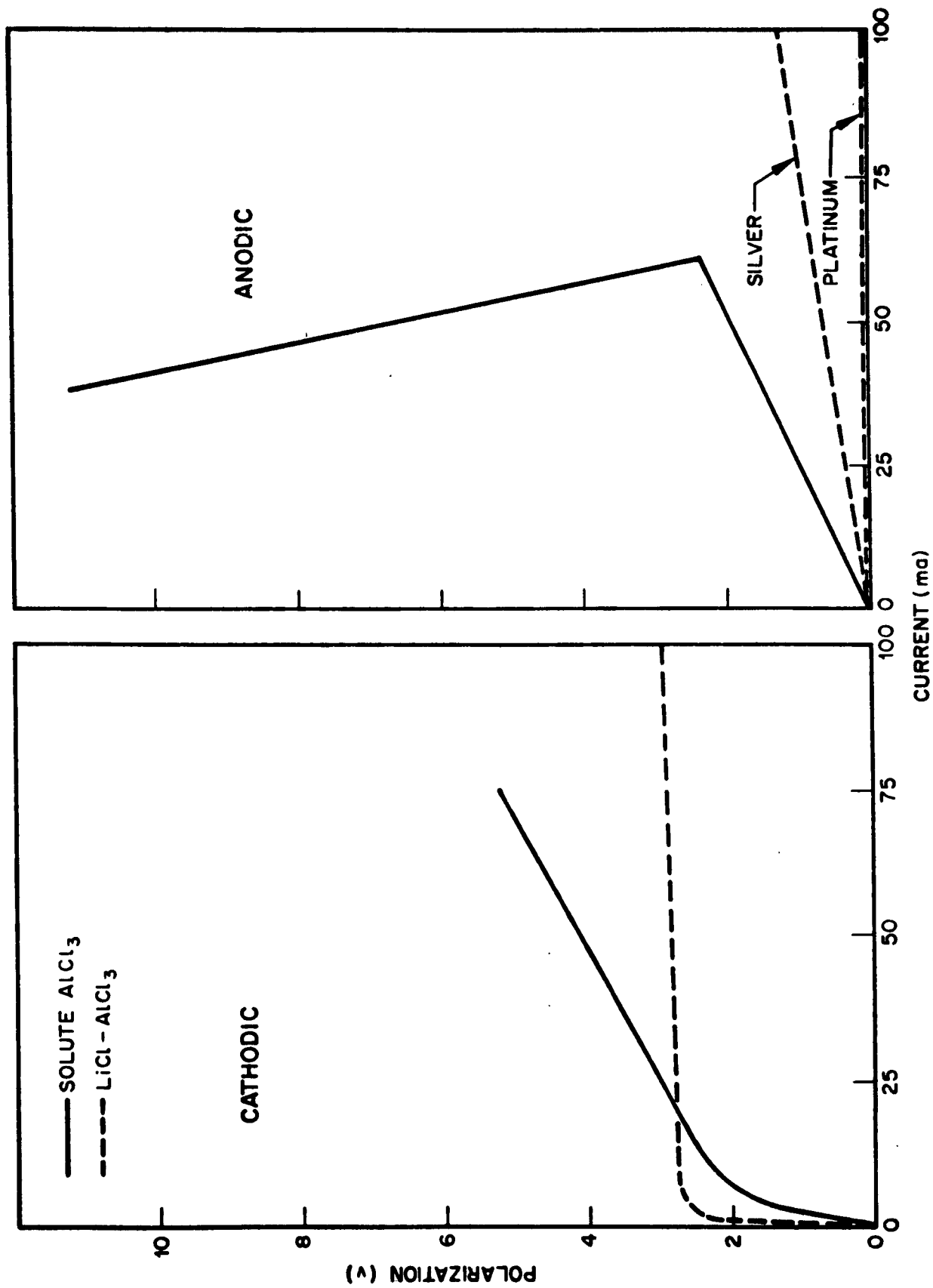


Fig. 9 Electrode Polarization in Nitromethane Solution

there is possible reduction of the AlCl_3 -nitromethane mixture at a potential lower than that for the production of lithium from similar solutions containing LiCl . It is also apparent that the addition of LiCl inhibits the reduction of the solvent. This is shown by the lower current at higher voltages (3 v and 7.5 ma). Previous work has shown that lithium metal is obtained with quite high efficiency under conditions of high aluminum chloride concentration.

2.2 SILVER ELECTRODE STUDIES

2.2.1 Anodic Oxidation of Silver

In the electrolyte system AlCl_3 , LiCl , propylene carbonate, the anodic oxidation of silver to silver chloride occurred at 100 percent efficiency for current densities up to 70 ma/cm^2 . Similar experiments with nitromethane as the solvent give similar results at current densities up to 35 ma/cm^2 .

The anodic reaction product was washed and weighed. The weight corresponded to that of silver chloride, within the experimental accuracy of 2 percent.

The anodic oxidation of silver was studied in both the propylene carbonate (PC) and nitromethane (NM) systems. The results are summarized in Table 1.

The use of LiClO_4 as the electrolyte solute resulted in a soluble silver oxidation product. Because of this fact, LiClO_4 alone cannot be used as the solute in a secondary battery electrolyte. Table 1 indicates that the addition of AlCl_3 results in the formation of insoluble AgCl . In the presence of sufficient AlCl_3 , the AgCl is formed as an adherent coating on the metal surface. The silver chloride formed in the propylene carbonate electrolytes is white, while that formed in nitromethane electrolyte is a dark grey or purple color.

Table 1
ANODIC OXIDATION OF SILVER IN SELECTED SYSTEMS

100 ml Solvent	Solution			Adhesion	Remarks
	LiClO ₄	AlCl ₃	LiCl		
Propylene Carbonate	8	0	0	----	Soluble AgClO ₄ Formation
	8	1	0	poor	AgCl deposit
	8	2	0	fair	in solution
	8	3	0	good	pale white color
	8	10	0	good	
	4	10	2.7	good	
	0	10	5.4	good	
Nitromethane	8	0	0	----	Soluble AgClO ₄ Formation
	0	3	0	good	Dark gray color
	8	3	0	good	Dark gray color

Note: In the following discussions of the optimization of the silver electrode, a propylene carbonate (100 ml) - AlCl₃ (10 g) - LiCl (sat.) electrolyte was used except where specifically noted.

2.2.2 Methods of Electrode Preparation

Many types of positive electrodes were tested in an effort to obtain electrodes with good operating characteristics. These characteristics are:

- High utilization of the incorporated silver chloride
- High electrode strength
- Low polarization
- High electronic conductivity
- High degree of uniformity
- Complete reversibility

In order to study the effect of surface, silver chloride was electroformed on the several electrodes prior to insertion into the cells. A current density of 17 ma/cm^2 was used with a propylene carbonate, aluminum chloride, lithium chloride electrolyte. Three surfaces were tested:

- Smooth silver sheet
- A silver plaque made by sintering silver oxide, water and polyvinyl alcohol onto expanded silver metal at 600°C
- A sintered silver plaque made by sintering $-150 + 200$ mesh silver powder onto a silver screen

These electrodes are quite different from one another in surface smoothness, the sintered silver powder being the most coarse.

Three electrodes were used in each cell – an anode, a cathode, and a reference electrode. The anodes were made by dipping silver-plated nickel into molten lithium. This lithium electrode was then enclosed in a glass fiber mat envelope. The cathodes made in the manner described above were also enclosed in similar envelopes. The reference electrodes were constructed from fine silver wire which was coated with fused silver chloride at the working end. This electrode was sheathed to near the tip with Teflon to prevent possible shorting. The cells were assembled so that the reference electrode was in the approximate center, between the anode and cathode. Spacers were used to provide tight packing of the type encountered in a normal operating cell.

The initial discharge showed lower polarization with coarser surfaces. After several cycles, only the sheet silver was polarized to a large extent. Figure 10 shows the comparative cathode polarizations for the second discharge.

The only practical method of introducing silver chloride is to combine it directly with the other electrode materials, since such methods as electroforming are difficult and additions of molten silver chloride are nonuniform. Sintered metal powders

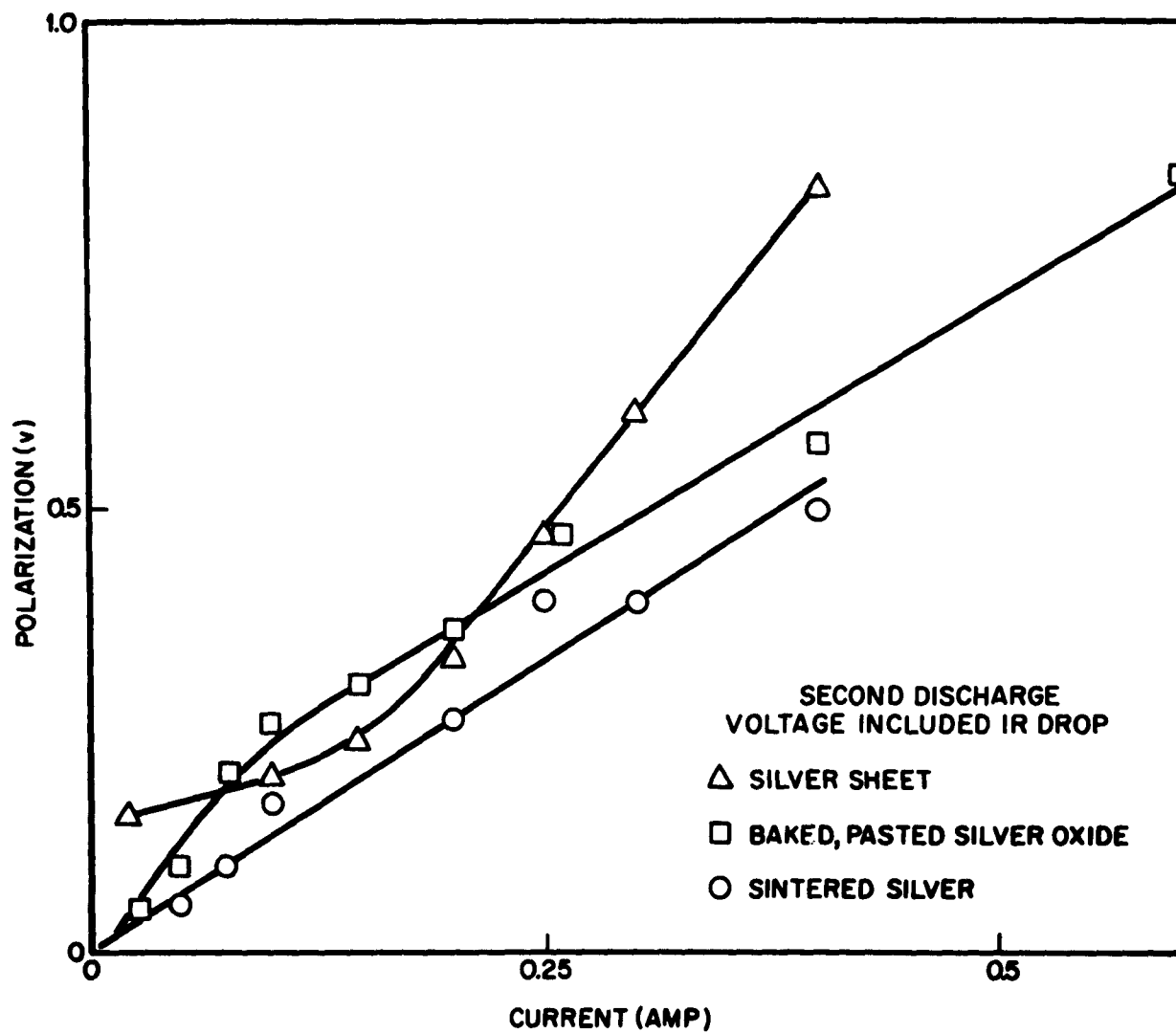


Fig. 10 Silver Discharge Polarization for Various Silver Surfaces

require high heats and more complex apparatus than pasted electrodes. Since both pasted and sintered electrodes have similar polarization characteristics after a few cycles, it was decided to use the former for future development.

Pasted electrodes were made which used commercial silver chloride or precipitated silver chloride. It was found that the commercial product resulted in electrodes with considerable nonuniformity. This could arise from the difference in drying treatment from batch to batch. The precipitated silver chloride electrode mixtures are made by adding sodium chloride to a stirred mixture of silver oxide, water, graphite, and silver nitrate and washing the precipitated and solid material.

2.2.3 Additives to Electrode Mix

Several types of additives were tried in an effort to produce high capacity-to-weight ratios. The following materials were used as electrode additives:

- Colloidal graphite
- Acetylene black
- Flake graphite
- Nickel powder
- Various forms of silver particles

The first two of these additives result in exfoliation of the electrode during the baking process due to oxidation by Ag_2O . The use of nickel powder appeared to offer no advantage and entailed the disadvantage of formation of oxides, which are eliminated only with great difficulty.

These studies indicate that the electrodes should be made of a mixture of silver oxide, precipitated silver chloride, graphite, and possibly a silver powder. This mixture pasted on a grid and baked at 400°C will allow a high degree of electrode uniformity to be achieved. The silver from the silver oxide reduction and the graphite form electrodes with high electronic conductivity. The form of the electrode surface is sufficiently good for electrochemical reversibility -- with porosity approaching 70 percent -- and for low polarization in the cell operating current density range. The exact

formulation depends upon the utilization efficiency for silver chloride and the strength desired for the electrode.

2.2.4 Silver Powder Size

It was thought that the addition of metallic silver with large particle size compared to the AgO powder might produce a more open structure, which would allow greater utilization of silver chloride in thick electrodes. The mix used was 25 parts silver chloride, 25 parts silver oxide, and 50 parts silver metal, all by weight. Three types of metal were used: precipitated powder - 150, 200, spherical silver, and flake silver. Figure 11 represents the data obtained as compared to electrodes of the following composition: 30 parts silver chloride, 60 parts silver oxide, 10 parts graphite, 30 parts silver chloride and 60 parts silver oxide. Figure 11 shows that the addition of graphite is preferable. Apparently the particulate silver blocks the efficient use of the silver chloride.

2.2.5 Graphite Effects

Graphite may be useful for reducing the weight of the cathode, providing a larger surface area, and allowing better penetration by the electrolyte. Figure 12 shows the silver electrode polarization in the absence of graphite. Graphite was added to the extent of 19 percent by volume with practically no effect on the polarization characteristics below 25 ma/cm^2 . Indeed, after 14 cycles, the cathode polarization was the same as for the third cycle discharge with no graphite present. The third discharge has been found, by previous experience, to be that with the lowest polarization. Figure 13 compares the 13th and 14th discharges for a cathode containing 3.85 wt-percent graphite (about 9.5 vol. -percent) with the 3rd discharge for a duplicate cell. It should be noted that the 13th discharge was a complete discharge at 2 ma/cm^2 (until that level of discharge could not be held). An examination of the 14th discharge shows the cathode polarization to be lower than that of the previous cycle. This would seem to indicate that there had been a build up of nonconducting silver chloride on the cathode. The silver chloride was reduced by the complete discharge.

Since graphite reduces the electrode weight-to-capacity ratio, it is important to determine the maximum amount of graphite that can be used. Electrodes were prepared that contained from 11 percent to 38 percent graphite (by volume) of the

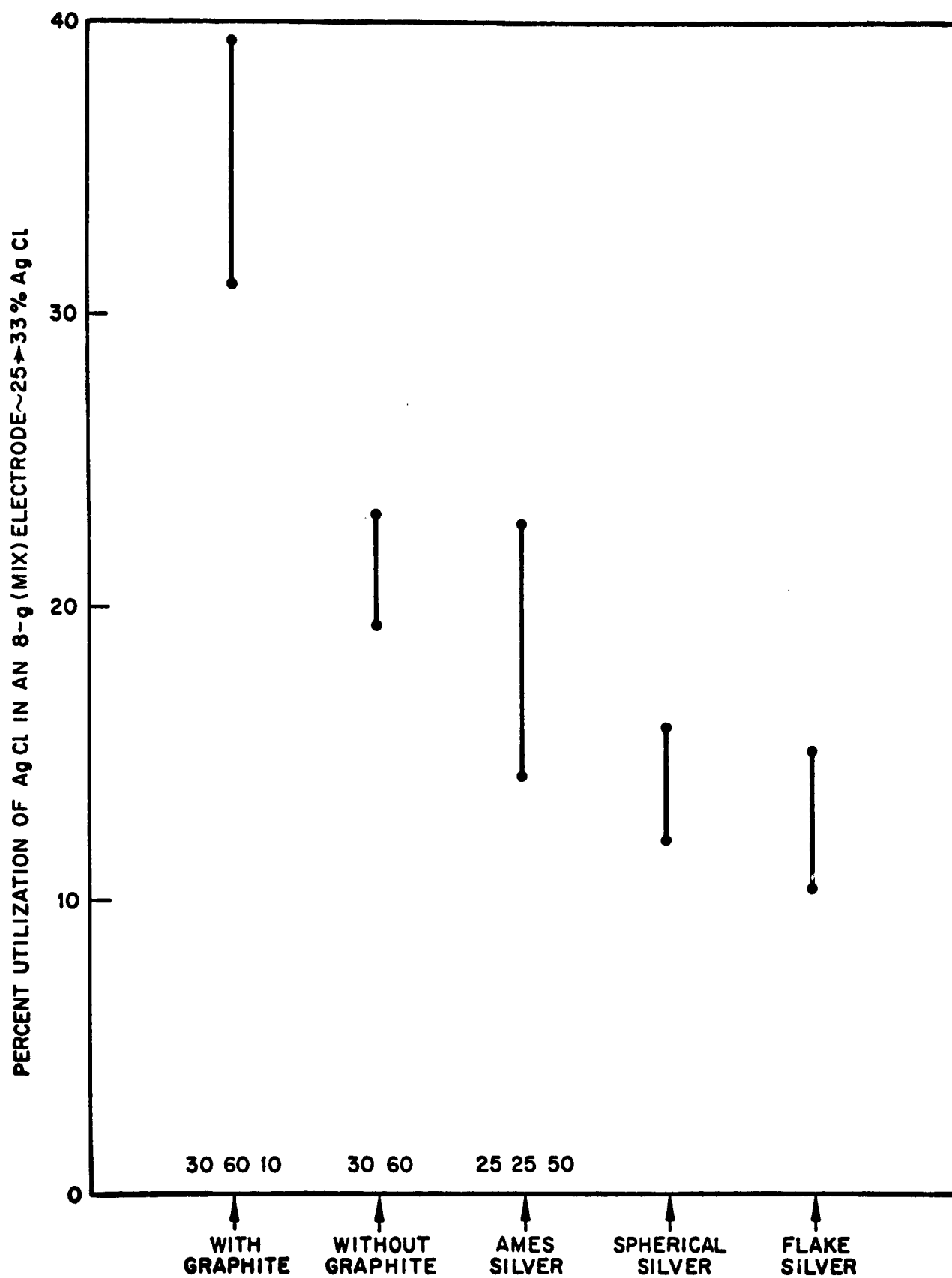


Fig. 11 Utilization of AgCl in Various Electrodes

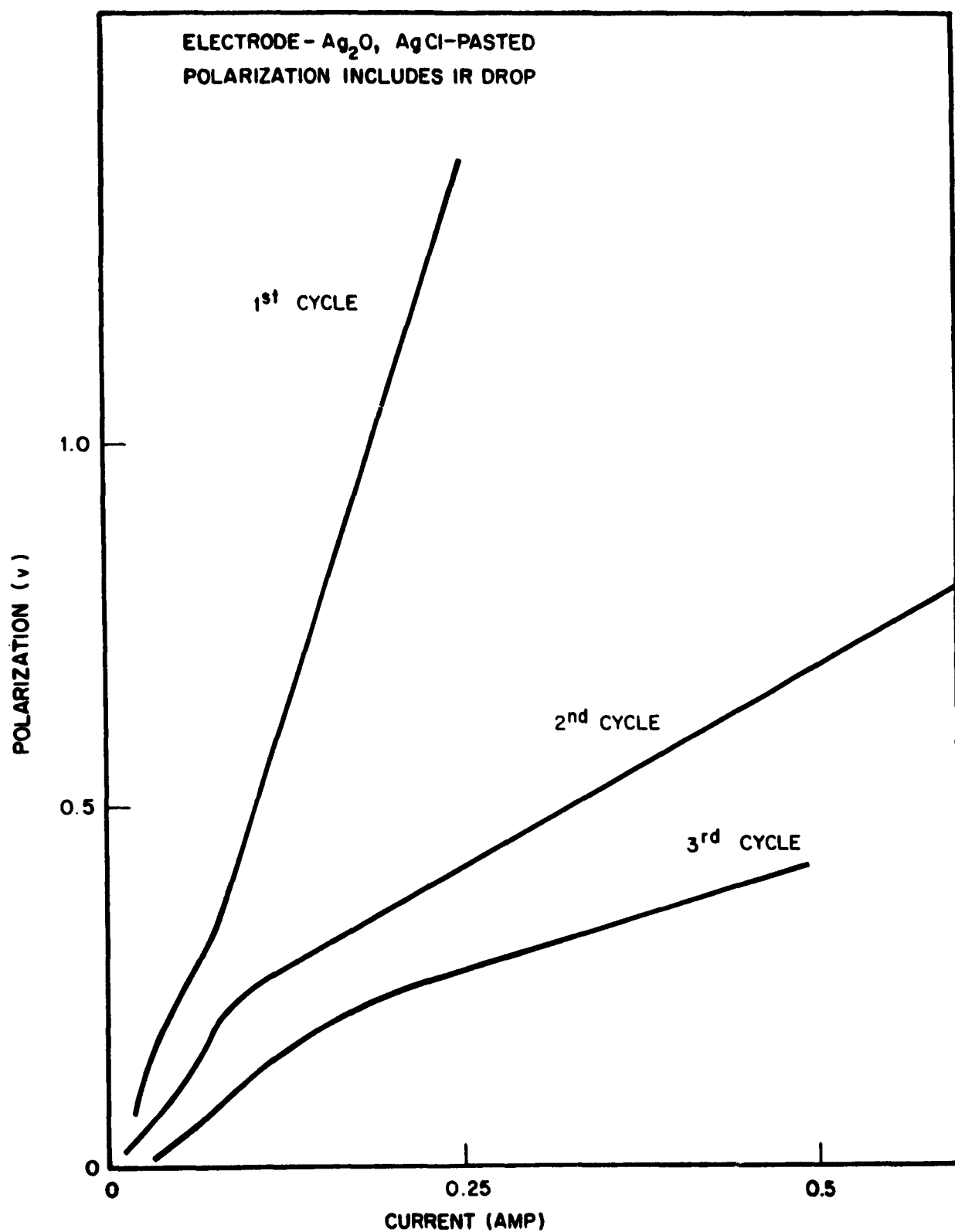


Fig. 12 Silver Discharge Polarization for Various Discharge Cycles

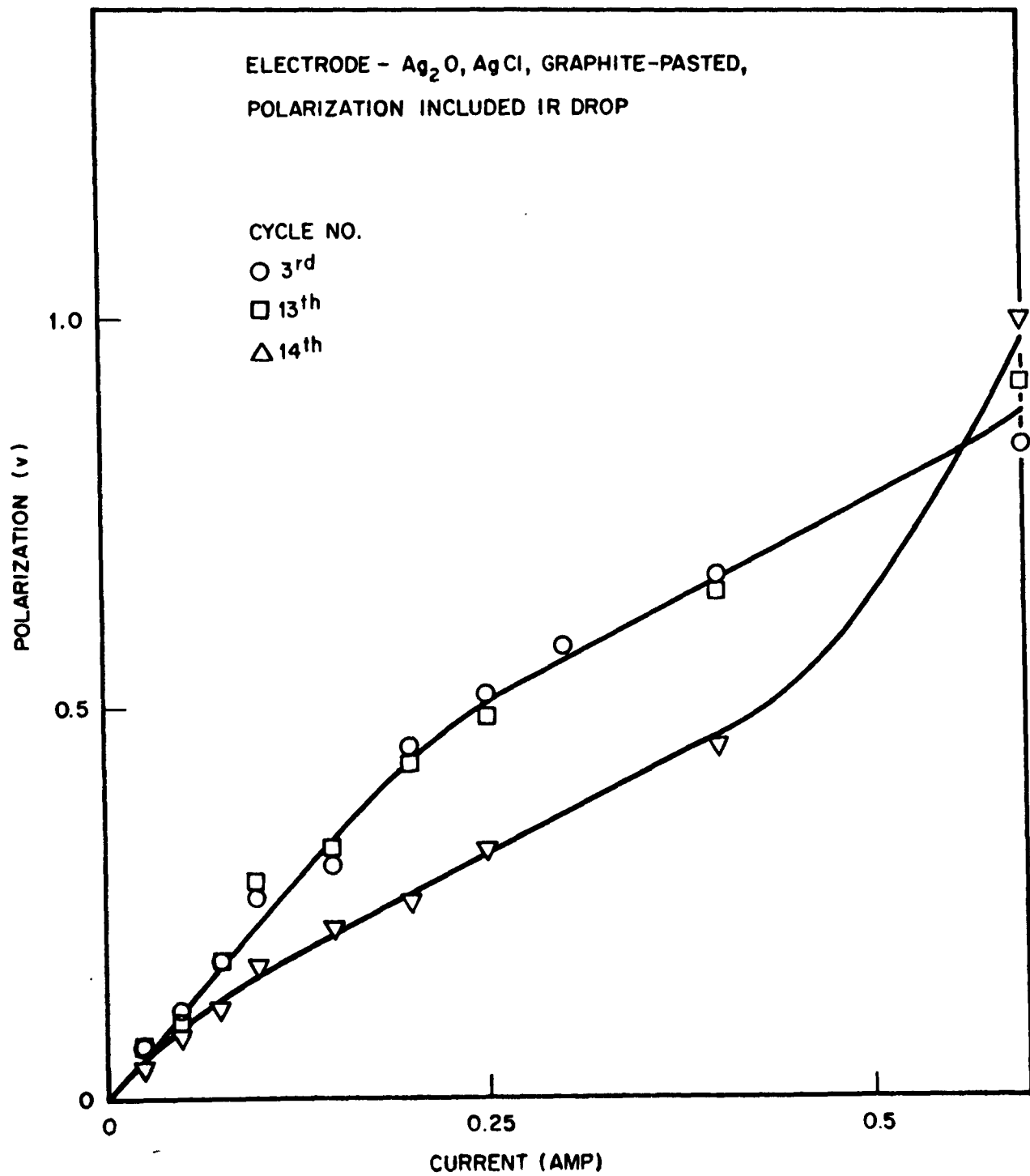


Fig. 13 Silver Polarization for Later Discharge Cycles

raw materials. These electrodes were thin (0.12 g/cm^2). The ratio of silver chloride to silver was held constant, so that as the percent of graphite was increased, the percent of silver chloride decreased.

The first discharges indicated that the availability of the silver chloride was approximately the same in all cases. The extent of discharge, compared to that calculated, indicated yields of 40 percent for a 20 percent voltage drop to about 75 percent for an end voltage less than 0.5 v. Polarization measurements showed no differences in the cathode for the third discharge cycle. Another type of experiment was carried out to determine how well these cells would perform under typical conditions. They were charged at 5 ma/cm^2 for 35 min. with the voltage limited to 4.5 v and discharged at 5 ma/cm^2 until the voltage dropped 30 percent (15 percent voltage regulation). Three cycles were run at two of the graphite concentrations with no appreciable differences. The resulting current efficiencies were found to range between 70 and 80 percent. Thus the characteristic limiting the amount of graphite that can be used is the structural strength of the electrode.

2.2.6 Silver Chloride Concentration

Another method for reducing the weight-to-capacity ratio is to increase the percentage of silver chloride in the electrode mix. To do this, cathodes were fabricated with a constant ratio of graphite to silver and a varying concentration of silver chloride. (The silver chloride content ranged from 18.6 percent to 31.3 percent by weight of the electrode mix.)

Previous studies indicated that with higher silver chloride concentrations, current efficiency decreased. In the present studies, then electrodes were used (0.12 g/cm^2). With these electrodes, no apparent relationship was found between silver chloride concentration and percent utilization. The average utilization was 42.5 percent, with 20 percent voltage variation and 65.1 percent utilization for an end voltage of less than 0.5 v. Polarization experiments were conducted with these cells. Figure 14 shows experimental results for two cells of very different silver chloride concentrations, second cycle. Note that cell polarization can be explained in terms of cell resistance (IR drop) up to a current density of nearly 30 ma/cm^2 .

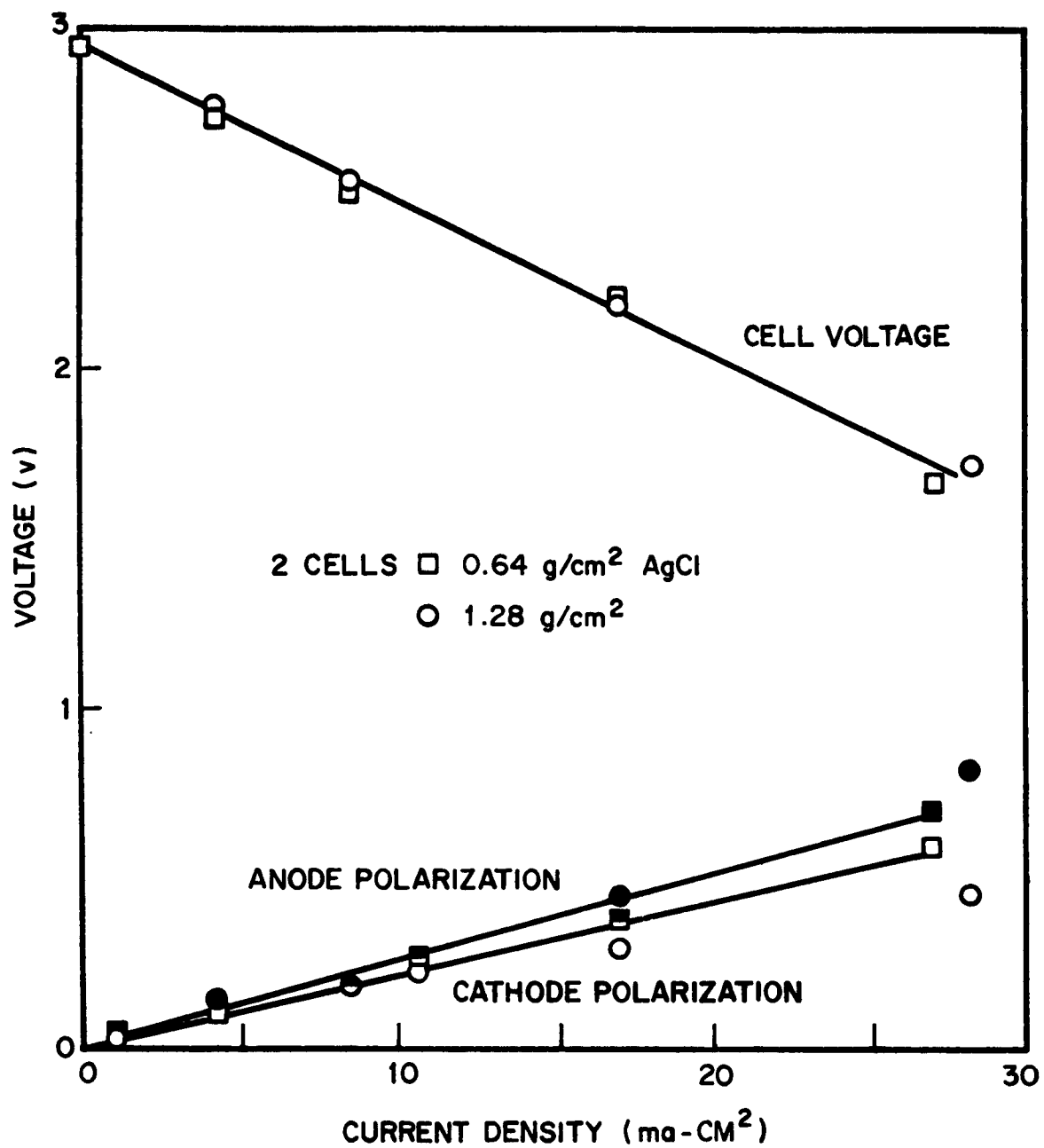


Fig. 14 Discharge Characteristics for a Lithium-Silver Chloride Cell

2.2.7 Electrode Thickness

To determine the maximum amount of active material that can be used, it is necessary to study the effect of electrode thickness upon utilization of silver chloride in the positive electrode. The mixes used were 30 parts silver chloride, 60 parts silver oxide, 10 parts graphite, and 30 parts silver chloride, 60 parts silver oxide. It had been found that with thin electrodes, both of these mixes gave good utilization and that with somewhat thicker electrodes, the graphite improved the characteristics. Figure 15 is a plot of the amount of silver chloride consumed as a function of the amount present in the electrodes themselves. The dotted line indicates 50 percent utilization, or 100 percent if both sides of the cathode were to be used. The lower ends of the vertical lines indicate the utilization for a 20-percent drop in voltage; the upper end indicates utilization for an end voltage below 0.5 v. Note that addition of graphite results in greater utilization of silver chloride. The technique used on each electrode is important; that is, graphite opens the structure, and proper pasting technique will give a less dense cathode. Figure 15 indicates that the cathode should contain between $1/4$ and $1/2$ gm/in² of silver chloride for 100 percent utilization of available active material.

2.2.8 Present Silver Electrode

As previously mentioned, the optimization studies were carried out using a propylene carbonate electrolyte. A few studies were made to learn the effects of using other electrolytes. The results showed that both polarizations and utilizations varied from one electrolyte to another. However, the trends were in the same direction, so that information gathered from one system can be directly applied to another.

The following electrode mix results in a strong electrode with good characteristics:

- 50 percent precipitated AgCl
- 10 percent graphite
- 40 percent Ag₂O

Wet with 2 percent polyvinyl alcohol and water solution, this material is pasted on silver expanded metal and sintered in air at 400° C.

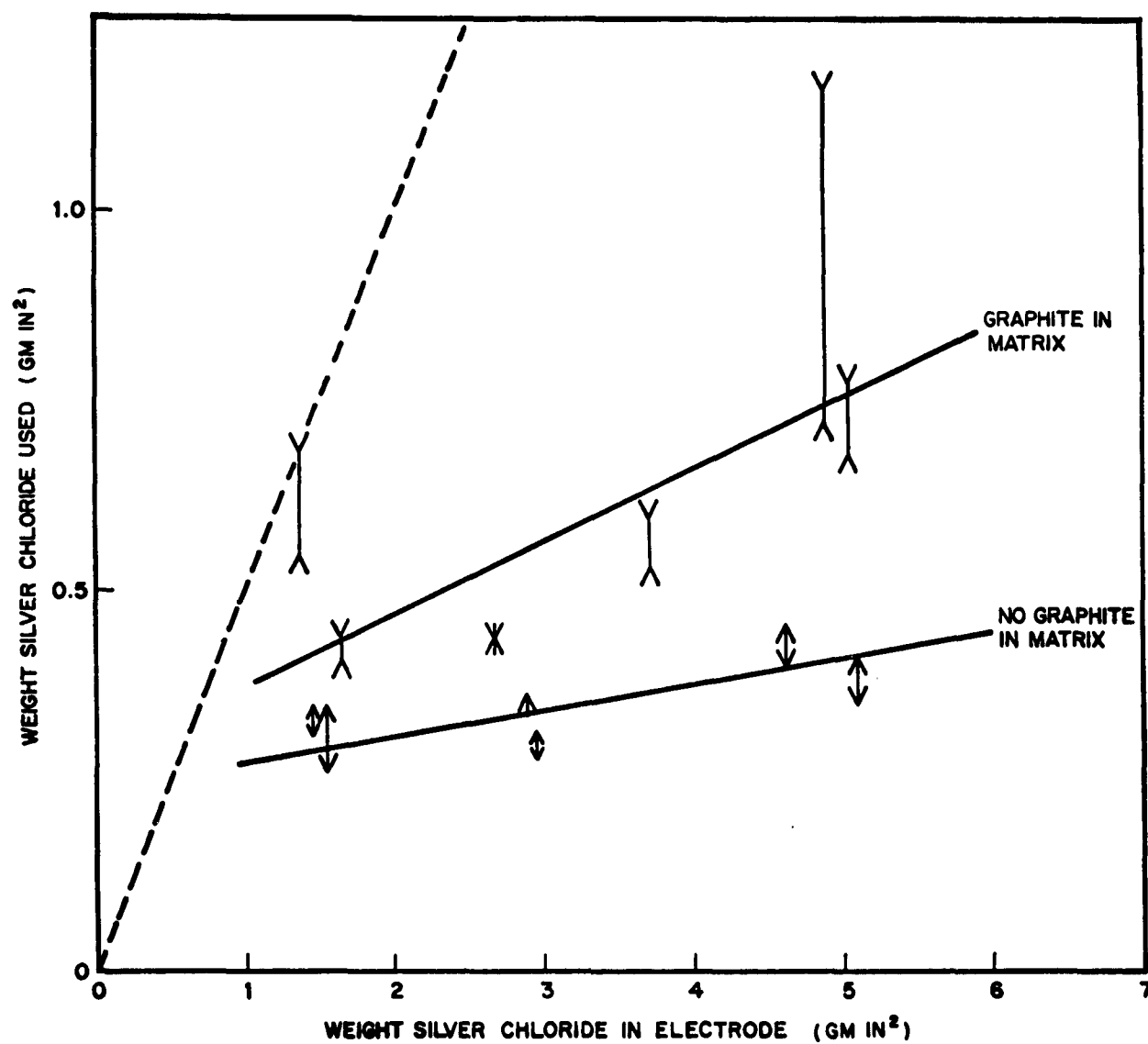


Fig. 15 Silver Chloride Concentration Effect on Utilization

The thickness of the electrode is determined by the maximum current density (maximum allowable polarization) and the length of discharge time. Electrode thickness of 0.030 has been obtained with 1 gm/in² of electrode mix weight. The structure has 70 percent porosity as evaluated by the ratio of the apparent density and the true density.

2.3 LITHIUM ELECTRODE STUDIES

Irreversibility of cycled cells and increase in anode polarization after long periods of charge - discharge cycling indicate need for a study of processes occurring at the lithium anode and, in particular, the lithium electrodeposition process.

2.3.1 Electrode Preparation

Lithium electrodes were initially produced by dipping silver plated nickel screen into a molten lithium pot. The present lithium electrode is constructed using lithium sheets. A lithium rod is rolled in an argon-atmosphere glove box to a 10- to 20-mil thick ribbon, 2-in. wide, using a hand-operated rolling mill with 3.5-in. diameter steel rolls which are 4-in. wide. A nickel, expanded-metal sheet is sandwiched between two pieces of the lithium ribbon, and the composite is again rolled. The lithium-nickel expanded metal assembly shows good strength. The lithium sheets are bonded together through the screen by the rolling pressure.

2.3.2 Lithium Electrodeposition

The electrodeposition of metallic lithium was studied with an electrolyte contained in a three-necked pyrex flask with ground glass fittings. The electrodes were introduced through two of the standard taper joints, and argon gas was led through the third fitting. The deposition of lithium was studied on various metal matrices. The current efficiency was found to be 100 ± 10 percent. The amount of lithium formed was measured by determining the amount of hydrogen formed on reaction of lithium with water. Deposition of lithium on silver and platinum resulted in formation of a black coating not easily removed with water, indicating alloying of the metal with lithium. Deposition of lithium on nickel and stainless steel did not produce the black coating. In general, the lithium deposits produced from nitromethane solutions

were light grey in color and dendritic in form. They were dark grey and amorphous in form from propylene carbonate solutions.

2.3.3 Deposition From Various Solvents

The electrodeposition of lithium was attempted from several solvents. Each solvent contained 100 gm/liter AlCl_3 and was saturated with LiCl . The results of this study are summarized in Table 2.

Table 2

LITHIUM-ELECTROLYTE DEPOSITION STUDY


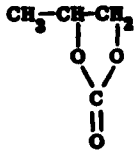

Solvent	Specific Conductivity $\times 10^{-3} \text{ ohm}^{-1} \text{ cm}^{-1}$	Remarks
Acetonitrile CH_3CN	8.87	polymerizes in presence of lithium
Nitromethane CH_3NO_2	26.20	grey lithium deposit plus gassing
Diethyl Carbonate $(\text{C}_2\text{H}_5)_2\text{CO}_3$	3.86	grey lithium deposit plus gassing
Dimethyl Carbonate $(\text{CH}_3)_2\text{CO}_3$	6.47	grey lithium deposit plus gassing
Dimethyl Sulfate $(\text{CH}_3)_2\text{SO}_4$	6.0	jells with AlCl_3
Diethyl Sulfate $(\text{C}_2\text{H}_5)_2\text{SO}_4$	—	jells with AlCl_3
N-Methyl-2-Pyrrolidone $\text{CH}_3\text{N}-\text{CH}_2-\text{CH}_2-\text{CH}_2-\text{CO}$	4.0	solvent decomposition no lithium deposition

An attempt was made to electrodeposit lithium from a propylene carbonate- PCl_5 - LiCl solution with a specific conductivity of $4.1 \times 10^{-3} \text{ ohm}^{-1} \text{ cm}^{-1}$. A small amount of grey lithium was obtained with a bright orange product, but this lithium was reactive in the solution. No heat of solution was noted when PCl_5 was dissolved in propylene carbonate, and the PCl_5 can possibly be reduced to PCl_3 or further to phosphorous. A high heat of solution for AlCl_3 in propylene carbonate was found and the AlCl_3 is in a complexed form in which it is not reduced by lithium.

2.3.4 Deposition from Mixed Solvents

The deposition of lithium metal on silver cathodes from selected nonaqueous solutions was studied in order to ascertain current efficiency for deposition and the form and adherence of the lithium particles obtained. With the standard propylene carbonate electrolyte, the electromechanical reversibility of the lithium deposition reaction has been shown to be very good, but the adherence of the metal particles has been poor. Loose metal particles not electrically in contact with an anode structure cannot be used in the cell reaction because utilization of the particles during discharge will be poor and electromechanical efficiency will be low. Thus, a study was made of the effect of change in solvent composition on the adherence of the lithium. The physical properties and chemical structure of several solvents are listed in Table 3.

Table 3
SOLVENT PROPERTIES (AT 25°C)

Solvent	Freezing Point (°C)	Boiling Point (°C)	Dielectric Constant	Viscosity cp	Density	Formula
Ethylene Carbonate	36	248	89 (at 40°)	1.9 (at 40°)	1.32 (at 40°)	
Propylene Carbonate	-49	242	64	2.5	1.19	
Butyrolactone	-43	204	39	1.7	1.12	
Nitromethane	-29	101	36	0.6	1.13	CH ₃ NO ₂
Water	0	100	78	1.0	0.99	HOH

The solvents listed have long liquid ranges and high dielectric constants, as indicated in comparison with water. Solutions were made with propylene carbonate and other organic solvents in a 50 vol.-% ratio and 10 gm AlCl_3 with 3 gm LiCl added per 100 ml of solution. Lithium deposition was studied in solution under argon gas with 1/4-in. diameter lithium rod anodes. The amount of lithium produced was determined by reaction of lithium with water and measurement of the hydrogen gas produced. Since some of the cyclic carbonate solvents decompose and produce CO_2 , a 6-M NaOH solution was used for hydrogen production with adsorption of any CO_2 produced. The current efficiency for lithium production, the nature of the deposit, and the solution conductivity are listed for mixed solvents in Table 4. Addition of water to propylene carbonate decreases the current efficiency for lithium production, but the other solutions have high efficiency. The most adherent deposit of lithium was obtained with the PC-nitromethane mixture that also had the highest electrical conductivity.

Table 4

LITHIUM DEPOSITION FROM MIXED SOLVENTS

Solution*	Volume (Percent)	Current Efficiency** (percent)	Lithium Deposit	Solution Conductivity ($\text{ohm}^{-1}\text{cm}^{-1} \times 10^{-3}$)
PC + Ethylene Carbonate	50	100	Dark grey, poor adherence	6.2
PC + Nitromethane	50	100	Light grey, den- dritic, good adherence	13.3
PC + Butyrolactone	50	100	Grey, poor adherence	7.2
PC + Water	1	65	Grey-white, fair adherence	—
Propylene Carbonate	100	100	Dark grey, poor adherence	6.7

*Solvent (100 cc) 10 gm AlCl_3 , 3 gm LiCl

**Current density 13 ma/cm²

2.3.5 Nitromethane Solution Deposition

Lithium deposition was also studied in nitromethane solutions with AlCl_3 and LiCl . As shown in Table 5, the production of lithium from these solutions was not efficient at lower AlCl_3 - LiCl concentrations. By increasing the AlCl_3 - LiCl concentration, the current efficiency for lithium production is increased, and the metallic character of the lithium deposit is substantially improved on addition of 10 vol.-percent water to the NM-AlCl_3 - LiCl solution; the production of lithium was reduced to 60 percent efficiency.

Table 5

LITHIUM DEPOSITION FROM NITROMETHANE SOLUTION

AlCl_3 - LiCl Concentration (gm/100 ml)	Current* Efficiency (Percent)	Remarks
10-3	80-80	Light grey, dendritic-growth adherent deposit
20-6	80-100	Adherent deposit
40-15	70-93	Adherent deposit
40-15	90-100	Vacuum treated, then run under fresh argon gas

*Current Density ma/cm^2 13-32

2.3.6 Deposition of Other Metals

A propylene carbonate solution containing 20 gm/liter AlCl_3 was saturated with either KCl or NaCl . These solutions were electrolyzed by means of smooth silver cathodes and massive lithium anodes, with the results given in Table 6.

Table 6
METAL DEPOSITION

Metal	Specific Conductance ($\times 10^{-3}$ ohm $^{-1}$ cm $^{-1}$)	Percent Efficiency	Remarks
Potassium	2.29	36	Light blue deposit K
Sodium	2.68	59	Grey-brown deposit Na
(AlCl ₃ only)	2.20	--	No deposit

When mixtures of these salts with lithium chloride or aluminum chloride are electrolyzed in propylene carbonate solvent, no improvement in the nature of the plated form is noticed.

2.3.7 Addition Agent Effects

Aqueous plating solutions may use addition agents to obtain a shiny or brilliant deposit or to produce a smoother or smaller or grained deposit. The effect of possible agents on the lithium structure in nonaqueous solutions was studied. The common addition agents used may contain water or may have reactive groups such as alcohols or acids, and these would affect the efficiency of the nonaqueous plating solutions. Nonreactive chemicals containing polar groups have been tested for their effect on the dendritic lithium deposits. An addition of 0.1 gm of the solid chemical was added to 50 ml of the solution and lithium electroplated onto smooth silver sheet by means of massive lithium anodes. The results are noted in Table 7. Improved adherence of the lithium particles was noted with the addition of Rhodamine B sodium salt, a dye material, and disodium fluorescein, an indicator, to the propylene carbonate system. The use of Rhodamine B sodium salt as an addition agent in the nitromethane solution produced no noticeable improvement in lithium form.

The effect of LiClO₄ addition on the lithium deposit from both propylene carbonate (PC) and nitromethane (NM) solution was determined and is summarized in Table 8. The lithium deposit was the most metallic in appearance of any solution yet tested in the PC LiClO₄ solution, and addition of AlCl₃ to the system decreased the metallic

character and adherence of the lithium. The deposit was very poor in the LiClO_4 -NM solutions, and the lithium was extremely reactive chemically.

Addition of mercuric chloride to nitromethane solution produced no improvement in adherence of the lithium deposit but changes the color of the deposited lithium from light grey to dark grey. The current efficiency for lithium production was reduced by HgCl_2 addition to the NM electrolytes. Similar observations were obtained by work with HgCl_2 addition to propylene carbonate solution.

Table 7

EFFECT OF ORGANIC ADDITIVES ON LITHIUM DEPOSITION
(Solution A: Propylene Carbonate 100 ml- AlCl_3 10 gm-LiCl 3 gm)

Solution	Current Efficiency (Percent)	Remarks
A	90	dark grey, poorly adherent
Rhodamine B, Sodium Salt	100	grey, fair adherence
4 Azobenzenesulfonic Acid, Sodium Salt	100	grey, fair adherence
Cholestane	100	dark grey, poor adherence
Sodium Lauryl Sulfate	80	extremely poor adherence
Methyl Red	80	extremely poor adherence
Victoria Blue B	90	poor adherence
Disodium Fluorescein	100	better adherence obtained than with electrolyte alone

Table 8

LITHIUM DEPOSITION FROM SYSTEMS WITH LiClO_4

Solution				Current Efficiency (Percent)	Remarks	Electrical Conductivity (ohm ⁻¹ cm ⁻¹ × 10 ³)
	LiClO ₄	AlCl ₃	LiCl			
PC*						
100 ml	8	0	0	100	Light grey, very adherent	4.9
	8	10	0	100	Dark grey, poorly adherent	4.0
	8	3	0	100	Dark grey, adherent	-
	8	2	0	100	Dark grey, fairly adherent	-
NM**						
100 ml	8	0	0	30	Black, adherent	-
	8	3	0	30	Black, adherent	-
	0	20	6	100	Grey, adherent	31.4

*Propylene Carbonate

**Nitromethane

2.3.8 Pressure Effects

The general appearance of the lithium anodes has been dendritic or mossy. It is known that in plating zinc from aqueous systems, the plate is firmer when formed under pressure. An attempt was made to study the effect of pressure on lithium deposits by running cells with the anode under pressure. Leaf springs were formed from chlorinated polyether plastic. When immersed in the standard electrolyte for several days, this material neither softened nor swelled. Several force constants were used, with forces varying from 7 to 220 gm/cm^2 . It was found that the force was not evenly distributed over the electrode surface even though 0.18-in. thick polyethylene plates were placed between the spring and the electrodes under test.

Thus, the results obtained were variable. The pressure helped to produce a more compact deposit. The electrode surfaces were quite dry (the electrolyte was apparently squeezed out of the glass separator material). For long-term runs, polarization studies indicated that the anode increased polarization. This result was found also when care was taken to prevent overcharging. At the present time there appears to be no good reason for spring loading of the cells. However, use of uniform packing of electrodes and separators may be adequate.

2.3.9 Coulombic Efficiency of Electroplated Lithium

Tests were begun to determine the efficiency of discharge for plated lithium. The positive electrode mix consisted of a sintered silver graphite mixture with no silver chloride present. The negative electrode consisted of a stainless steel screen on which LiCl was fused over an open flame. Some precautions were taken to limit the amount of water taken up by these electrodes. The cells were assembled in an argon atmosphere dry box.

The current densities were low for both charge and discharge, 0.8 and 1.2 ma/cm² respectively. The solvents used were propylene carbonate plus ethylene carbonate and nitromethane. At the end of the tenth discharge the cells were allowed to stand on open circuit for three days. The next few cycles resulted in 100 percent coulombic efficiency for the electrolyte utilizing propylene carbonate and 60 percent for the one utilizing nitromethane. At the end of the fifteenth charge the cells were allowed to stand at open circuit overnight. The first discharges were considerably worse than preceding and subsequent ones by about 15 percent for both solvents, indicating a loss of active material. This procedure was repeated for the twentieth cycle with a similar 15 percent drop in current efficiency. At about the twenty-fifth cycle, the current efficiencies had dropped back to levels obtained for the first few cycles. The maximum, in the coulombic efficiency versus cycle number curve, was very pronounced in the propylene carbonate case, and only slightly discernable in the nitromethane case. The average efficiency for the cell using propylene carbonate as the solvent was 70 percent while for the one using nitromethane it was 45 percent.

From lithium plating experiments, one would expect the adherence of the plated lithium to be better in the nitromethane electrolyte; however, the cell cycling data are dependent on the action of both lithium and the silver chloride electrodes.

2.3.10 Lithium Polarization

Lithium electrodes were used in studies of lithium oxidation, and the polarization was measured by steady state methods with propylene carbonate AlCl_3 -LiCl electrolyte. In Figure 16, the average polarization curve obtained from three runs is compared with one obtained using electrolyte with 5-percent addition of water. The values were uncorrected for reference to electrode resistance. The presence of water increases the electrode polarization.

2.4 SEPARATOR MATERIAL STUDY

In the lithium-silver chloride cell, electronic shorting between the positive and negative electrodes is prevented by a separator. The properties that a separator should have for useful service in the nonaqueous electrolyte cells can be summarized as follows:

- Minimum resistance when saturated with electrolyte
- No chemical reaction or solubilization with electrolyte
- No degradation by electrolysis
- Good mechanical strength
- Good electrolyte retention properties during periods of high acceleration

Also, a useful property of separator materials is the ability to be heat-sealed or easily joined. If the material is wet by the electrolyte, separators with very small pores may be used. In addition, separators which incorporate water into the physical structure or have reactive hydrogen atoms in the molecular structure cannot be used with nonaqueous solvents. Since separators must be electronic nonconductors, their effect when used in cells is to increase the solution resistance through the separator by lowering the electrolyte and ionic conductivity volume. The glass mat material used as separator in present cells has a resistance when saturated with electrolyte of 3 to 4 times that of an equal volume of electrolyte alone. The separator resistance R_s (ohm cm^2) saturated with electrolyte can be expressed as:

$$R_s = \frac{2t}{kP}$$

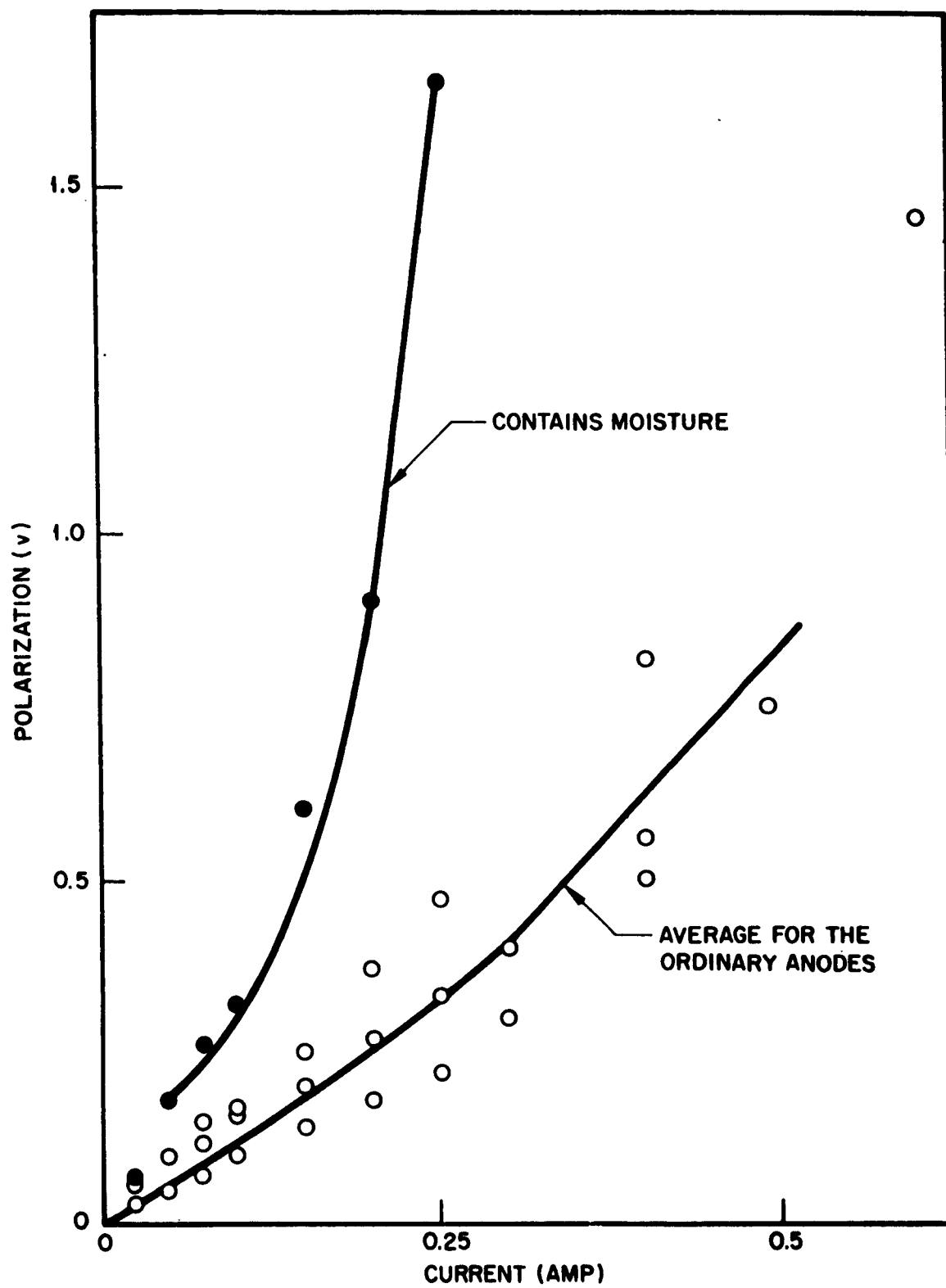


Fig. 16 Lithium Electrode Discharge Polarization

where $t(\text{cm})$ is the separator thickness, $2t$ the length of an average pore, P the porosity (assuming that the pores are continuous throughout the material and are all wet with electrolyte) and k the electrolyte conductivity in $\text{ohm}^{-1} \text{cm}^{-1}$. Useful separators should be thin and porous for minimum resistance. Because of the assumptions necessary for this formula, it is easier to measure resistance directly instead of evaluating pore length or material porosity with continuous pores. The resistance of an electrolyte-saturated separator can be directly measured by AC or DC methods. In the DC method, the voltage drop across a separator is measured with silver-silver chloride reference electrodes when current is passed through the separator by external working electrodes. The resistance R_{dc} is calculated from the slope of the voltage-drop (V) and current (I) curves, which are linear. Thus

$$R_{\text{dc}} = \frac{\Delta V}{\Delta I} \quad (1)$$

For the AC method of determining resistance, circular disks of separator saturated with electrolyte are positioned between silver plated dies and the capacity C and dissipation factor D measured with a standard resistance bridge operating at a frequency of 1,000 cps. The resistance R_{ac} is calculated as follows

$$\text{where } w = 2 \pi 1,000 \quad R_{\text{ac}} = \frac{D}{wC} \quad (2)$$

Using a glass mat separator and propylene carbonate- $\text{LiCl}-\text{AlCl}_3$ electrolyte, we measured both AC and DC resistances and the results are summarized as follows:

<u>Sample</u>	<u>$R_{\text{dc}} (\text{ohm}^{-1} \text{cm}^2)$</u>	<u>$R_{\text{ac}} (\text{ohm}^{-1} \text{cm}^2)$</u>	<u>Percent Deviation AC to DC</u>
1	3.4	3.9	12
2	4.1	3.7	-10

Thus, the two methods give the same results, but the AC method of measuring resistance is faster than the DC method. Because the measurements are taken across the entire sample area in the AC method, small imperfections do not appreciably affect the resistance values obtained.

The thickness of a separator is measured conveniently with the help of the silver plated dies which are used in the AC resistance measuring method. By taking thickness readings with a dial gauge on the dies with and without the separator between them, the average thickness of a 1-in. diameter circle is determined for a 240-gm loading (the weight of the upper die).

The compatability of the separator to electrolyte was determined by immersion of sample in the electrolyte and noting dimensional changes such as swelling, solubility, color change, and weakening of the separator structure.

The properties of separators studied by means of a propylene carbonate 100 ml, LiCl 3.3 gm, AlCl_3 10 gm electrolyte are given in Table 9. The standard glass mat is used in present cell design because of the low resistance measured when saturated with electrolyte and because the material is moderately strong.

Single anode and cathode cells were run using as separators the standard mat and mats A and B. The initial cell resistances of all were the same (within experimental error), ranging from 1.2 to 1.4 ohms for 2-in.² electrode with the AlCl_3 -LiCl-NM solution for electrolyte.

Wetting of the separator by the electrolyte and penetration of the electrolyte into small pores are problems limiting the conductivity of the porous polyethylene separators. In theory, the resistance of the porous polyethylene separators should be lower than that of the standard glass mat since they are thinner and have 75 to 80 percent porosity.

2.5 CELL ASSEMBLY TECHNIQUES

2.5.1 Cell Assembly Dry Boxes

Two dry boxes are used for cell preparation. One is constructed of 0.5-in. thick aluminum and can be evacuated for complete changes of atmosphere. In this box dry operations are performed, such as forming negative electrodes by dipping

Table 9
SEPARATOR MATERIALS

Material	Form Thickness (In.)	Source	Resistance (Ohms) (a)	Remarks
Porous Polyvinyl Chloride (b)	Sheet 0.008	A	13.0	Softened
Asbestos	Paper 0.005	B	6.0	Very fragile
Glass Cloth	Woven 0.003	C	2.4	Open pore
Polyamide Cloth	Woven 0.003	D	3.4	Open pore
Polytetrafluoroethylene	Woven 0.0075	E	25.0	
Glass Polytetrafluoroethylene	Mat 0.0025	F	4.2	Open pore
Polyethylene	Perforated Sheet 0.035	G	20.0	
Fiber Frax (aluminum silicate)	Mat 0.040	H	10.0	
Standard Glass Mat	Mat 0.016	I	4.4	
Glass Mat	Mat 0.014	C	3.6	Fragile
Polypropylene	Mat 0.010	J	10.0	

(a) Resistance in ohms of a one-inch diameter circle saturated with electrolyte.

(b) Leached in 30 percent KOH previously.

Table 9 (cont.)

Material	Form Thickness (In.)	Source	Resistance (Ohms) (a)	Remarks
Glass Mat A	Mat 0.005	K	6	Very fragile
Glass Mat B	Mat 0.012	K	9	
Irradiated Polyethylene	Sheet 0.006	L	400	Brittle
Porous Polymonochlorotri- fluoroethylene	Sheet 0.020	A	470	Not wetted by solution.
Porous Polyethylene	Sheet 0.010	A	9	10 pores
Porous Polyethylene	Sheet 0.005	A	14	1.5 pores
Epoxy Resin Fiber Material	Sheet 0.020	M	16	Stiff material

(a) Resistance in ohms of a one-inch diameter circle saturated with electrolyte.

(b) Leached in 30 percent KOH previously.

nickel screen into molten lithium, or rolling lithium rod into sheet form and processing into electrodes, formation of silver electrodes with glass separators and lithium electrodes into cell packs, and assembly of cell packs in cell cases. The aluminum box has an argon atmosphere purified by recirculation over titanium sponge heated to 700°C. A second dry box, obtained commercially, is used in preparation of electrolyte, filling of cells, and conducting experiments in argon gas with electrolyte vapor present. This box cannot be evacuated because of its low-strength structure, but atmosphere is purified by alternately filling and collapsing a balloon inside the chamber with fresh argon. By repeating the ballooning technique three times, a final argon purity of 99.94 percent was obtained. The argon atmosphere is recirculated over specially treated alumina spheres. This process removes water and hydrochloric acid.

2.5.2 Materials

Sealed cells are necessary to isolate the cell components from external atmosphere, for lithium is reactive with both oxygen and water vapor. Although test cells were assembled in machined polypropylene cases, which were convenient for assembly and could be reused, it was evident that metal cell cases offered advantages in more complete sealing.

Metal cases were needed, too, in obtaining realistic weight and volume figures for evaluation of the system and for ultimate working hardware.

Tests with isolated strips of aluminum alloy type 1100* placed in operating test cells showed no signs of corrosion following cell cycling.

Commercially available cans of this alloy were procured drip-drawn to 1 by 2 by 4 in. These cans, with the open end the 1- by 2-in. dimension, were made from 0.019-in. thick material. Lids were procured of the same material and thickness and were nominally 1 by 2 in with a 1/8-in. lip. These lids were formed to fit inside the open end of the can.

*1100 alloy: 99.00 percent minimum aluminum, 644° - 650°C - melting point.

The intent of the design of this "canned" battery is that the terminals be attached to the lid but electrically isolated. The electrodes are attached to the terminals, the battery pack is inserted into the can, and the assembly is hermetically sealed. These final steps of the operation must be accomplished in an inert-atmosphere glove box, and the sealing method must neither harm either electrode or separator material nor leave any residual material on or in the can which may impair the operation of the battery. The cell must be subsequently filled with electrolyte and the filling tube sealed. The battery so assembled and sealed must be gas tight.

Terminals were made from such materials as copper, nickel, silver, and aluminum. Tests showed that the copper and aluminum terminal materials corroded during cell cycling. Furthermore, the salts formed from the corrosion of these materials were soluble in the electrolyte, whereas the salts formed from nickel or silver corrosion—should any occur—are insoluble and probably would not be a detriment to cell operations.

2.5.3 Initial 5-Amp-Hr Cells

The first work with the 5-amp-hr cell utilized a polypropylene plug cover rather than the aluminum lid. This plug-type cover was machined for an "o-ring" seal on the face of the plug so that the seal was effected on the sides of the can. Screws inserted through the can sides into the plastic above the "o-ring" seal provided mechanical clamping. Terminals inserted through the plastic top were also sealed with "o-rings." Cells of this construction were built but usually failed because this sealing arrangement leaked.

2.5.4 Final 5-Amp-Hr Cells

A more effective method for sealing the cases was desired, and a device for attaching the terminals to the aluminum lid was made from aluminum rod stock. The bushing was machined from 1100-type aluminum alloy and was subsequently torch-brazed onto the can lid with an aluminum filler rod* and a commercial flux.

*9.3-10, 7 percent Si, 3.3-4.7 percent Cu, 0-80 percent Fe, 0.20 percent Zn, 0.15 percent Mg, 0.15 percent Mn, 0.15 percent Cr, remainder Al.

Terminals made from nickel bar stock and tetrafluoroethylene inserts were placed in the bushing. The design provides for positive keying of the terminal to the can so that the terminals can be tightened without stressing the electrodes by twisting. Tightening of the terminal pulls the plastic insert into the cone of the bushing providing a seal around the terminals and the bushing by utilizing the plastic flow properties of the tetrafluoroethylene inserts. The electrode pack is then attached to terminals and the assembly is placed into the aluminum can. These last steps, as well as the sealing step to follow, must be conducted in the glove box to protect the lithium.

A lid assembly complete as shown in Fig. 17 was weighed and placed in the standard nitromethane electrolyte to test for corrosion, especially at the brazed joints. The lid was examined 14 days later, and no corrosion was found at the brazed joints, although reweighing of the lid was not practical since the nitromethane attached and dissolved the nylon washers.

2.5.5 Lid-to-Can Sealing

A number of procedures were evaluated for sealing the lid to the can. Among those tested were brazing, spot welding, soldering and arc-fusion welding. Of these, only arc-fusion welding was chosen for use because the other methods either could not be accomplished without heating the can-electrode system to too high a temperature or required a flux to do an adequate job of sealing. Spot welding could not be accomplished without the use of special fixtures and equipment.

Since the arc-fusion method of welding employs an inert gas over the work piece during the arc process, this procedure can be accomplished in the glove box, utilizing the inert gas (argon) in the box. This procedure was tried and was successful.

The temperature of an electrode was measured during the welding process by placing a thermocouple on a screen attached to a terminal on a standard lid assembly. This simulated electrode rose to a maximum of 75°C during the welding process and cooled rapidly when the weld was finished.

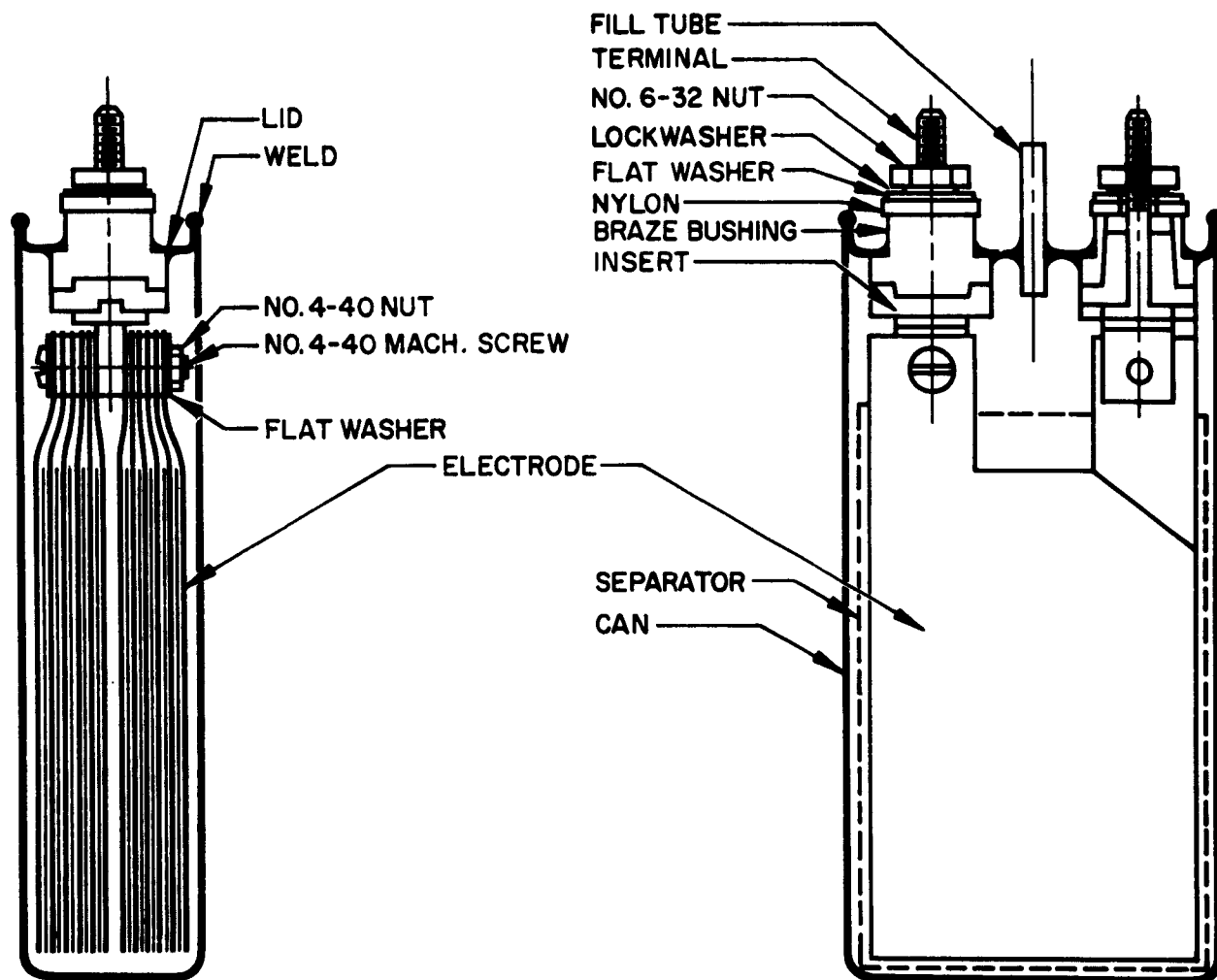


Fig. 17 5-Amp-Hr Lid and Can Assembly

Figure 18 shows the assembly sequence for a sealed can. The lid is sized to press into the can by placing it on the filling die and pressing to stretch the lid slightly. The lid is then degreased and caustic etched. The aluminum bushings are pressed into the lid along with the filler tube. The assembly is fluxed and brazed. The lid is then cleaned of all flux with water and acid dyes, and is dried. The terminals and insulating inserts are put into place. This lid is once more straightened and fitted with the fitting die. The assembly is placed into the glove box at this point, and the electrodes are attached to the terminals with stainless steel machine screws. The battery pack is slipped into the can with an insulating plastic wrapper* around the pack to prevent shorts to the can.

When the lid and chill plate are in place on the can, the clamp is attached and the can is welded where the lip of the lid meets the lip of the can. The copper chill plate keeps the weld joint from spreading apart during the welding. The can is then visually checked for leaks and pressure tested. The electrolyte is then introduced into the can and the filler tube is pinched shut and welded. The battery is now ready to be tested in the atmosphere. The finished battery is shown in Fig. 19 (the chill plate is still in place on the battery).

Several batteries using this assembly and sealing technique have been made and successfully tested.

2.6 TEST APPARATUS

2.6.1 Constant-Current Cell Cycling Apparatus

Constant-current charge - discharge cycling of secondary cells simplifies comparison between cells, and the efficiency calculations for a given cell. By fixing the current, cells (or batteries) may be compared on the basis of voltage, which reflects the power output. Coulombic efficiencies may be readily obtained from the ratios of the constant-current charge and discharge periods as the products with time. This is related to the theoretical electrochemical equivalents for the active electrode materials present.

*Polyester film.

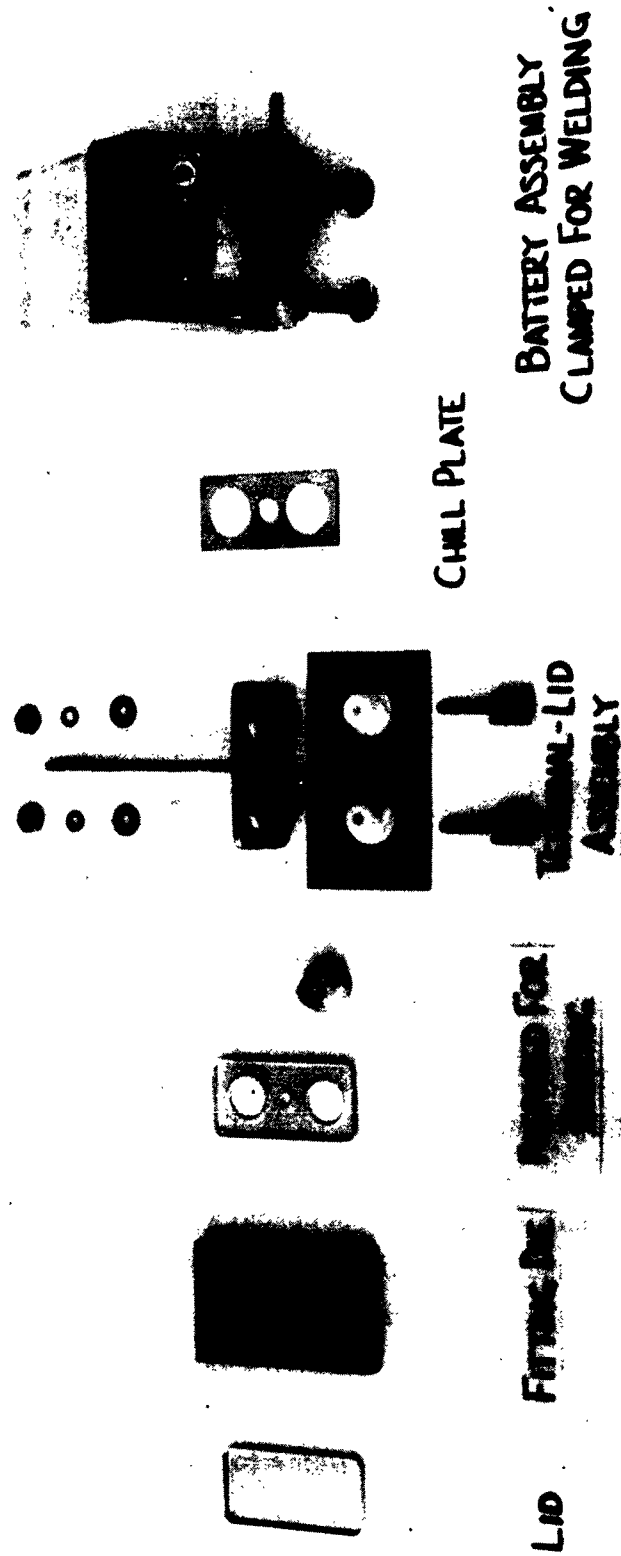


Fig. 18 Lid Assembly Sequence

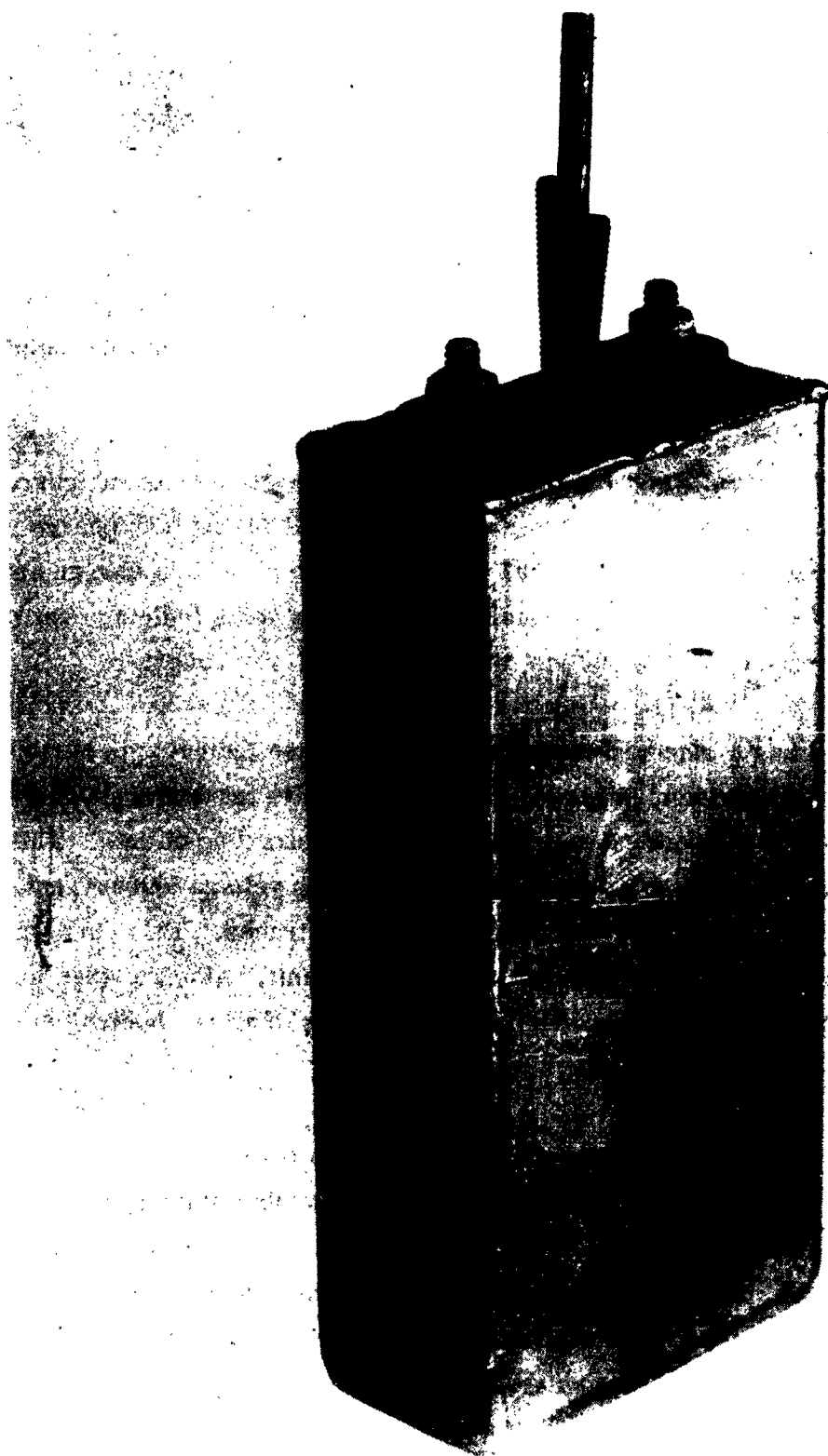


Fig. 19 Arc-Welded Cell Assembly

Equipment for such constant-current cycling of both cells and batteries has been devised. Figure 20 is an electrical schematic of a power and control unit with individual recorders and circuitry for each cell station.

A power and control unit (Fig. 20) is used with four charge - discharge units. It supplies filtered direct current at 0 to 24 v adjustable for charging of either cells or battery. It also supplies timing power for charge - discharge switching relays and for the recorder function relay. A numerical indicator records the total number of charge - discharge cycles.

The charge - discharge circuit (see Fig. 21) contains a solid-state constant-current element similar to that suggested by Greiner,* which is used during both charge and discharge. A switching relay changes circuit component values so that charge and discharge rates may be independently adjusted. Preliminary tests indicate control of ± 2 percent with currents of 50 to 300 ma over a 1.5- to 4.0-v range.

The recorder selected has a standard motor movement, whose indicator is periodically clamped against the clock-driven, pressure-sensitive paper to leave a connected line of dots. This recorder is economical and also allows the recording of dots. This recorder is economical and also allows the recording of both voltage and current on a single channel without smears by input switching between traces. This function relay is switched every 7.5 sec by power from the control unit. Also included in the circuit are range switches for the recorder inputs and jacks to allow checking of the recording trace with precision meters.

Because the charge - discharge equipment will be used with both low-rate experimental cells and higher rate batteries as developed, considerable flexibility is required in the assembly. The individual charge - discharge units are readily replaced with others built for different ranges, and the recorders are readily replaced as a matter of maintenance. At the present time, a total of eight stations have been constructed with separate cycle times and charge voltages available from the control unit serving each

*R. A. Greiner, Semiconductor Devices and Applications, McGraw Hill, p. 329, 1961.

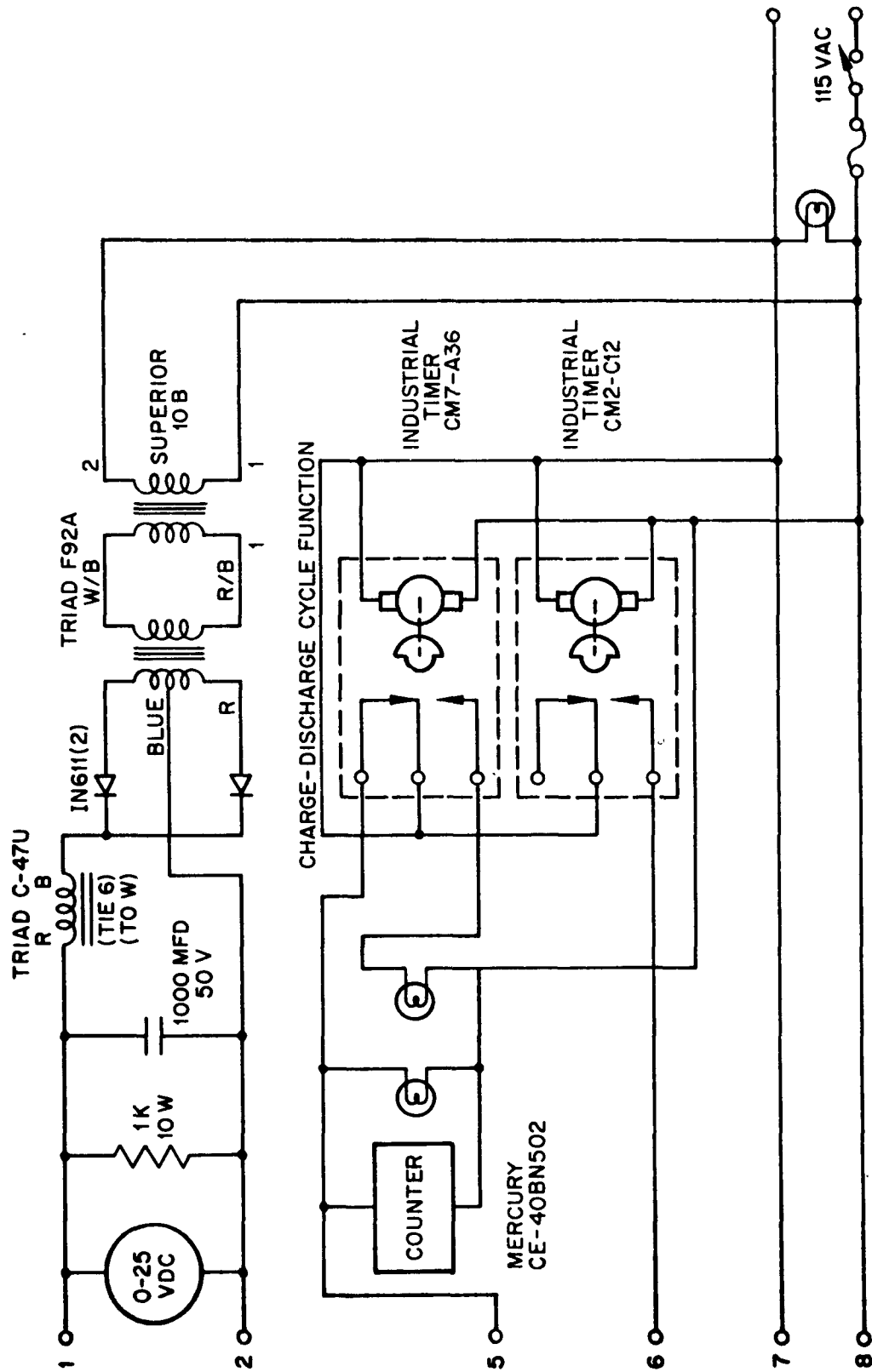


Fig. 20 Cell Power and Control Circuit

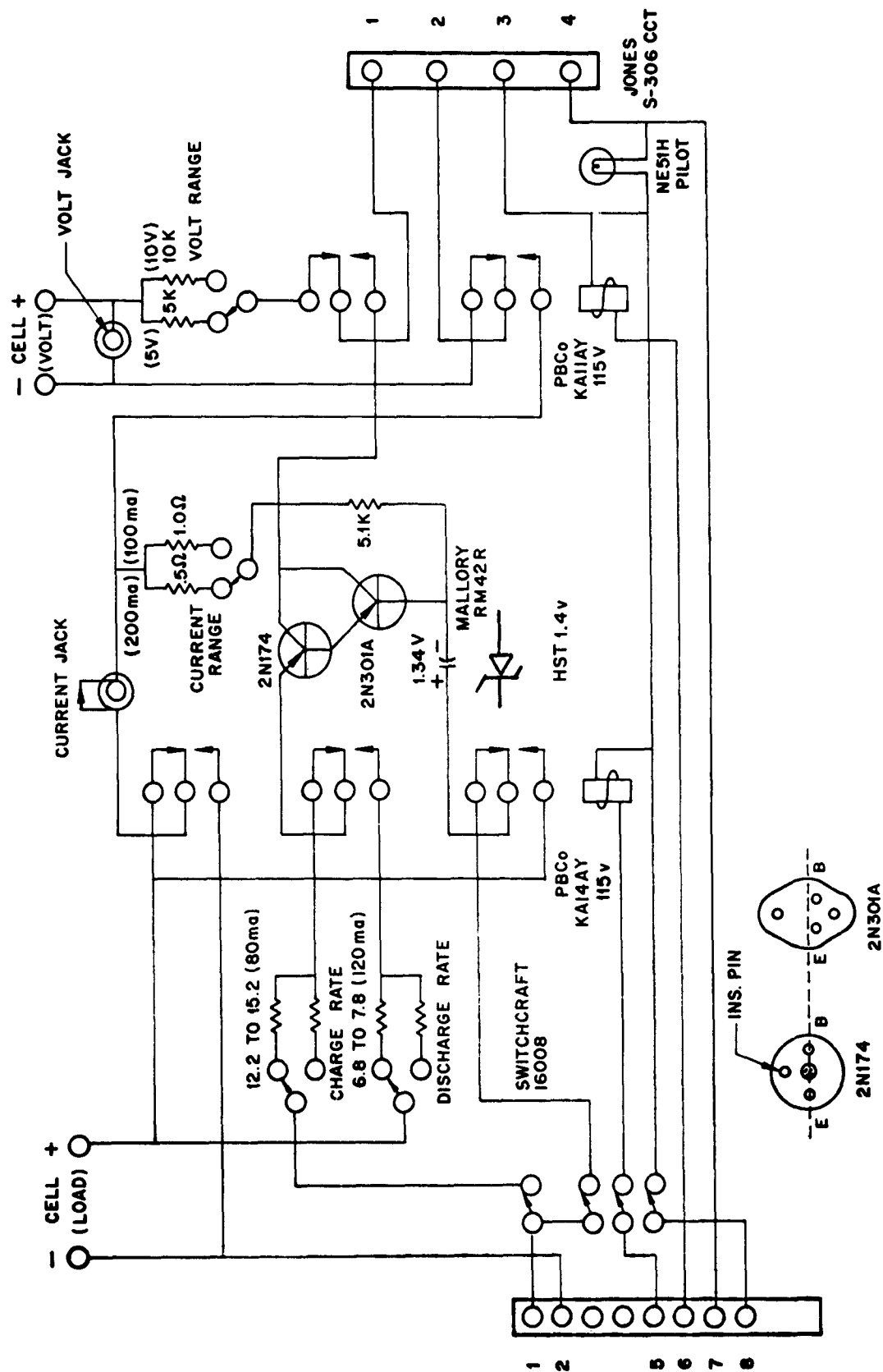


Fig. 21 Charge-Discharge Circuit

four stations. In Fig. 22 are seen front and back views of the cell cycling equipment in use.

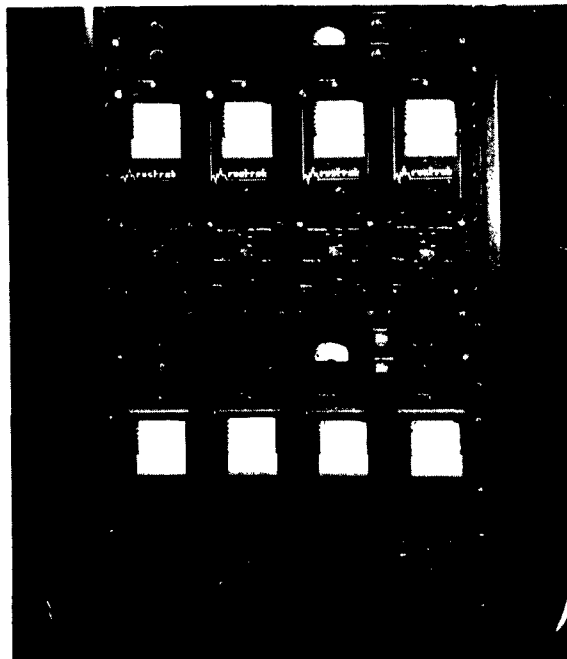
A charge - discharge curve obtained with a Li, NM-AlCl₃-LiCl, AgCl-Ag cell is shown in Fig. 23. The current during charge remains constant until the cell charging voltage becomes limited by the apparatus input voltage. Current during discharge remains constant until the discharge voltage falls below the control-transistor bias voltage.

2.6.2 Battery Testing Equipment

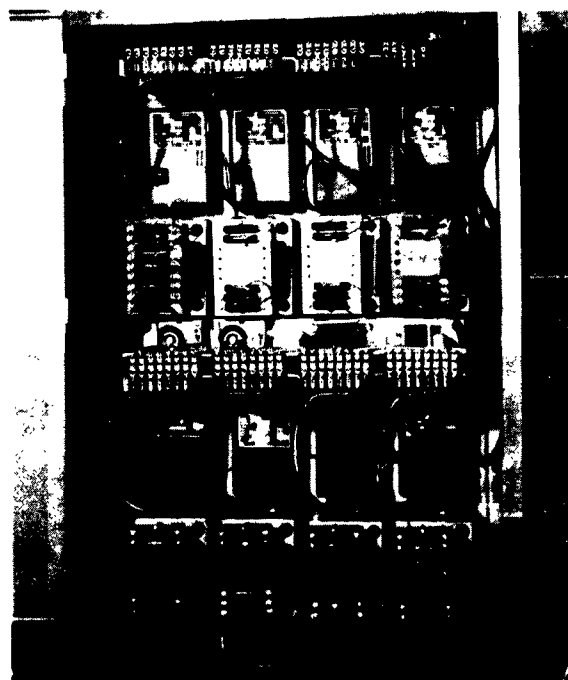
Charge - discharge cycling equipment for up to 5-cell batteries has been built. This was designed for 5-amp-hr batteries but the load can be altered to allow its uses with smaller test cells. The unit layout of the circuit is shown on Fig. 24. The power and control unit, Fig. 25, is similar to that previously shown (Fig. 20) except for the 5-amp capability of the battery charging power supply. The cell voltage switch, Fig. 26, connects the individual cells to the recorder for 10-sec periods so that all cell voltages may be monitored. The recorded traces show as a series of dashed lines. A longer dwell time is used for one cell, and this results in a longer recorder trace for that position and allows subsequent recorder traces to be identified. The charge - discharge unit, Fig. 27, is similar to that used with the cell test unit, Fig. 21, except for the higher voltage regulating range and the greater power dissipation capability of the regulating components. The circuit was derived from the schematic given by Honeywell Semi-Conductor Products.* This unit can charge or discharge either single cells or batteries at rates of 100 ma to 5 amp. Parallel tetrode transistors were used to lower the impedance of the regulator so that high-rate discharges could be obtained from each single cell.

Front and back views of the battery cycling equipment are seen in Fig. 28.

*Minneapolis-Honeywell Company, Application Note AN3.



Front View



Rear View

Fig. 22 Current Charge-Discharge Apparatus

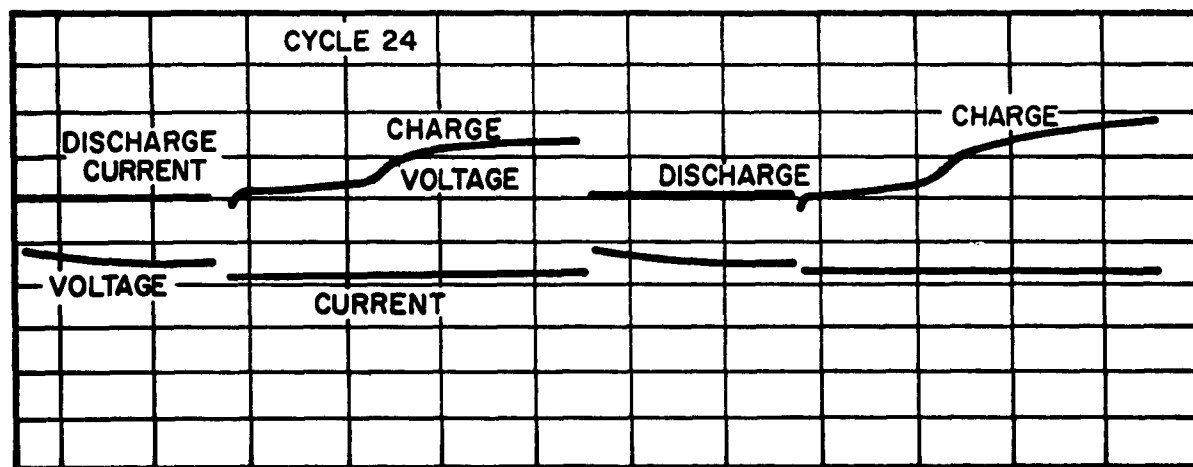
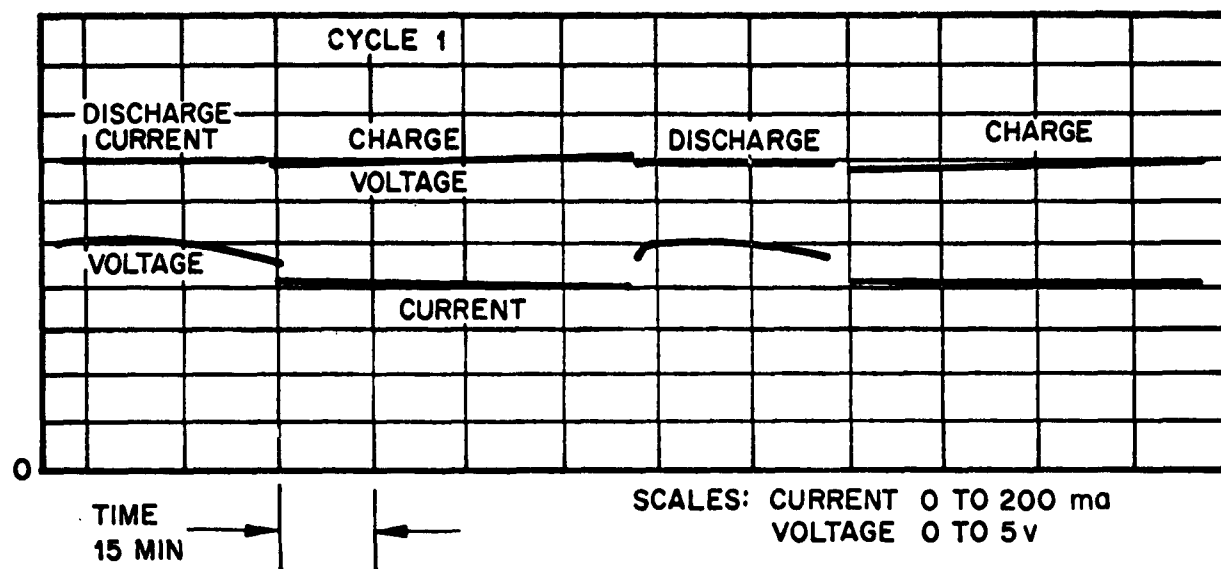


Fig. 23 Charge-Discharge Curves Obtained With Li-AgCl Nitromethane System

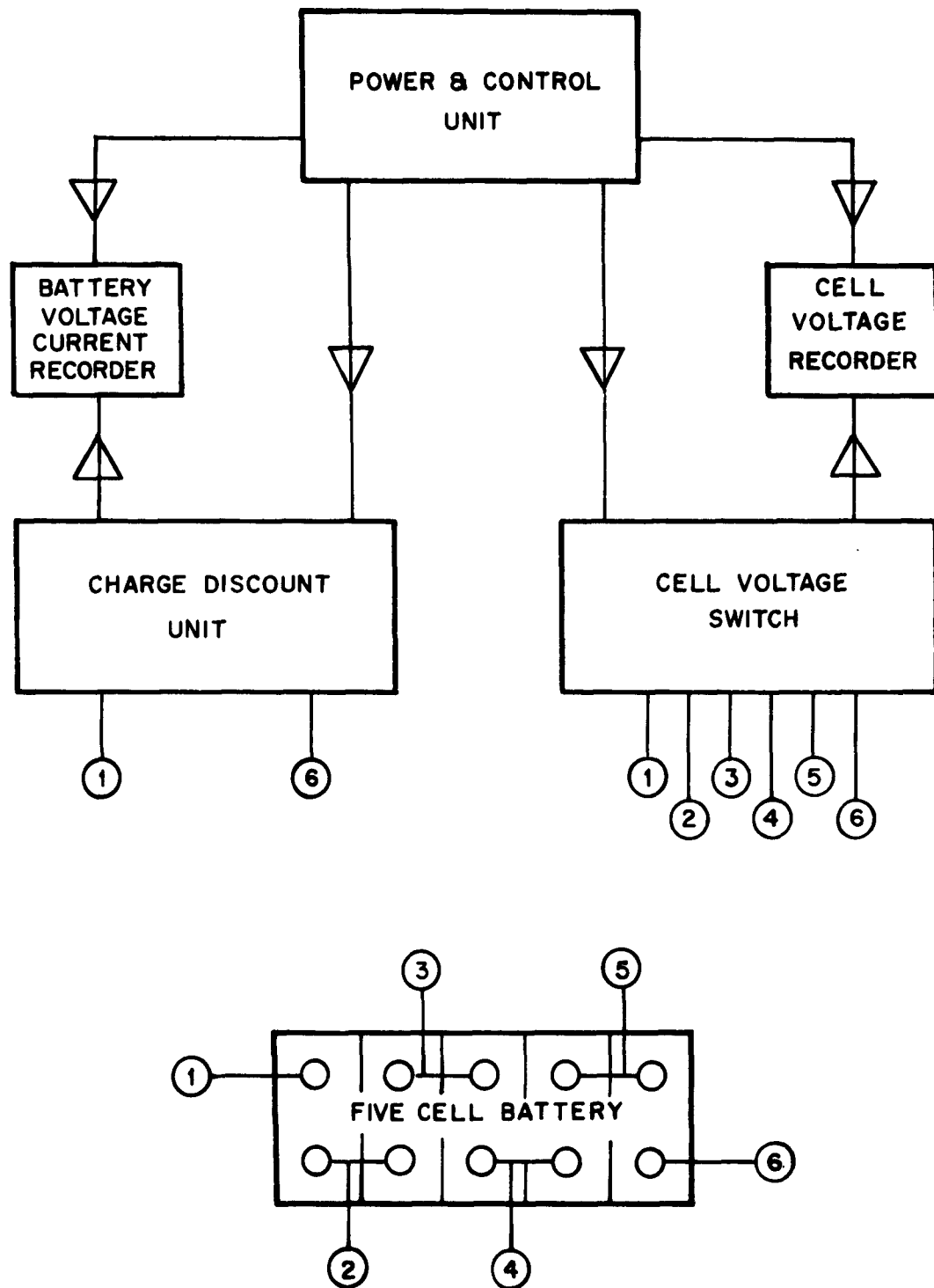


Fig. 24 Battery Cycle Diagram

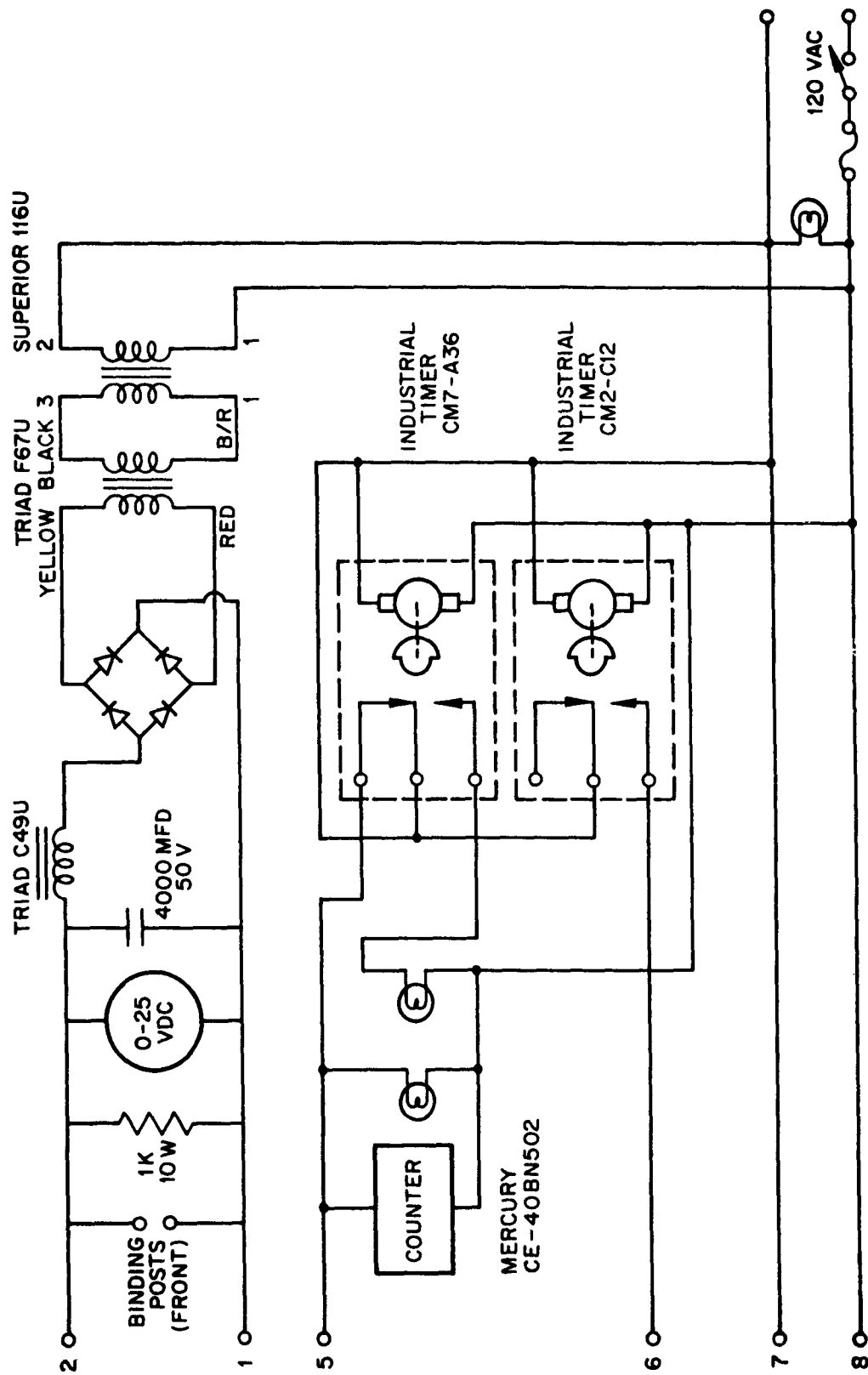


Fig. 25 5-Amp Power and Control Unit

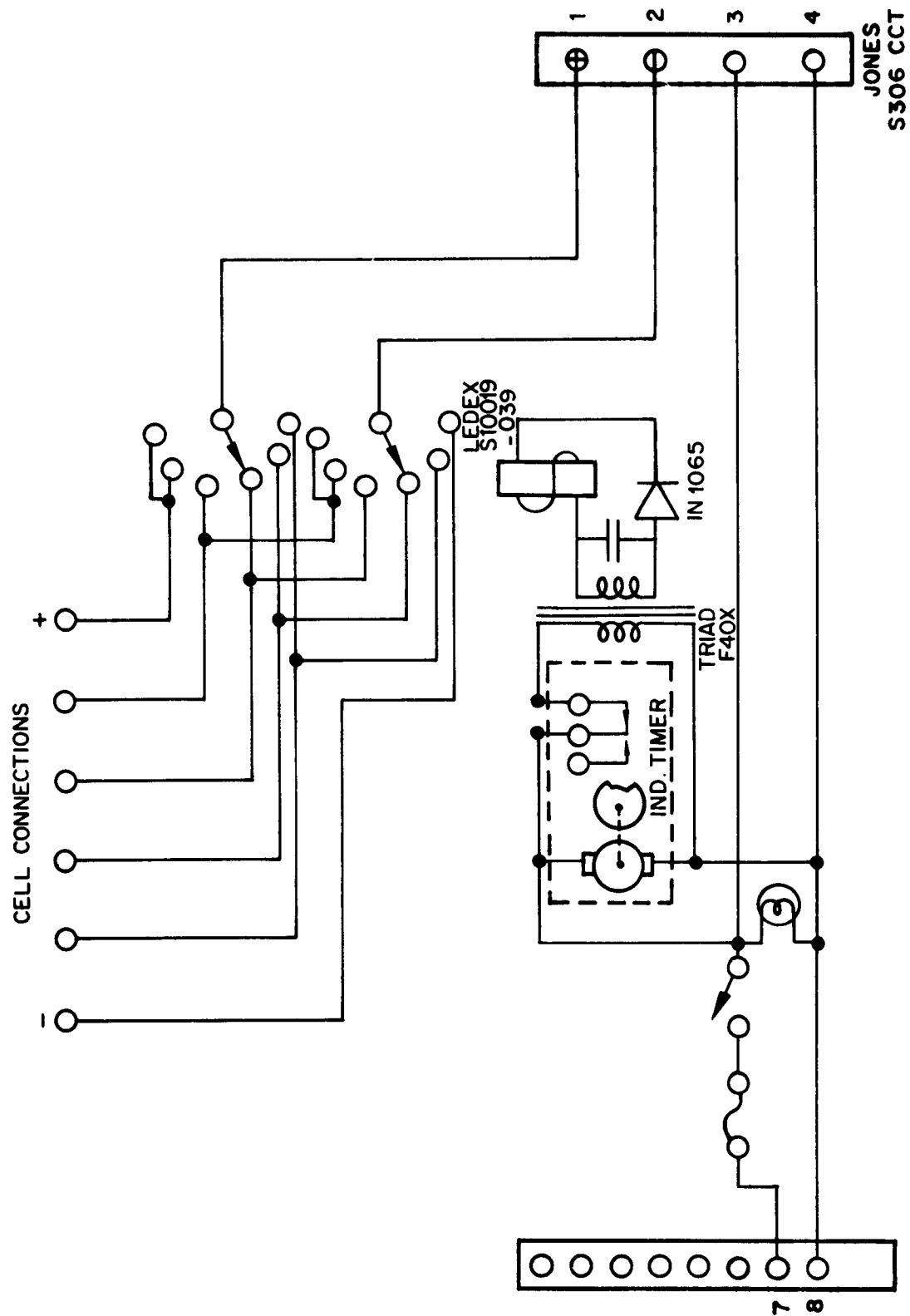


Fig. 26 Cell Voltage Switch

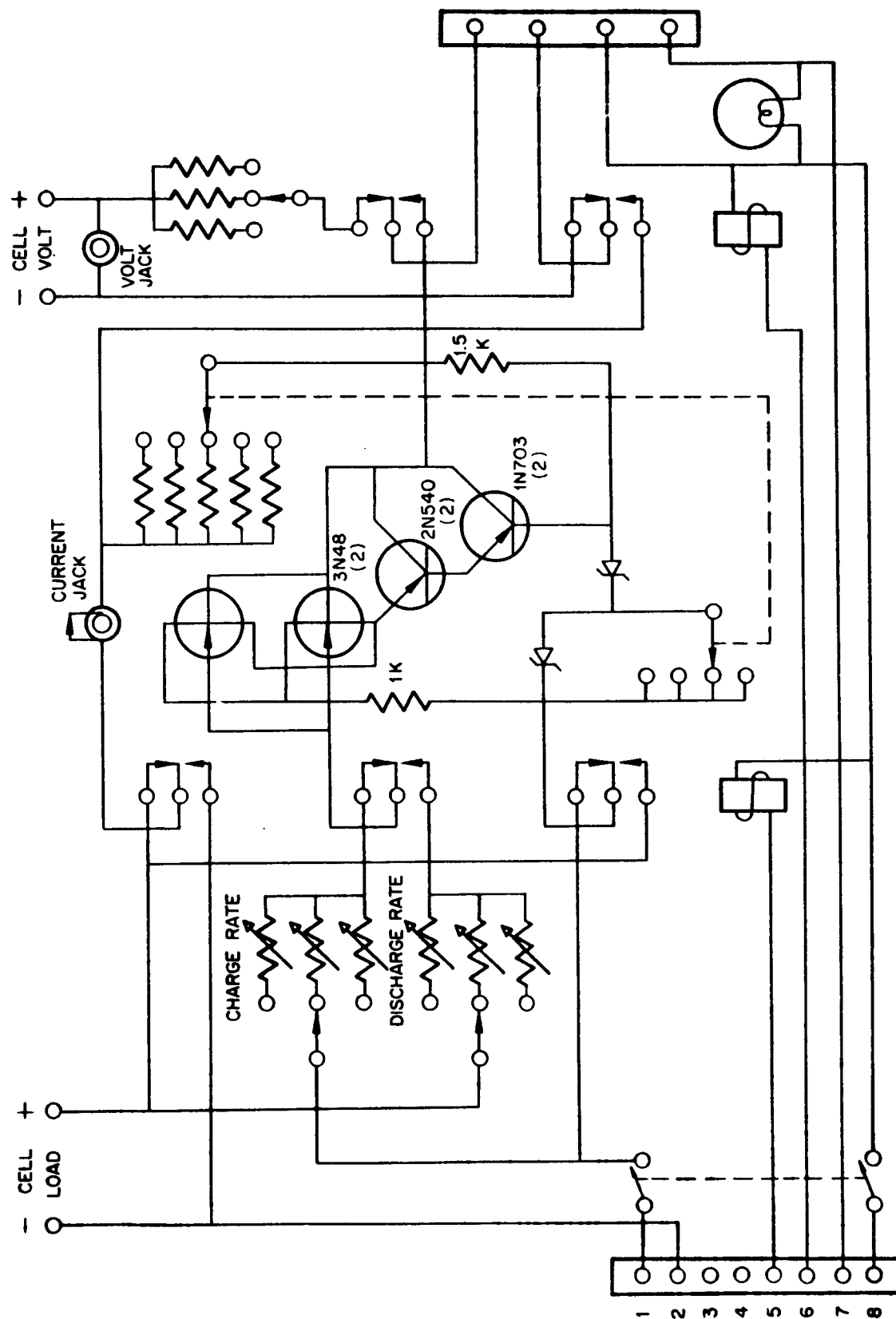
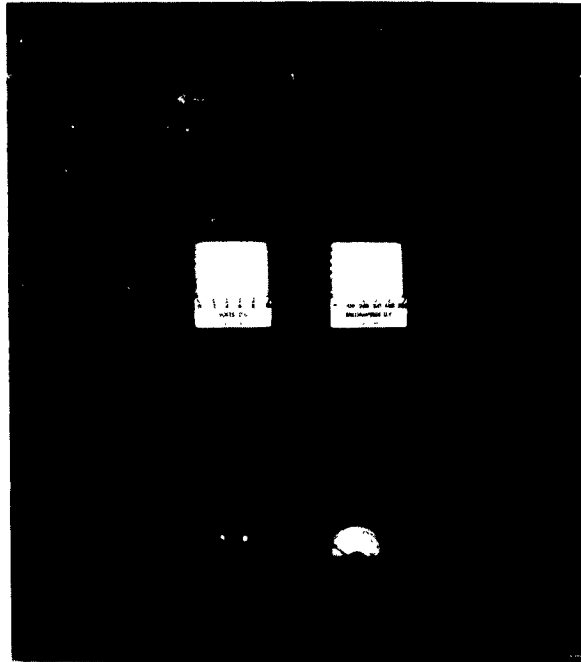
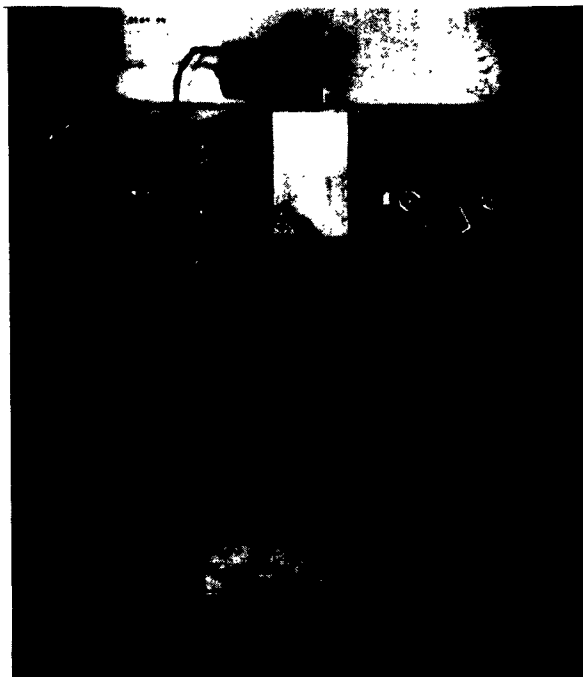


Fig. 27 Variable Charge-Discharge Unit



Front View



Rear View

Fig. 28 Battery Cycling Unit

2.7 CELL TESTING

2.7.1 Cells With 4-In.² Electrodes

Many combinations of cell components were tested by charge - discharge cycling of cells. A 35-min discharge and a 55-min charge period was used for the time cycle. The cells were contained in polypropylene cases with each electrode 23 cm² in area. Cells made with two silver and three lithium electrodes had capacities of about 0.5 amp-hr, with silver chloride being the limiting material. The cells were charge - discharge cycled as assembled or were initially discharged to 0.5 v and recharged before cycling; current and voltage values were recorded as functions of time. Initially, electrical testing was done with a constant load, but later tests were run on constant-current equipment. The cell make-up is described in Table 10, and the type of cells and the results of the cell testing are presented in Table 11. The data presented include the coulombic efficiency (E) defined as follows:

$$E = \frac{\left[\int_0^t i_d \, dt \right]_{\text{(discharge)}}}{\int_0^t i_c \, dt_{\text{(charge)}}} 100$$

where i_d is discharge current and i_c the charge current. The integration is performed graphically from the cell current - time recording with a polar planimeter. The cell resistance is measured with an AC bridge operating at 1,000 cps and is corrected for lead resistance. The data presented are the average results for the indicated number of similar cells.

Some of the results of these tests have been reported in other sections on specific cell components. The following further conclusions can be drawn from the data presented:

- Polyethylene separators produce cells with higher initial resistance than do cells formed with asbestos or glass mat, as would be expected from the previous resistance measurement of electrolyte-saturated separators.

Table 10

KEY TO CELL COMPONENTS

Designation	Ingredients	Treatment
St.	Propylene carbonate Aluminum chloride Lithium chloride	Combine at low (less than zero degrees centigrade) temperature
St. ¹	As above only Sodium chloride instead of LiCl	As above
St. ²	As above with lithium perchlorate instead of lithium chloride	As above
St. EC	Eutectic mixture of propylene carbonate and ethylene carbonate, otherwise the same as St.	As above
CH ₃ NO ₂	Nitromethane Aluminum chloride Lithium chloride	As above
E ¹	Silver sheet plus silver chloride	
F	Silver powder Graphite	Sintered in H ₂ atmosphere
F ¹	Silver powder Graphite Silver chloride	Sintered plaque with silver chloride added
H ¹	Silver oxide, silver chloride 1 percent polyvinylalcohol-water	Past on F-S Ex-met (silver), dry for an hour at 85°C
H ²	As above plus graphite	As above
H ³	As H ₂ plus nickel powder	As above
H ⁴	H ¹ plus precipitated silver	As above
H ⁵	H ¹ plus spherical silver	As above
H ⁶	H ¹ plus flake silver	As above

Table 10 (cont.d)

Designation	Ingredients	Treatment
M ¹	Sodium chloride	NaCl fused into a sintered silver powder plaque
N	Lithium	Silver plated nickel screen dipped into molten lithium
Q	Asbestos paper	None
U	Glass-fiber filter paper	Flame sealed edges
U ¹	Glass-fiber mat (thin)	Flame sealed edges
U ²	Glass-fiber mat	Flame sealed edges
V	Polyethylene separator	Heat sealed edges

Table 11
CELL TEST DATA

Electrolyte	Anode	Cathode	Separator	Configuration Anode-Cathode	Number of Cells	Average No. of Cycles	Percent Efficiency	Initial R (ohms)	ΔR (d)	Voltage (b) Ch. (v) i (c) f	Ch. (ma) i f	Current Disch. i f
PC	N	E ¹	U	1-1-1	1	48	100	9.0	---	2.8 2.8 2.4 0.2	60 12	96 6
A _{PC} Ka		F		1-3-1	1	44	86	3.1	---	2.7 3.4 2.7 2.1	80 80	120 120
PC		F ¹		1-1-1	10	40	94	3.5	-1.1	3.0 4.1 2.4 1.8	95 55	110 95
		F ¹		1-3-1	2	—	—	—	—	—	—	—
		H ¹		1-1-1	20	45	91	6.25	-1.7	2.8 4.2 2.5 1.2	80 80	120 96
		H ¹		2-3-1	2	59	53	2.1	1.0	3.1 4.6 3.1 1.7	72 42	92 70
		H ²		1-1-1	34	44	84	5.25	1.0	2.9 4.3 2.4 1.2	80 60	116 100
		H ³		1-1-1	4	29	92	7.1	1.4	2.8 3.7 2.3 1.4	81 67	140 94
		H ⁴		1-1-1	2	45	82	8.0	-5.4	2.9 4.3 2.0 1.2	80 48	116 92
		H ⁵		1-1-1	2	50	78	12.0	-8.0	2.9 4.4 2.4 1.2	76 72	120 88
		H ⁶		1-1-1	3	30	85	16.0	-11.6	2.9 3.4 3.1 1.8	76 40	124 72
PC ¹	M	F		1-1-1	1	50	10	6.5	-1.8	3.4 4.6 2.0 0	39 14	13 0
PC ²	N	H ²		1-1-1	7	46	84	4.0	-1.5	3.2 4.2 2.4 1.4	90 65	130 80
PC+EC		H ¹		2-3-1	2	29	100	1.7	1.0	3.2 5.0 2.3 0.7	270 120	420 150
NM		F ¹		1-1-1	2	—	90	0.8	---	2.9 3.3 2.2 1.6	85 80	95 65
		H ¹	Q	1-1-1	3	22	78	3.1	7.2	3.1 3.2 2.1 1.1	80 94	112 28
			U	1-1-1	6	30	79	2.0	-4.8	2.9 3.0 2.6 2.5	80 80	118 118
			U	2-3-1	3	15	70	0.5	-18.0	3.1 4.3 2.5 2.3	310 305	480 480
		U ¹		1-1-1	3	26	92	1.3	-3.3	2.9 3.2 2.4 2.1	78 78	116 116
		U ²		1-1-1	4	24	80	3.1	-6.0	2.9 3.0 2.3 1.9	78 78	116 116
		V		2-3-1	4	14	76	5.5	2.5	3.2 4.8 2.4 1.9	290 180	490 460
		U		1-1-1	4	26	78	2.6	1.2	3.0 3.3 2.4 2.3	84 84	120 120
					Total	120						

(a) Cell made 8/6/62 Cycled 2/25/63

(b) Characteristics on tenth cycle

(c) i = initial f = final

(d) Initial minus final resistance

- Cells using a high- AlCl_3 concentration propylene carbonate electrolyte produce runs with lower coulombic efficiency than do cells using the standard PC electrolyte.
- The best lithium support is nickel or stainless steel and aluminum cannot be used as lithium support.
- Soldered, electrode tab-to-terminal connections are attacked during charging and fail.
- Too low a discharge current may be obtained on cycling for set time cycles, thus limiting the coulombic efficiency values by the apparatus rather than by cell reactions.

A summary of the best results obtained with cycled cells is given in Table 12. The number of cycles obtained with a given percent discharge capacity are listed for various levels of current density, electrolyte, and total capacity. For low discharge rates, over 100 cycles have been obtained with propylene carbonate electrolyte cells. A life of 110 cycles was obtained from one cell containing propylene carbonate electrolyte, with ± 10 percent voltage regulation at 12 percent discharge capacity.

The limiting of the cell-cycle life and failure of the cells tested has been found due to several causes which are listed as follows:

- Loss of capacity by mechanical separation. Soldered lithium electrode tabs fail during charging or silver electrode tabs are eroded by anodic oxidation on overcharge.
- Increased cell resistance. Cell resistance increases by mechanical and electrical separation of electrodes and by loss of electrolyte through leaks in cell cases or tops.
- Internal cell shorting. Separator tearing at electrode edges in packed cells allowed loose graphite or silver to bridge both lithium and silver electrodes.
- Destruction of cell by electrolyte ignition. This occurs with leaking cells, generally on charging cycle.
- Electrode Nonreversibility. During charging, the electrode reactants are not completely reformed in reusable condition.

Table 12

CELL CYCLING RESULTS

Electrolyte			Cycle Time (min) Discharge - Charge	Area (cm ²)	Current Density (ma/cm ²)	Capacity ^a (Amp-Min)	Percent Discharge Capacity	Number of Cycles
Nitromethane	AlCl ₃	LiCl						
(ml)	(gm)	(gm)						
100	40	14	35-55	93	1.3	55 ^b	10	38
100	20	7	35-55	46	2.5	14.5	22	26
100	20	7	35-55	46	2.5	15.1	20	29
100	40	14	35-55	93	4.9	120 ^b	13	4
100	40	14	35-55	93	4.9	50 ^b	10	10
Propylene Carbonate	AlCl ₃	LiCl						
(ml)	(gm)	(gm)						
100	10	3	35-55	93	1.3	24	12	110
100	10	3	8-12	46	1.5	1.8 ^c	50	192
100	10	3	35-55	46	2.0	15 ^b	13	33
100	10	3	35-55	93	4.8	120 ^b	3	10

^aCapacity measured on initial discharge.^bTheoretical capacity based on AgCl equivalents.^cCell with initial silver electrode, AgCl formed on initial charge.

The first four failure methods may be suppressed by adequate design of cell components, and most of these failure causes have been corrected by the cell design which was finally evolved during the present work.

2.7.2 5-Amp-Hr Cell Tests

High-capacity cells were made by assembling nine silver-silver chloride electrodes and eight lithium electrodes of dimensions 3 in. by 1-3/4 in. in cells. Each silver electrode contained 9.5 gm average of a mix with 40 percent silver chloride and was 40 to 55 mil thick. Other cells were constructed with eleven silver-silver chloride electrodes with 5 gm average weight of mix with 50 percent silver chloride and twelve lithium electrodes. Each lithium electrode contained 0.6 gm lithium rolled onto the nickel screen with an overall thickness of 18 to 25 mil. Glass fiber filter paper separators were sealed over the silver electrodes. Both nitromethane and propylene carbonate electrolytes were used. This combination of materials and construction resulted in a completed cell weight of from 268 to 290 grams. A summary of the results for several cells is presented in Table 13 for cells discharging to a 20-percent voltage drop.

Cells containing nitromethane electrolyte show higher capacities than do those containing propylene carbonate. This in part is due to the higher electrical conductivity of the nitromethane electrolyte. The highest energy density obtained is 25 w-hr/lb of cell weight. This value is over 1/10 the theoretical energy density of 240 w-hr/lb of active materials, and improvement has been made over the previous values obtained. Further minimization of inactive cell components and incorporation of low resistance separators into the final cell structure will result in higher actual energy densities for the lithium-silver chloride cell under study. At the higher currents considerable heating of the cells was noted in both charge and discharge conditions, with final temperatures of 20°C over ambient obtained.

Table 13

RESULTS OF 5-AMP-HR CELL TESTING

Cell No.	Electro-lyte	Current (amp)	Current Density (ma/cm ²)	Average Voltage* (v)	Capacity (amp-hr)	Energy Density (w-hr/lb)
.01	NM	4.5	9.0	2.1	2.25	8
		1.0	2.0	2.55	4.60	18
		0.12	0.24	2.7	6.00	25
.02	NM	1.0	2.1	2.47	5.50	21
.04	NM	1.0	2.0	2.55	4.75	20
		2.0	4.0	2.44	6.50	26
.05	NM	2.0	4.0	2.31	4.26	16.7
.06	PC	1.0	2.0	2.3	2.63	9.5
.07	NM	1.0	2.0	2.38	5.40	19.9
.08	PC	1.0	1.4	2.42	2.06	9.1
.010	PC	0.144	0.23	2.73	5.62	28.6
.010	PC	1.0	1.6	2.55	2.44	10.4

*

$$V_{\text{average}} = \frac{\int_0^{t(.8 V_o)} \int_0^v v \, dv \, dt}{\int_0^{t(.8 V_o)} dt}$$

2.8 BATTERY TEST RESULTS

Several batteries utilizing nitromethane electrolyte were studied. The 5-cell batteries were on a 90-min cycle with a nominal 35-min discharge. The rates were approximately 380 ma, charge, and 520 ma, discharge.

The construction of each cell in the several experiments was the same, using 3 silver and 2 lithium electrodes. Initially, the silver electrodes were pasted with 5 gm of a mix - 50 percent Ag_2O , 40 percent AgCl and 10 percent graphite, by weight. Later the Ag_2O was reduced to 40 percent and the AgCl increased to 50 percent, by weight. These electrodes had a center thickness of from 55 to 69 mil. The average side to center variation was 16 mil, or sides about 25 percent thinner than the center.

The lithium electrodes were rolled to thickness on the order of 25 mil. Because lithium is rolled onto the grid, it is necessary to fasten the electrode to the terminal by a suitable means in a protective atmosphere. Initially, soldering was used to fasten the electrode to the terminal; in final runs mechanical connections using bolts and nuts were used with assembly performed in an argon atmospheric chamber.

Cells fabricated with aluminum screen lithium electrodes failed because of an aluminum-lithium alloy formation which disintegrated during cycling. Cells with electrodes joined to terminals by soldering were found to fail when lithium was deposited on the soldered joint. Mechanical fastening of electrodes to terminals works very well in practice, but assembly in an inert atmosphere glove chamber is difficult.

Envelope type glass mat separators were fitted around the silver electrodes. Spacers were used in some of the cells to reduce the variation in electrode separation and to limit the amount of electrolyte required.

The data which is obtained in the charging and discharging of batteries is not as easily presented as that for single cells.

Since complete results have been obtained for few batteries, it is best to present a raw data sample and tables of the results. A pictorial representation of a charge-discharge cycle is shown in Figure 29. One set of curves shows the current and voltage of the

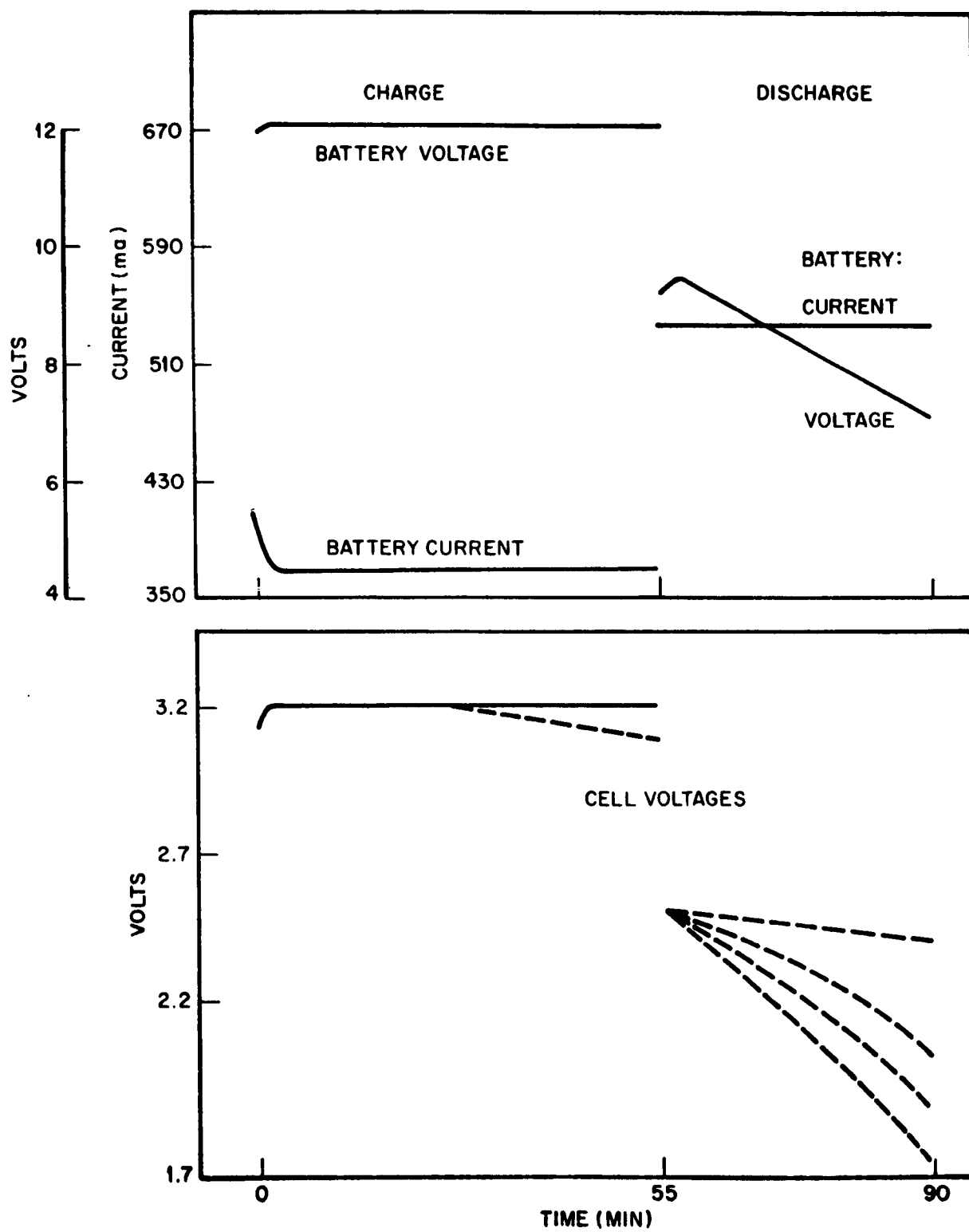


Fig. 29 Battery Cycling Data Record

complete battery. The other shows the voltages of the individual cells. Because the markings for the cell voltages are made by the same striker, the mark for the first cell in the battery is made twice as long as the others in order to allow identification of each individual cell's voltage.

Typical data which is recorded for our files is presented in Table 14. The current capacity of the battery as used in these tables is determined by integrating the battery current over the time for the initial discharge to a 2-v cutoff potential.

2.9 CELL THERMAL EFFECTS

2.9.1 Low-Temperature Studies

Because of the high energy density of these systems, it seemed desirable to perform a few experiments to determine their suitability for use at low rates at very low temperatures. The low temperatures were obtained with a large Dewar containing an alcohol-water mixture with dry ice which iced at about -55°C (-67°F). However, this means of controlling the temperature is very poor when the temperature must be held constant for many hours. Cooling liquids to -55°C is even less satisfactory. As a result, the long-term temperature variation was from -75°C to -40°C (-103°F to -40°F).

This is unsatisfactory for quantitative experimentation, but the results are indicative of whatever might be expected. In the following experiments the temperature was held at the indicated level for about an hour prior to the performance of the experiment. The experiments were of a very short time duration so that the temperature should have been constant.

Standard nitromethane electrolyte is composed of the following:

CH_3NO_2	100 ml
AlCl_3	40 gm
LiCl	14 gm

The conductivity of this solution at room temperature is 4.3×10^{-2} mho/cm, at -57°C it is 4.3×10^{-3} mho/cm. At the low temperature the conductivity seemed to drop over an extended length of time; this appeared to be due to the precipitation of some of the solute.

Table 14

BATTERY TEST RESULTS

Battery No. B003

Cell Components

Negative Electrode - Rolled lithium on silver plated nickel, soldered to terminal.

Positive Electrode - Silver, Silver Chloride - sintered.

Separator - Glass fiber filter paper.

Electrolyte - 30 ml CH_3NO_2 -12 g ACl_3 -4.2 g LiCl .

Discharge Current Density - 5.75 ma/cm².

Capacity from first Discharge of Battery to 10 v end voltage - 0.385 amp-hr
23.1 amp-min

Battery Resistance - 3.3 ohms

Cells 2 and 4 removed before cycle 7; cell 4 was replaced before cycle 7.

Battery Characteristics

Cycle	State	Current (ma)	Voltage (v)	Efficiency (Percent)	Capacity (Percent)
1	C	320-300	14-14.8	Current runaway	
	D	600-700	12-11		
3	C	450-320	14-15	100	90
	D	500-540	12.6- 9.5		
6	C	420-380	15.6-16	100	89
	D	550-420	10- 5		
7	C	420-380	12.5-12.7	100	89
	D	540-540	10- 9		
13	C	390-410	12-12.5	100	88
	D	540-400	11.5- 4.9		

Table 14 (Cont.)

Battery No. B003

Cell Data

Cell No.	Cycle No.	State	Voltage (v)	Notes
1	1	C	2.9-3.0	initial R = 0.75 ohms
		D	2.6-2.5	final R = 1.8 ohms
	3	C	3.0-3.1	
		D	2.6-2.49	Lithium at bottom of cell case.
	6	C	3.25-3.35	
		D	3.1-2.35	
	7	C	3.2-3.3	Cathode - soft
		D	2.6-2.4	
	13	C	3.2-3.2	
		D	2.5-0.6	
2	1	C	2.9-3.0	initial R = 0.64 ohms
		D	2.5-2.4	final R = 0.96 ohms
	3	C	3.0-3.2	
		D	2.5-0.71	
	6	C	3.2-3.1	
		D	2.5-neg.	
3	1	C	3.0-3.0	initial R = 0.75 ohms
		D	2.6-2.3	
	3	C	3.0-3.1	
		D	2.5-2.3	
	6	C	3.3-3.3	
		D	2.5-2.5	
	7	C	3.25-3.4	
		D	2.6-2.3	
	13	C	3.2-3.2	
		D	2.5-2.1	

Table 14 (Cont.)

Cell No.	Cycle No.	State	Voltage (v)	Notes
4	1	C	3.0-3.0	initial R = 0.76 ohms
		D	2.6-1.9	final R = 3.8 ohms
	3	C	3.1-3.1	Lithium at bottom of case
		D	2.6-2.3	
	6	C	3.2-3.2	
		D	2.5-neg.	
*	7	C	3.2-3.3	initial R = 2.68 ohms
		D	2.7-2.3	
	13	C	3.2-3.2	
		D	2.5- .6	
5	1	C	2.9-3.2	one soldered anode connection failed
		D	2.6-1.5	
	3	C	3.1-3.3	
		D	2.6-1.75	
	6	C	3.2-3.3	Lithium at bottom of case
		D	2.5-2.3	
	7	C	3.0-3.0	
		D	2.7-2.3	
	13	C	3.2-3.15	
		D	2.5-neg.	

*This is a new cell.

Table 14 (Cont.)

Battery No. B005

Cell Components

Negative Electrode - Rolled lithium on nickel screen bolted to terminal.

Positive Electrode - Silver, silver chloride - sintered.

Separator - Glass fiber filter paper.

Electrolyte - 30 ml CH_3NO_2 -12 g AlCl_3 -4.2 g LiCl .Discharge Current Density - 5.6 ma/cm²

Capacity (to 2 v worst cell) - 0.315 amp-hr, 18.9 amp-min

Initial Battery Resistance - 2.4 ohms

Cell 2 replaced before cycle 8

Cells 1, 4, and 5 removed before cycle 9

Cell 3 dead before cycle 11

Battery Characteristics

Cycle	State	Current (ma)	Voltage (v)	Efficiency (Percent)	Capacity (CH) (Percent)
3	C	310-290	15.6-16.6		50
	D	500-530	12.4-11.6	126	
7	C	795-305	15.6-15.2	116.5	50
	D	540-460	12.0- 4.0		
9	C	295-170	5.9- 6.5		46
	D	520-440	4.5- 1.0	132	

Table 14 (Cont.)

Battery No. B005

Cell Performance

Cell No.	Cycle No.	State	Voltage (v)	Notes
1	3	C	3.2-3.4	Res. -0.5-1.4 ohms
		D	2.6-2.4	
	7	C	3.2-3.2	
		D	2.5-0.8	
2	3	C	3.2-3.4	Res. -0.5-1.1 ohms
		D	2.6-2.4	
	7	C	3.2-3.2	
		D	2.5-neg.	
*	9	C	3.1-3.2	Res. 0.6-0.7 ohms
		D	2.6-2.3	
3	3	C	3.2-3.6	Res. -0.5 0.5 ohms
		D	2.6-2.4	
	7	C	3.2-3.2	
		D	2.5-2.2	
	9	C	3.2-3.9	
		D	2.5-neg.	
4	3	C	3.2-3.4	Res. 0.5-1.0 ohms
		D	2.6-2.4	
	7	C	3.2-3.0	
		D	2.5-1.1	
5	3	C	3.2-3.6	Res. 0.6-1.4 ohms
		D	2.6-2.4	
	7	C	3.2-3.0	
		D	2.5-0.6	

Table 14 (Cont.)

Battery No. B006

Cell Components

Negative Electrode - Rolled lithium on nickel screen - bolted to terminal.

Positive Electrode - Silver, silver chloride - sintered.

Separator - Glass mat fiber filter paper.

Electrolyte - 30 ml CH_3NO_2 -12g AlCl_3 -4.2 g LiClDischarge Current Density - 5.5 ma/cm²

Capacity (to 2 v - worst cell) - 0.553 amp-hr, 33.2 amp-min

Battery Resistance - 4.5 ohms

Changed cell No. 3 before cycle 8.

Stopped battery run before cycle 9.

Battery Characteristics

Cycle	State	Current (ma)	Voltage (v)	Efficiency (Percent)	Capacity (CH) (Percent)
2	C	310-310	14.6-15.3		29.1
	D	540-520	12.7- 9.6	126	
7	C	150-150	15.1-15.2		14.1
	D	540-430	12.0- 3.0	237	

Table 14 (Cont.)

Battery No. B006

Cell Performance

Cell No.	Cycle No.	State	Voltage (v)
1	2	C	3.0-3.2
		D	2.6-2.3
	7	C	3.15-3.15
		D	2.40-0.60
2	2	C	3.0-3.3
		D	2.6-2.2
	7	C	3.15-3.2
		D	2.40-neg.
3	2	C	3.0-3.0
		D	2.6-0.8
	7	C	3.0-3.0
		D	2.6-1.3
4	2	C	3.0-3.2
		D	2.6-2.3
	7	C	3.15-3.15
		D	2.40-1.0
5	2	C	3.0-3.2
		D	2.6-2.4
	7	C	3.15-3.15
		D	2.40-0.5

Table 14 (Cont.)

Battery No. B007

Cell Components**Negative Electrode** - Rolled lithium on nickel screen bolted to terminal.**Positive Electrode** - Silver, silver chloride - sintered.**Separator** - Glass fiber filter paper.**Electrolyte** - 30 ml CH_3NO_2 -12g AlCl_3 - 4.2g LiCl **Discharge Current Density** - 5.43 ma/cm²**Capacity** - not determined (No preliminary discharge)**Battery resistance** - 3.1 ohms**All cells removed before cycle 10; two removed on cycle 9.****Battery Characteristics**

Cycle	State	Current (ma)	Voltage (v)	Efficiency (percent)
1	C	320-320	14.6-15.6	
	D	500-500	13.3-12.5	109
4	C	320-200	15.8-17.6	
	D	500-500	13.0-11.9	119
7	C	320-140	15.8-18.3	
	D	500-460	12.4- 7.5	123

Table 14 (Cont.)

Battery No. B007

Cell Data

Cell No.	Cycle No.	State	Voltage (v)	Notes
1	1	C	2.9-3.0	Very weakened tab on positive electrode
		D	2.6-2.5	
	4	C	3.1-3.7	
		D	2.6-2.4	
	7	C	3.2-3.4	
		D	2.5-2.3	
2	1	C	2.9-3.1	Very weakened tab on positive electrode
		D	2.6-2.5	
	4	C	3.1-3.3	
		D	2.6-2.4	
	7	C	3.2-3.0	
		D	2.5-2.3	
3	1	C	2.9-3.2	Little electrolyte remaining at end of test
		D	2.6-2.5	
	4	C	3.1-4.2	
		D	2.6-2.2	
	7	C	3.2-4.7	
		D	2.5-2.4	
4	1	C	2.9-2.9	Yellow electrolyte at end of test
		D	2.6-2.5	
	4	C	3.1-3.5	
		D	2.6-2.4	
	7	C	3.2-4.4	
		D	2.5-2.4	

Table 14 (Cont.)
Battery No. B007

Cell Data				
Cell No.	Cycle No.	State	Voltage (v)	Notes
5	1	C	2.9-3.3	Yellow electrolyte at end of test
		D	2.6-2.5	
	4	C	3.1-3.2	
		D	2.6-2.4	
	7	C	3.2-3.0	
		D	2.5-2.4	

Table 14 (Cont.)

Battery No. B008

Cell Components

Negative Electrode - Rolled lithium on nickel screen bolted to terminal.

Positive Electrode - Silver, silver chloride - sintered.

Separator - Standard glass fiber filter paper.

Electrolyte - 30 ml nitromethane - 12g AlCl_3 , 4.2g LiClDischarge Current Density - 5.2 ma/cm^2

Capacity - 0.657 amp-hr - 39.4 amp-min

Battery Resistance - 3.6 ohms

(Cells 2 and 3 failed on cycle 5 - charge)

Cycle	State	Battery Characteristics			
		Current (ma)	Voltage (v)	Coulombic Efficiency (percent)	Discharge Depth (percent)
1	C	320-160	14.6-16.4		
	D	500	12-11	95	41.5
3	C	320-80	15-17.8		
	D	500	12-11	129	41.5
4	C	320-80	15-18		
	D	500	12-10.9	126	41.5

Table 14 (Cont.)

Battery No. B008

Cell Data

Cell No.	Cycle No.	State	Voltage (v)
1	1	C	3.0-3.2
		D	2.6-2.5
	3	C	3.2-3.6
		D	2.5-2.4
	4	C	3.2-4.0
		D	2.5-2.4
2	1	C	3.0-3.2
		D	2.6-2.5
	3	C	3.2-3.8
		D	2.5-2.3
	4	C	3.2-3.8
		D	2.5-2.3
3	1	C	3.0-3.4
		D	2.6-2.2
	3	C	3.2-4.0
		D	2.5-2.4
	4	C	3.2-3.2
		D	2.5-2.4
4	1	C	3.1-3.8
		D	2.6-2.4
	3	C	3.2-3.6
		D	2.5-2.1
	4	C	3.2-3.1
		D	2.5-2.0

Table 14 (Cont.)

Battery No. B008

Cell Data

Cell No.	Cycle No.	State	Voltage (v)
5	1	C	3.1-3.5
		D	2.6-2.5
	3	C	3.2-3.6
		D	2.5-2.3
	4	C	3.2-4.0
		D	2.5-2.4

The 25°C (77°F) discharge characteristics of a lithium-silver chloride cell were compared to those at -30°C (-22°F). Figure 30 indicates the cell voltage-current density data for these two temperatures. A drop in potential was observed for this cell. The linear portions of the cell voltage-current density curves yield slopes which correlate well with the values determined for the cell resistance.

Figure 31 shows the cell voltage as a function of current at -57°C. Colder temperatures results in lower cell current and voltage under a constant load. At -57°C, a current drain of 6 ma (60 ma/cm²) resulted in a slow drop in the cell voltage. The drop was minimal after 35 min with the total voltage drop at 0.2 v. Subsequent to the preceding experiments, the cell was discharged at about 1 ma (temperature about -55°C) for several days, so that over 1/4 amp-hr was drawn. The cell was operating satisfactorily when this test was ended.

By making use of a eutectic of propylene carbonate and ethylene carbonate, a solvent is obtained which has a freezing point of about -55°C (-67°F). The following electrolyte was used:

136 ml propylene carbonate
14 ml ethylene carbonate
15 gm aluminum chloride
4 gm lithium chloride

The conductivity of this solution at room temperature is $6 \times 10^{-3} \text{ ohm}^{-1} \text{ cm}^{-1}$ while at -55°C it is $2 \times 10^{-4} \text{ ohm}^{-1} \text{ cm}^{-1}$.

Figure 32 presents the low-temperature (-55°C) cell polarization (current vs voltage). Subsequent to obtaining this data, the cell was discharged at about 1 ma for several days at temperatures below -55°C (at times as low as -75°C). After about 1/4 amp-hr of discharge, the cell was brought to room temperature. The cell was then cycled at a 5 ma/cm² discharge rate. When the cell discharge characteristics became poor (after 14-16 cycles) the rate was reduced to 1 ma/cm² for another 14-16 cycles. The cell was not completely inoperable at the end, but the cycle current efficiency was down to 60 percent. The silver electrode tabs were in a very weakened condition.

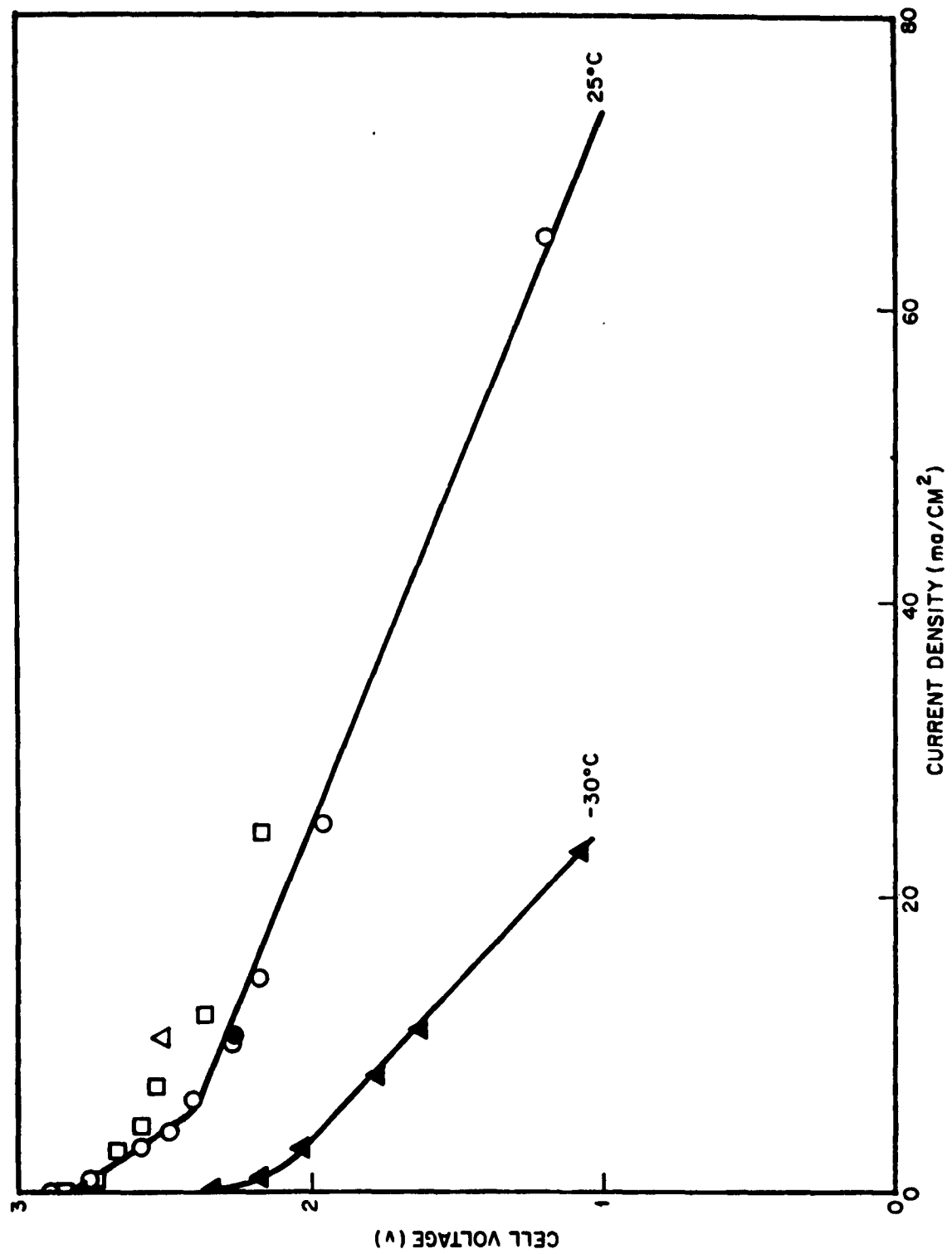


Fig. 30 Cell Discharge Characteristics at 25°C and -30°C

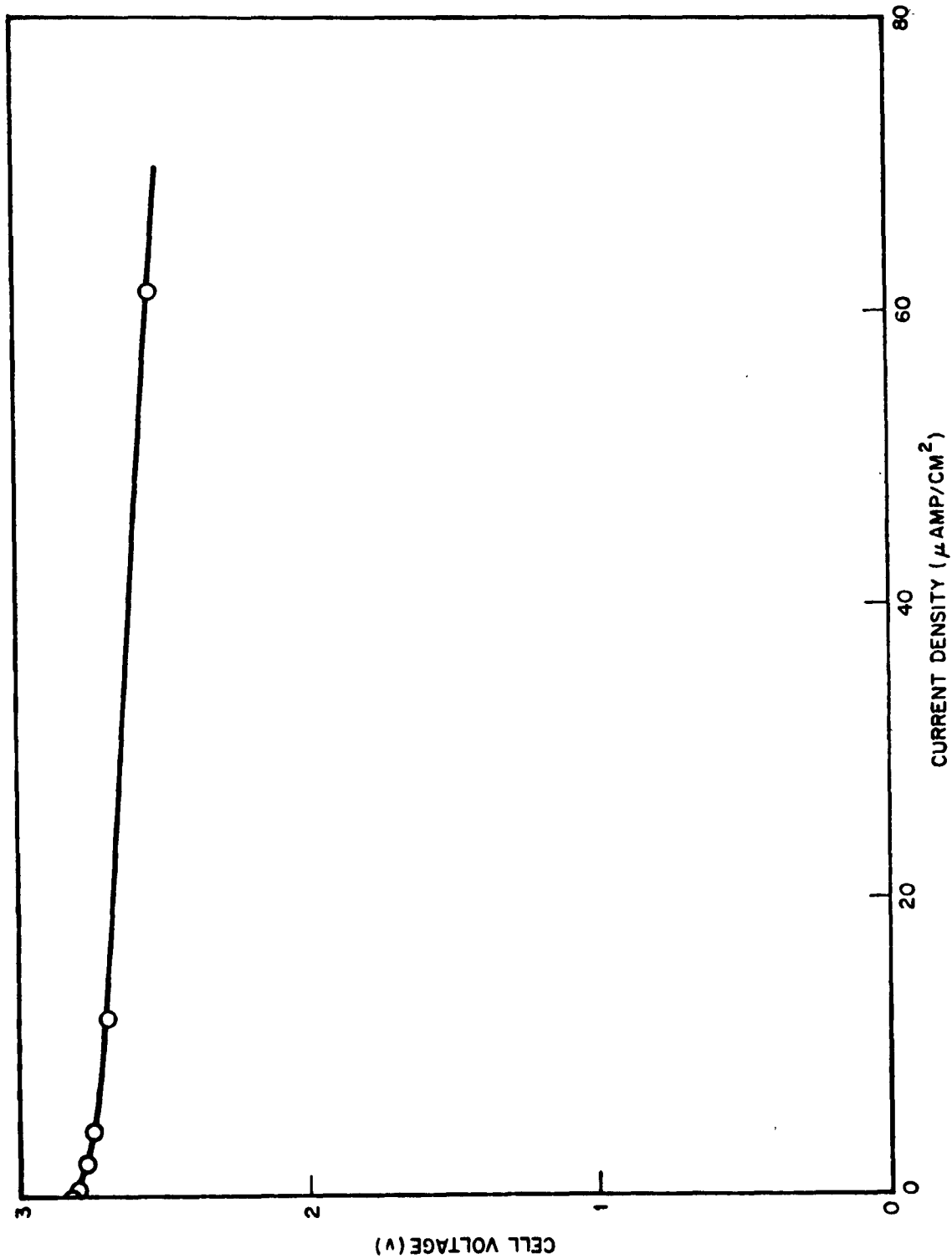


Fig. 31 Cell Characteristics at -57°C

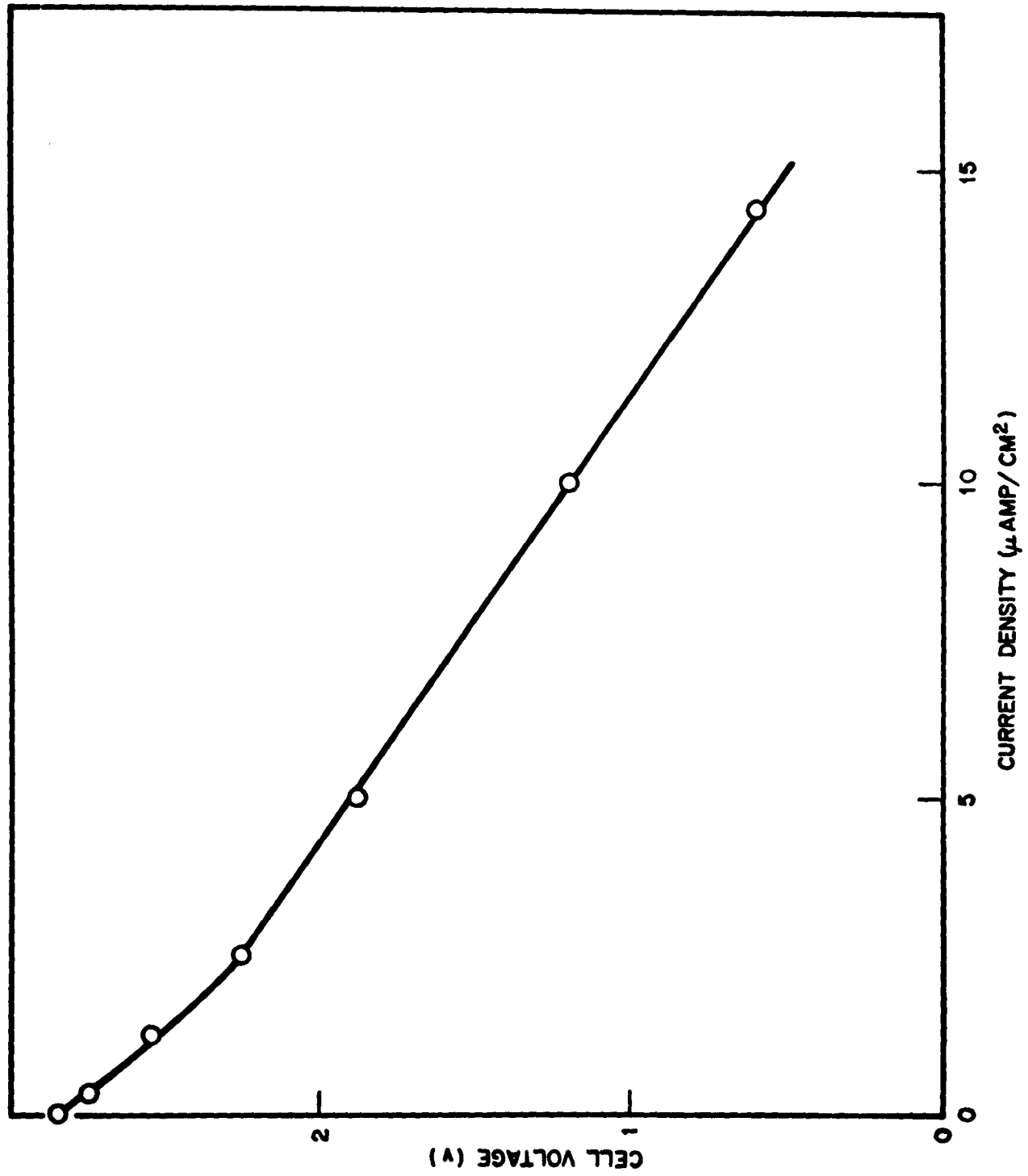


Fig. 32 Cell Characteristics at -56°C

2.9.2 High-Temperature Study

It is of interest to study the operation of nonaqueous cell systems. The cell cases used are not necessarily well sealed.

The flash point of nitromethane is 35°C, and the fire point is 42°C. Because of these facts, it was decided not to test the nitromethane system.

The propylene carbonate-ethylene carbonate electrolyte, used for the low temperature study, was also studied at a high temperature. The cell was heated in an oven at 74.5°C (166°F). Figure 33 presents the high temperature cell polarization. In order to study the pressures produced, a gauge was inserted in order to observe any gassing which might occur. Initially there was some gassing. This subsided after two days to a pressure difference on the order of 0.2 psig or 10 mm of mercury. This pressure is still somewhat greater than the estimated 3-mm solvent vapor pressure. The gage used did not allow readings to be taken accurately enough to determine the pressure precisely. After taking the polarization data and measuring the pressure over a period of several days, the cell was cooled to room temperature and cycled as the low-temperature cell described in the previous section. The results obtained for both cells were similar.

2.9.3 Temperature Dependence of Cell Voltage

The temperature dependence of the EMF of a reversible cell is related to the entropy of the cell reaction by the following expression:

$$\frac{dE}{dT} = \frac{\Delta S}{nF} \quad (3)$$

where E is the open circuit cell voltage, T the absolute temperature, S the entropy of reaction; n the number of equivalents per mole and F the faraday.

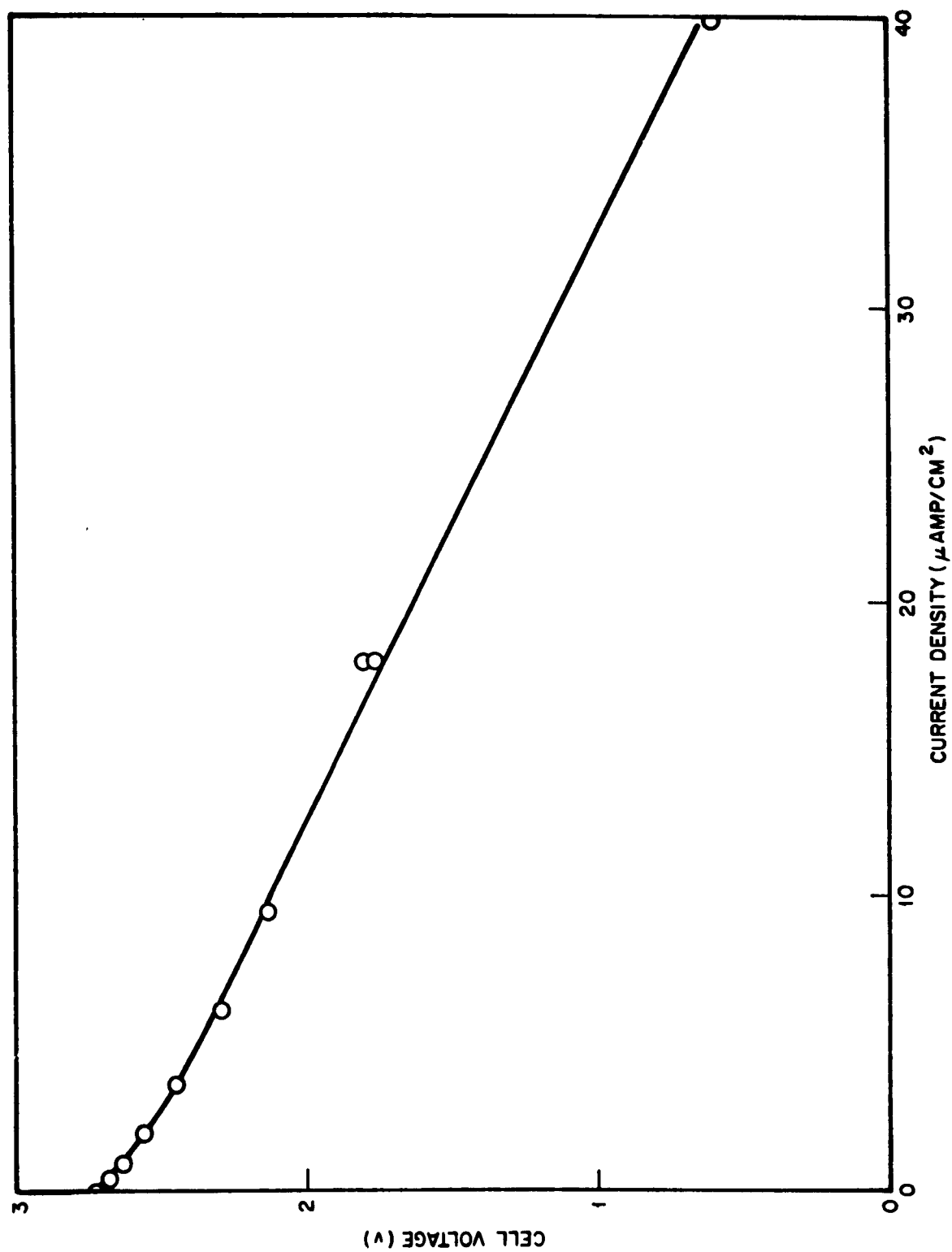
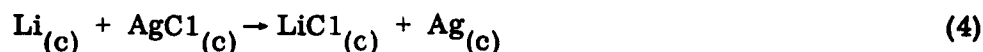


Fig. 33 Cell Characteristics at 74°C

When the cell reaction is written:



where (c) represents the solid crystalline, state, the entropy change is computed to be -6.3 eu at 25°C. The values of the entropy of the individual components in the solid state (l) are used

For the following reaction:



The entropy change for the solid components is estimated as -12 eu at 25°C from an estimate for the entropy of $\text{LiAlCl}_{4(c)}$ of 50 eu.

The open circuit voltage of the lithium/lithium chloride-aluminum chloride-propylene carbonate/silver chloride-silver cell has been measured from -30°C to 40°C and the data is presented in Figure 34. A three-necked flask was partially filled with the electrolyte. Lithium rods were used as anodes and silver wire covered with fused silver chloride as cathodes. These were inserted through each neck by means of standard taper glass joints. The silver electrodes were interconnected electrically for 48 hours in order to bring each electrode to a similar state. This same procedure was used with the lithium electrodes. The emf's of the three cells were then measured at various temperatures with stand times up to 16 hours. After this stand time, the cell potentials were nearly identical.

The experimental value of entropy change for the cell obtained from the slope of the cell voltage-temperature curve is -6.5 eu at 25°C and -17 eu at -10°C. The room temperature cell entropy change value is near the estimated value obtained for equation (4). The reaction indicated by equation (4) would be the net reaction expected to occur in the cell if the electrolyte is saturated with respect to LiCl before the run.

1. W. M. Latimer, Oxidation Potentials, Prentice-Hall, New York, 1953.

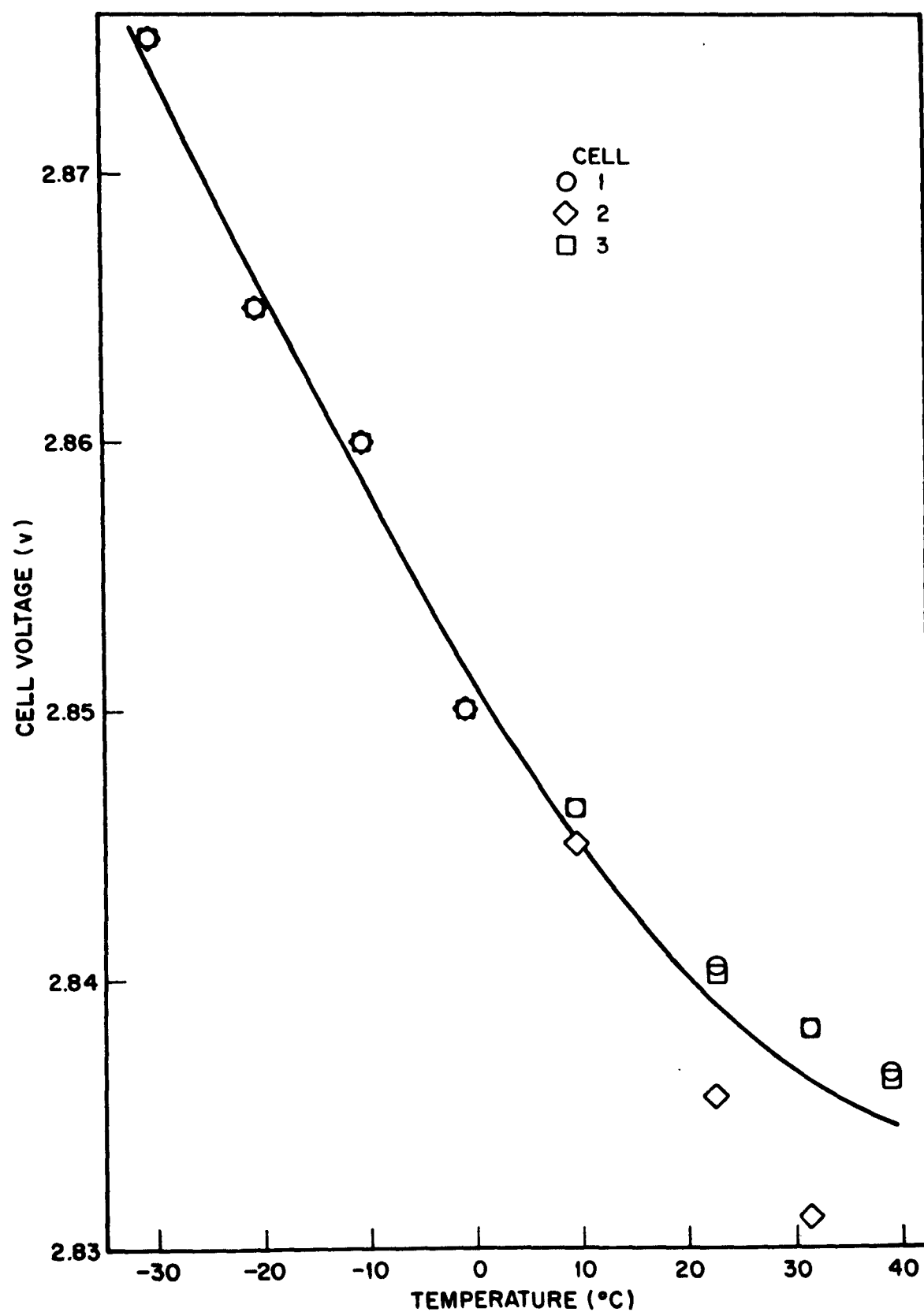


Fig. 34 Temperature Dependence of Open-Circuit Cell Voltage in Propylene Carbonate Solution

At 25°C the cell reaction is uncomplicated by solvent interaction.

The decrease in entropy change at -10°C is greater than can be accounted for in terms of the specific heat change for the net reaction. This low entropy change value may indicate solvate formation with lithium chloride at low temperature.

The emf of the lithium-silver chloride cell using nitromethane instead of the propylene carbonate has been measured as a function of temperature. Reaction entropies calculated from this data given in Figure 35 are -8 eu at 25°C and -14 eu at -10°C temperature.

The differences in entropies measured for the propylene carbonate and nitromethane systems may indicate more solvent interaction with the ionic species in the nitromethane solution. The experimental data with the nitromethane solvent was difficult to obtain. Reaction of the metal clip holding the lithium sample in the electrolyte, successively cadmium plated steel, silver, and platinum, seemed partly responsible for the scatter of data at the higher temperatures.

2.9.4 Cell Heat Production

The heat produced on cell discharge has been evaluated for nitromethane and propylene carbonate electrolytes in 5-amp-hr-size lithium-silver chloride cells. A cell with an aluminum case and a 6-ohm heating coil were placed in a Dewar flask containing water. The coil was heated electrically with measured voltage (V), current (I) and length of time (t). The temperature of the Dewar contents were recorded as a function of time and the thermal capacity of the cell and heat transfer liquid calculated from the following equations:

$$\text{Heat input } Q_1 = IVt \quad (6)$$

$$\text{Heat Capacity} = \frac{Q_1}{\Delta T_1} \quad (7)$$

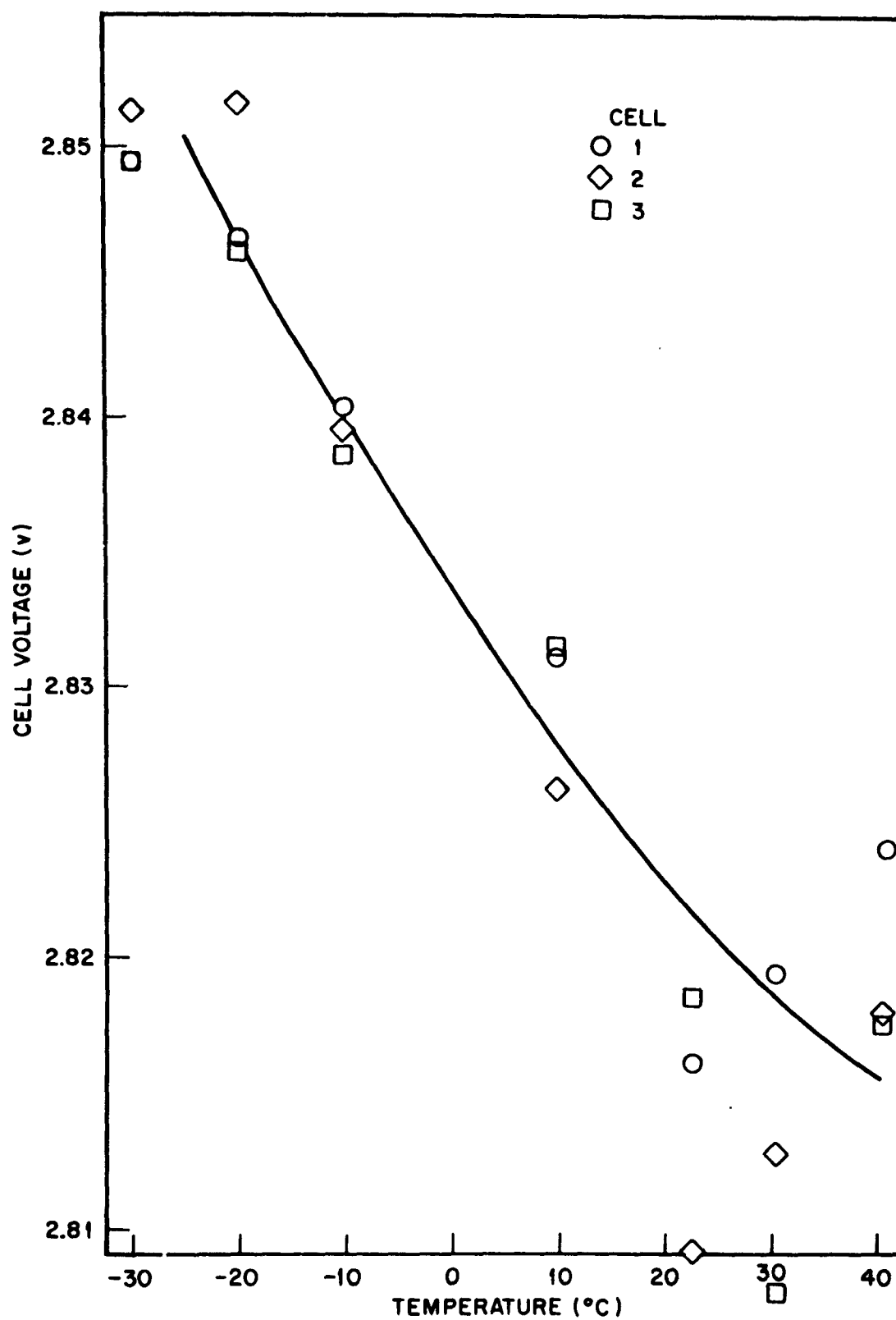


Fig. 35 Temperature Dependence of Open-Circuit Cell Voltage in Nitromethane Solution

where T_1 is the temperature change for the heat input Q_1 . The cell heat capacity from 25°C to 28°C is $0.207 \text{ cal gm}^{-1} \text{ }^\circ\text{C}^{-1}$. While discharging the cell at constant current, the temperature of the Dewar contents and cell voltage were recorded as functions of time. The heat produced by cell discharge Q_2 is calculated from the measured temperature change ΔT_2 (see Fig. 36) as follows:

$$Q_2 = Q_1 \frac{\Delta T_2}{\Delta T_1} \quad (8)$$

The heat produced by cell discharge can also be expressed as the sum of the irreversible heats and reversible heat as follows:

$$Q_2 = \frac{I(V_0 - \bar{V}t)}{J} - T \Delta S \frac{(It)}{F} \quad (9)$$

where I is the current (amp), $V_0 - \bar{V}$ the difference between the open circuit cell voltage and the average cell voltage during discharge $\left[\bar{V} = \int_0^t V dt(v) \right]$, t time of discharge (sec), J a constant equal to 4.186 joules per cal, T the temperature $^\circ\text{K}$, and ΔS the entropy of reaction for the cell ($\text{cal mole}^{-1} \text{ }^\circ\text{K}^{-1}$), and F 96500 ($\text{amp-sec equivalent}^{-1}$). The irreversible heat term $I(V_0 - \bar{V})$ consists of the effects from electrode polarization and cell resistance. The cell resistance was measured with a standard AC bridge operating at 1,000 cps at intervals during the discharge period. The heat measured from the cell discharge was equal to the sum of the irreversible and "reversible" heats within 8 percent deviation. Q_2 was calculated by means of experimental voltage values and the previously determined values of ΔS from the data of the temperature coefficient of the cell voltage at open circuit. The heat from the lithium-silver chloride cell containing propylene carbonate electrolyte consisted of "reversible" heat ($T \Delta S$) 13 percent, resistance heat 17 percent, and electrode polarization heat 70 percent at a discharge rate of 1 amp. The heat from the cell with nitromethane electrolyte consisted of "reversible" heat 14 percent, resistance heat 33 percent, and electrode polarization heat 53 percent at a discharge rate of 2 amp. For cell discharges to 20 percent of the original voltage, the total heat effects are predominantly from electrode polarization. Resistance heating is a predominant source of cell heat during initial discharges as indicated by

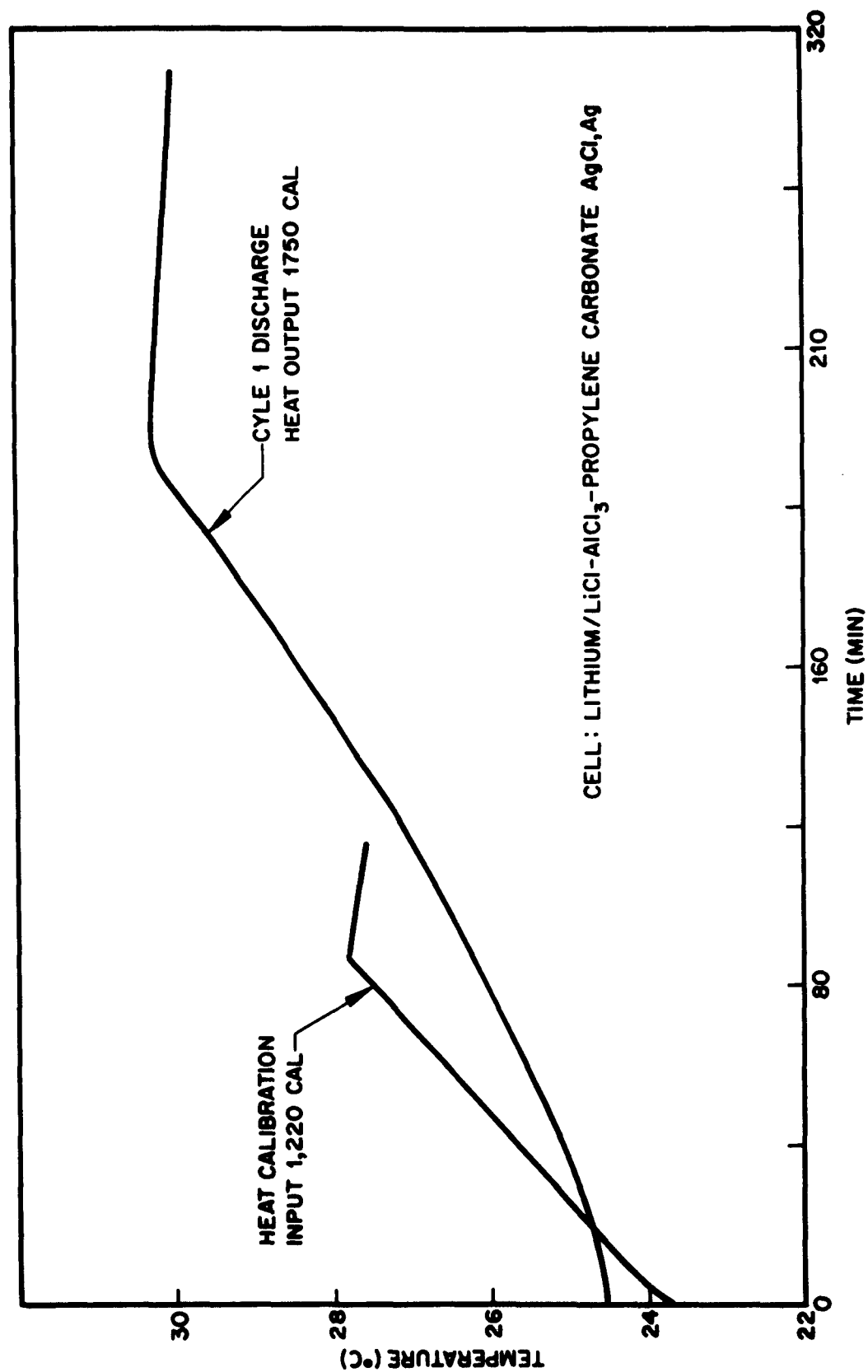


Fig. 36 Cell Heat Production Measurements

the resistance-limited polarization curves obtained by steady-state current-voltage measurements on initial cell discharge. Cell heating is one factor limiting cell performance with the present design. A temperature increase of 20°C was recorded for the 2-amp rate discharge during the 2-hr run.

2.10 CELL POLARIZATION STUDY

2.10.1 Steady-State Measurements

The lithium-silver chloride electrode polarization has been measured as a function of current density and cycle number for the nitromethane electrolyte system. A silver-silver chloride reference electrode was inserted in the cell between the separator-covered electrodes. The electrode polarization plotted in Fig. 37 is the measured voltage between one electrode and the reference. Thus, this value includes half the voltage drop due to solution-separator resistance between electrodes as well as electrode polarization and electrode resistance. The half-cell resistance was calculated from the cell resistance measured after each discharge cycle by use of an AC bridge operating at 1,000 cps. Figure 37 represents cell discharge values for the charge-discharge cycle numbers 2, 10, 24, and 34 for a lithium-silver chloride cell system charging for 60 min at 60 ma current and discharging 30 min at 120 ma current. A gradual decrease in cell voltage at a given current density is noted from cycle 2 to cycle 34. There is also a gradual increase in cell resistance with increasing cycle number, with a larger contribution to resistance from the lithium electrode.

2.10.2 Transient Measurements

Electrode polarization of lithium-silver chloride electrodes has been determined using a current interrupter technique which measures the voltage recovery at an open circuit as a function of time after a cell discharge. The polarization is determined from the voltage, measured with an oscilloscope, between an electrode and a silver-silver chloride reference electrode inserted equidistant between the lithium and silver chloride electrodes.

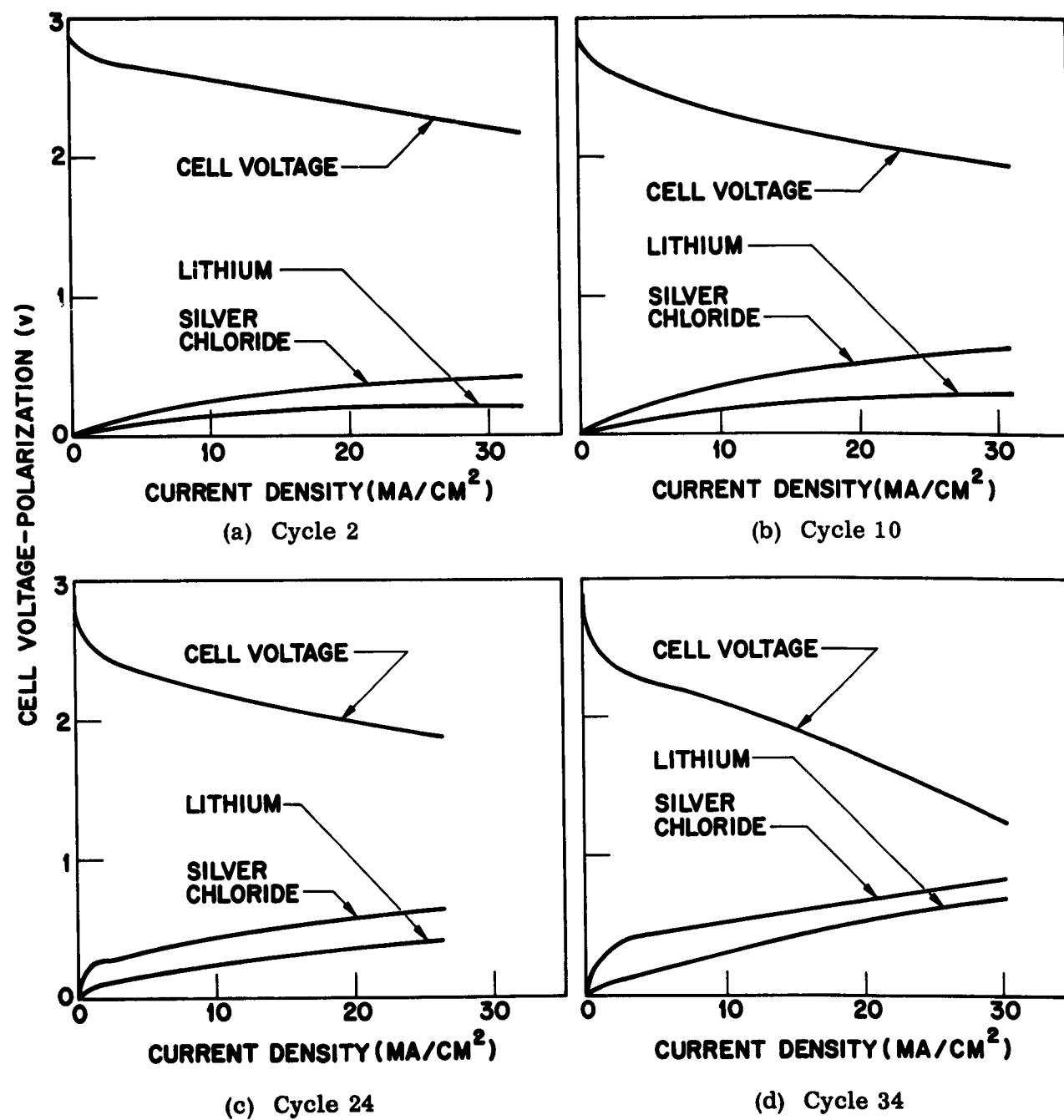
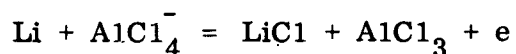
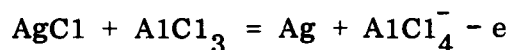


Fig. 37 Discharge Characteristics and Electrode Polarization Study

Resistance polarization due to film formation and solution resistance between reference electrode and working electrode is obtained by extrapolating voltage to time zero and measuring the instantaneous voltage drop. Transport polarization due to mass transport of reacting species from solution to electrode or a slow rearrangement of electrode deposit is assumed to be the time-dependent function and is measured from the initial portion of the time-dependent part of the voltage curve to the final voltage or 1 sec time (oscilloscope time base 0.1 sec per cm). The sum of the resistance polarization measurements for both electrodes is in agreement with the cell resistance measured by AC bridge techniques. The transport polarization at the lithium electrode which would be expected to be an inverse function of the LiCl-AlCl_3 concentration as indicated by the following reaction



but has not been measured with sufficient precision to determine if such a relationship exists. The silver chloride electrode transport polarization would not be expected to depend on the AlCl_4^- concentration as represented by the following reaction:



Polarization measurements obtained on lithium-silver chloride cells with nitromethane electrolyte on charge-discharge cycling show increasing resistance polarization on the lithium electrode. This is also true for cells run with propylene carbonate electrolyte.